NASA CONTRACTOR REPORT

N73-18202
NASA CR-2193

NASA CR-2193



# PROCESSING FOR SPACEBORNE SYNTHETIC APERTURE RADAR IMAGERY

*by M. Lybanon*

*Prepared by*
COMPUTER SCIENCES CORPORATION
Huntsville, Ala.
*for George C. Marshall Space Flight Center*

NATIONAL AERONAUTICS AND SPACE ADMINISTRATION • WASHINGTON, D. C. • FEBRUARY 1973

TECHNICAL REPORT STANDARD TITLE PAGE

| 1. REPORT NO. | 2. GOVERNMENT ACCESSION NO. | 3. RECIPIENT'S CATALOG NO. |
|---|---|---|
| NASA CR-2193 | | |

| 4. TITLE AND SUBTITLE | 5. REPORT DATE |
|---|---|
| PROCESSING FOR SPACEBORNE SYNTHETIC APERTURE RADAR IMAGERY | February 1973 |
| | 6. PERFORMING ORGANIZATION CODE |
| 7. AUTHOR(S) M. Lybanon | 8. PERFORMING ORGANIZATION REPORT # M540 |
| 9. PERFORMING ORGANIZATION NAME AND ADDRESS Computer Sciences Corporation Computer Systems and Simulation Operation Huntsville, Alabama | 10. WORK UNIT NO. |
| | 11. CONTRACT OR GRANT NO. NAS 8-21805 |
| 12. SPONSORING AGENCY NAME AND ADDRESS National Aeronautics and Space Administration Washington, D. C. 20546 | 13. TYPE OF REPORT & PERIOD COVERED CONTRACTOR |
| | 14. SPONSORING AGENCY CODE |

15. SUPPLEMENTARY NOTES

16. ABSTRACT

This report considers the data handling and processing in using synthetic aperture radar as a satellite-borne earth resources remote sensor. The discussion covers the nature of the problem, the theory, both conventional and potential advanced processing techniques, and a complete computer simulation. The report shows that digital processing is a real possibility and suggests some future directions for research.

| 17. KEY WORDS | 18. DISTRIBUTION STATEMENT |
|---|---|
| Synthetic Apeture Radar<br>Earth Resources<br>Digital Processing | |

| 19. SECURITY CLASSIF. (of this report) | 20. SECURITY CLASSIF. (of this page) | 21. NO. OF PAGES | 22. PRICE |
|---|---|---|---|
| Unclassified | Unclassified | 104 | $3.00 |

MSFC - Form 3292 (May 1969)

* For sale by the National Technical Information Service, Springfield, Virginia 22151

## Acknowledgement

A number of people have graciously contributed to the work described here. Their advice and suggestions are sincerely appreciated. The author wishes to give special thanks to Dr. A. D. Bond of Computer Sciences Corporation for many hours of fruitful discussion. Thanks are also due to the Project Monitor, Mr. B. Hodges, Chief, Applications Development Branch, Computation Laboratory, for his helpful contributions and support during the project.

TABLE OF CONTENTS


Page

SECTION I. INTRODUCTION

A. Earth Resources Remote Sensing with Imaging Radar . . . 2
B. Synthetic Aperture Radar . . . . . 2

SECTION II. DATA GENERATION AND PROCESSING FOR SPACEBORNE SAR IMAGERS . . . . . 5

A. The Synthetic Aperture Principle . . . . . 5
B. Data Rate for Orbital Payloads . . . . . 10
C. Processing Techniques . . . . . 18

SECTION III. MATHEMATICAL THEORY OF SAR DATA PROCESSING . . . . 20

A. Summary of Previous Results . . . . . 20
B. The Received Signal . . . . . 21
C. Matched Filtering and the Linear FM Signal . . . . . 22

SECTION IV. OPTICAL AND DIGITAL SAR SIGNAL PROCESSING . . . . . 29

A. Optical Processing of Synthetic Aperture Radar Signals. 29

1. The Radar Signal . . . . . 29
2. Coherent Optical Correlation . . . . . 30
3. The SAR Optical Processor . . . . . 32

B. Digital Processing of Synthetic Aperture Radar Signals. 35

1. Possibility of Digital Processing . . . . . 35
2. Basic Processing . . . . . 37
3. Variations on Fundamental Algorithm . . . . . 39
4. A Proposed Real-Time SAR Digital Processor . . . . 41
5. Alternate Approaches . . . . . 44

SECTION V. SYNTHETIC APERTURE RADAR SYSTEM SIMULATOR . . . . . 56

A. Introduction . . . . . 56

1. Experiment Simulator Concept . . . . . 56
2. Overall Concept of Simulator . . . . . 56

B. Structure of Simulator . . . . . 57

1. Target Model and Data Representation . . . . . 58

a. Internally-Generated Targets . . . . . 58
b. Externally Input Targets . . . . . 61

TABLE OF CONTENTS
(Cont'd.)


Page

2. Radar System . . . . . 61

a. Antenna and Construction of Received Signal . . 61
b. Radar Receiver . . . . . 64

3. Processor . . . . . 64

a. Preprocessing Modules . . . . . 64
b. Processing Variations and Options . . . . . 65

4. Output Options . . . . . 67

a. Tabulations . . . . . 67
b. Plots . . . . . 68
c. Images . . . . . 68
d. Statistical Analyses . . . . . 68

C. Examples . . . . . 69

SECTION VI. CONCLUSIONS . . . . . 76

APPENDIX A. FUNDAMENTAL OPTICAL PRINCIPLES . . . . . 80

APPENDIX B. OPTICAL PROCESSING . . . . . 85

LIST OF ILLUSTRATIONS


| Figure | Title | Page |
|---|---|---|
| 1 | Sidelooking Radar Configuration | 3 |
| 2 | Synthetic Aperture Radar Slant Range Plane Geometry | 6 |
| 3 | Synthetic Aperture Radar Cross-Track Geometry | 11 |
| 4 | Maximum Data Rate vs. Altitude for SAR in Circular Earth Orbit | 13 |
| 5 | Radar Data Film Format | 15 |
| 6 | Maximum SAR Data Rate vs. Resolution at Skylab Altitude | 17 |
| 7 | A Coherent Optical Multichannel Cross-Correlator | 31 |
| 8 | Light Transmitted by the Line $y = y_1$ of the Film Transparency | 31 |
| 9 | Development of an Anamorphic Lens System for Compensation of the Radar Image | 36 |
| 10 | Algorithm Employed with Quadrature Detection | 38 |
| 11 | Pipeline Processor Concept | 47 |
| 12 | Parallel Structure of ILLIAC IV | 47 |
| 13 | Signal Flow Graph for Cooley-Tukey Algorithm | 50 |
| 14 | Pipeline FFT m Module | 51 |
| 15 | FFT Pipeline Processor Flow Diagram, N = 16 | 52 |
| 16 | FFT Pipeline Diagram, Two Interleaved Channels, N = 8 Each | 54 |
| 17 | Synthetic Aperture Radar Simulator System Diagram | 59 |
| 18 | Schematic of SAR System Simulated | 62 |
| 19 | CYCLE Target Pattern, Full Focused Processing | 71 |
| 20 | LINEAR Target Pattern, Full Focused Processing | 71 |
| 21 | POINT Target Pattern, Full Focused Processing | 72 |

LIST OF ILLUSTRATIONS (Continued)


| Figure | Title | Page |
|---|---|---|
| 22 | POINT Target Pattern, Full Zone Plate Processing . . | 72 |
| 23 | POINT Target Pattern, Unfocused Processing . . . . . | 73 |
| 24 | Computer Generated SAR Images--Comparative Processing Study . . . . . | 73 |
| 25 | Computer Generated SAR Images--Continuation of Comparative Processing Study . . . . . | 74 |
| A1 | Region of Integration for Kirchhoff Integral . . . . | 81 |
| A2 | Construction for Derivation of Fresnel-Kirchhoff Diffraction Formula . . . . . | 81 |
| B1 | Fourier Transforms In an Optical System . . . . . | 87 |
| B2 | Optical Processing Examples . . . . . | 87 |

LIST OF TABLES


| Table | Title | Page |
|---|---|---|
| 1 | Cases Portrayed in Figures 19-23 . . . . . | 70 |
| 2 | Representative SAR Design Details . . . . . | 78 |

## DEFINITION OF SYMBOLS

The following is a list of some symbols that appear at several places in the text, along with their most frequent definitions.

| Symbol | Definition |
|---|---|
| $A$ | Amplitude of (azimuth) return signal pulse |
| $A(\omega)$ | Envelope of spectrum of SAR azimuth point response |
| $A_p$ | Pth stage in recursive FFT calculation |
| $B$ | Nominal bandwidth of SAR azimuth signal |
| $c$ | Speed of light |
| $D_h$ | Radar antenna length |
| $f$ | (1) Frequency<br>(2) Focal length |
| $f_i$ | Instantaneous frequency |
| $k$ | Linear FM rate |
| $N$ | (1) Number of samples (resolution cells) in return azimuth signal from a point<br>(2) Number of points in FFT sequence |
| PRF | Pulse repetition frequency |
| $R$ or $R_0$ | Slant range |
| $S(f)$ | Signal spectrum |
| $s(t)$ | Return signal from point target |
| SAR | Synthetic aperture radar |
| $T$ | Length of time target remains in beam |
| $t$ | (1) Time<br>(2) Amplitude transmission function |
| $v$ or $v_a$ | Speed of vehicle carrying radar |
| $v_f$ | Speed of film in recorder |
| $W$ | Principal Nth root of unity |

DEFINITION OF SYMBOLS (Continued)

| Symbol | Definition |
|---|---|
| $x$ | (1) Coordinate along film<br>(2) x-coordinate in plane of lens or transparency |
| $y$ | (1) Coordinate across film<br>(2) y-coordinate in plane of lens or transparency |
| $\theta$ | Phase in frequency domain |
| $\lambda$ | Wavelength |
| $\rho_a$ | Azimuth resolution |
| $\tau_g(f)$ | Group delay |
| $\phi$ | Phase in time domain |
| $\Omega$ | Doppler bandwidth (radians/second) |
| $\omega$ | Angular frequency |

PROCESSING FOR SPACEBORNE SYNTHETIC APERTURE RADAR IMAGERY


## SUMMARY

Synthetic aperture radar, and the processing required to produce high-resolution imagery, are discussed. Particular attention is paid to the use of SAR as a satellite-borne earth resources remote sensor, and the associated data handling and processing problems, which are different from those associated with airborne radars. A computer simulation of a complete synthetic aperture radar system is described, and examples of its output are presented. It is pointed out that the simulator could be useful in preparing for the new applications of SAR.

The report may be meaningfully read in parts. Sections I and II introduce the basic principles and simplified theory. The analysis is sufficient to allow realistic estimation of data rates; a discussion of limiting data rates for the orbital case is provided. Sections III and IV go more deeply into the mathematical theory and details of the processing. Section III is a thorough analysis of the properties of the received radar signal and the mathematical operations required to produce imagery. Section IV discusses both the conventional coherent optical processing technique (Appendices A and B cover the physical principles involved) and the possibility of real-time SAR digital processing. A proposed on-board real-time SAR digital processor is described, a number of concepts relevant to the design of this and more sophisticated digital processors are discussed. Section V describes a complete SAR digital computer simulation, discusses its use, and gives examples of output. Conclusions are presented in Section VI.

The nature of these conclusions is that satellite-borne SAR systems will require some new design considerations, particularly with regard to data management, that digital processing is a real possibility, and that a simulator like the one described here could be useful in the design tradeoff studies. Since this report is not the result of such a study, it does not propose a specific design for a synthetic aperture radar processor. But it does contain discussion of a great many of the principles and concepts involved.

# SECTION I. INTRODUCTION

## A. Earth Resources Remote Sensing with Imaging Radar

Side-looking imaging radar is a potentially valuable sensor for geoscience, hydrological, and other applications. Since radar provides its own illumination and has the ability to penetrate cloud cover, its use for viewing is not restricted to periods of good weather in daylight. Radar operates in the microwave region; therefore, it can be expected to provide information not seen in visible and infrared images. With the addition of the synthetic-aperture processing technique, imaging radar achieves resolution comparable to photography.

In considering putting a synthetic aperture radar on a satellite, the size, weight, and power requirements are considerable. Aside from this, there are significant questions concerning data processing, storage, and transmission, which this report will investigate. The intention is to discuss the relevant points in some detail; the solution of the design problems and choice of a particular configuration depend on the goals and constraints of specific missions.

## B. Synthetic Aperture Radar

The synthetic aperture radar (SAR) technique was developed as a method of improving the angular resolution of airborne imaging radars [1,2]. The configuration involved is shown in Figure 1. In order to be carried on an aircraft, the radar antenna must fit into a "package" that is small enough and whose shape will not destroy the aerodynamic characteristics of the plane. A streamlined cover, or radome, big enough to contain a long rotating antenna has very serious effects on the flying abilities of an aircraft, so the necessary sweeping cannot be done in this way. But a non-rotating antenna intended to look only to the side (a fixed antenna which looks straight down has no cross-track resolution) has its greatest dimension extended along the length of the aircraft, so side-looking radars can use larger airborne antennas than can rotating radars.

In principle, the cross-track, or range, resolution can be made as fine as desired by pulsing the radar signal and choosing the pulse width small enough. However, the antenna simply "adds up" the return from the reflected beam (plus noise), so the along-track, or azimuth, resolution of a side-looking system is apparently the width of the beam at the ground, which can be considerable. From satellite altitudes, imagery with this resolution would be worthless.

It is easy to see that the return signal actually contains more detail about the location of objects than the simplest approach yields.

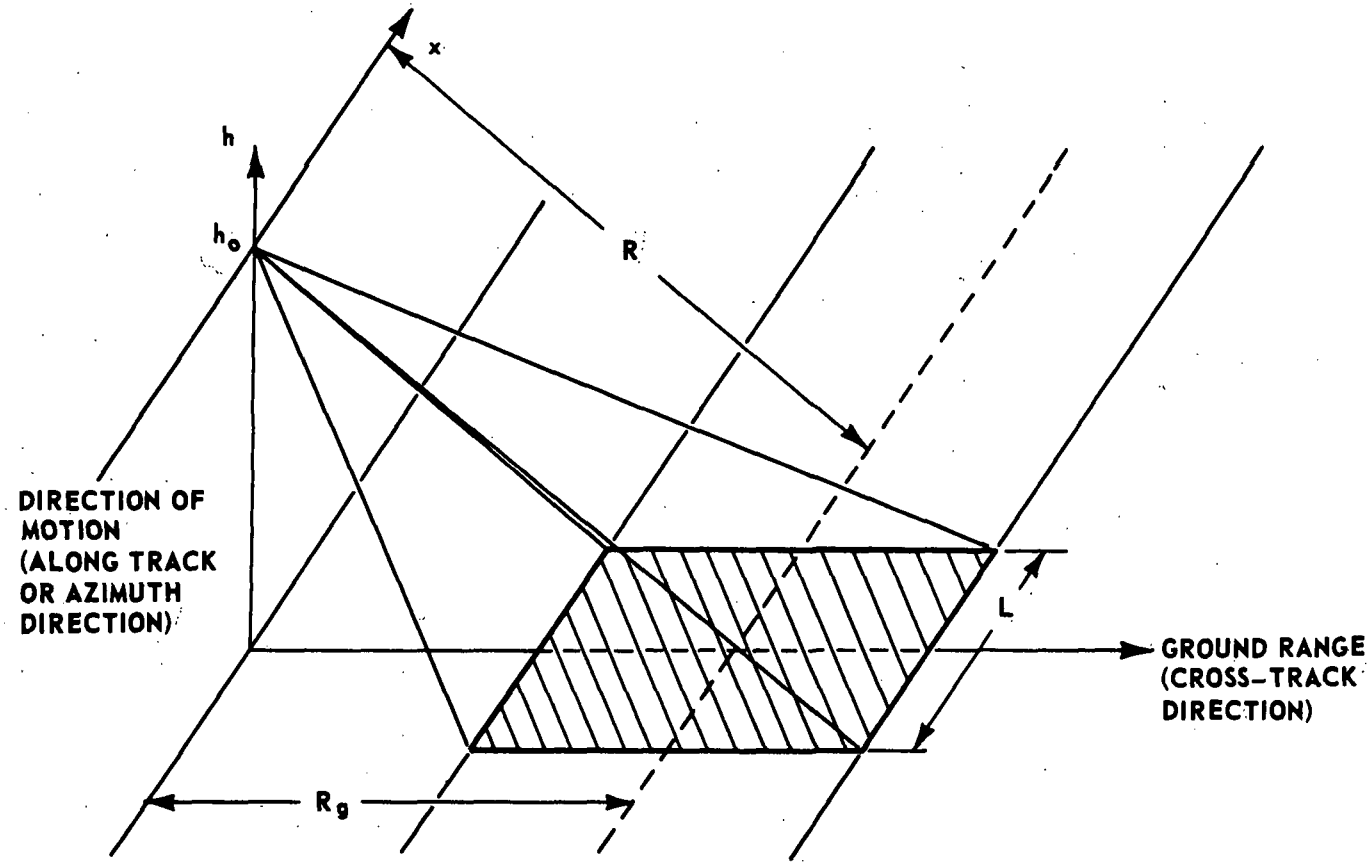


FIGURE 1. SIDE LOOKING RADAR CONFIGURATION

When one considers the return from a point scatterer illuminated by the radar beam, it is seen that there is a time-varying Doppler shift depending on the instantaneous component along the radius vector from the antenna to the target of the scatterer's velocity relative to the antenna. The total signal is a composite of such returns, with a complex Doppler spectrum. The analysis of this Doppler spectrum is achieved by the SAR processing. It produces the effect of using a (synthetic) antenna whose length is much greater than that of the actual physical antenna, hence the angular resolution is much finer. The theory will be discussed more fully in subsequent sections.

The mathematical operations involved in SAR processing are conventionally done by recording the received signal on photographic film and using optical processing techniques [3,4,5,6] . It will be shown that the data rate is very great, especially for a satellite-borne SAR. Thus a large quantity of data is received in a short time. Film is an efficient storage medium, permitting very fast, dense recording of the data. And, if film is used, the video data record is available for direct insertion into an optical channel. The azimuth processing is range-dependent; each range interval must be processed differently. Optical systems are readily adaptable to performing the two-dimensional mathematical operations required [7] . However, there are certain drawbacks to applying this method in a satellite system. An airplane can land after taking data for a few hours, but on a satellite, disposing of the exposed film and replacing it with fresh film is a more serious problem. Therefore, it is sensible to consider alternatives to the conventional method.

Some authorities have considered digital processing of SAR data to be impossible [5] . However, at least one group which has been working on the problem takes the opposite view [8,9,10] . According to this group, in the immediate future digital processing of SAR data should be practical using a special-purpose processor [9] . Methods, tradeoffs involved, and other considerations will be discussed in later sections of this report. It is worth mentioning that the special-purpose processor might be of value in other image-processing applications.

## SECTION II. DATA GENERATION AND PROCESSING FOR SPACEBORNE SAR IMAGERS

### A. The Synthetic Aperture Principle

A short antenna that radiates a relatively wide beam is moved through space in a straight line perpendicular to its radiating direction, which is to the side and downward at an angle. The phase of each reflected signal is measured very accurately (with coherent detection) and recorded, along with the amplitude, typically on a CRT-photographic film recorder.

A point reflector passing through the beam would be recorded as a Doppler beat pattern, decreasing in frequency as the point approaches broadside, passing through zero, and increasing as the point leaves the beam. This recorded signal can be subsequently compressed by coherent correlation with a reference function (matched filter), to produce an image of the point reflector. An extended object may be regarded as a collection of point reflectors, producing a complex recording which can be compressed to form the image of the object. Therefore, along-track resolution is made substantially better than the along-track beamwidth, which would be the resolution length in the absence of processing. Cross-track resolution is obtained by transmitting short pulses.

Since antenna beams are fan-shaped, points at far range stay in the beam for a longer period of time than those at near range. If the correlation interval is long enough to include the entire Doppler history at each range, then each recorded point history, regardless of range, will compress to the same size on the output image in the along-track direction, resulting in equal resolution at all ranges. Therefore, an SAR image can readily be given an appearance similar to a photograph taken straight downward from an aircraft or spacecraft, even though the radar antenna is side-looking.

The synthetic aperture technique, then, consists of mathematical processing to analyze the Doppler spectrum of the received radar signal. Subsequent analysis will show that the mathematical operations simulate the physical situation of a long array antenna. Without the detailed development this requires, however, it is possible to proceed from the foregoing verbal description to a simplified, non-rigorous mathematical analysis that quickly provides some useful information concerning data rate and resolution.

We consider first the return from a point scatterer (an object whose dimensions are small compared to lengths of interest in the following discussion). The situation is shown in Figure 2: The radar antenna is taken to be at rest at the origin of a reference frame moving with the aircraft (or spacecraft). P is the scattering object's instantaneous relative position, v its relative total velocity, $C_t$ its relative trajectory, and c stands for the speed of light. For simplicity, suppose that the

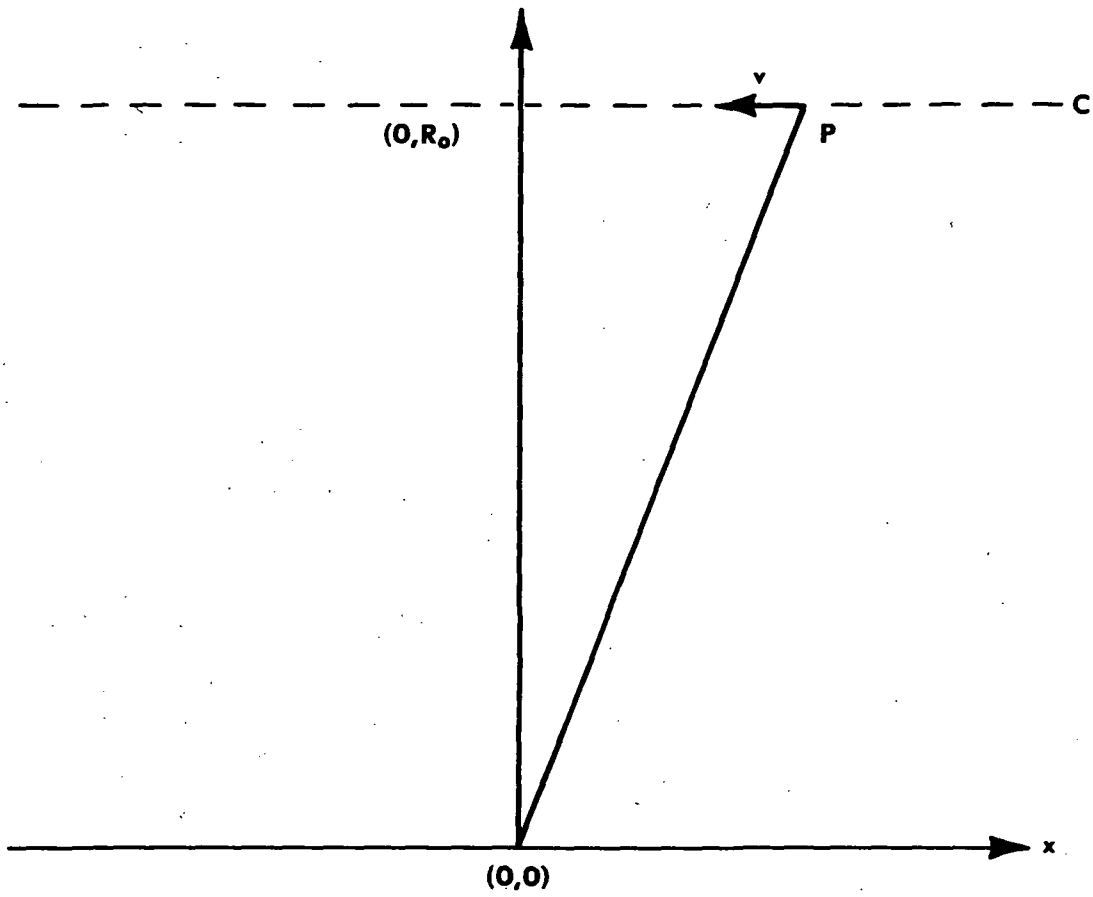


FIGURE 2. SYNTHETIC APERTURE RADAR SLANT RANGE PLANE GEOMETRY

time behavior of the radiated signal is given by $\cos \omega_o t$. Then the received signal depends on $\cos \{\omega_o[t - \tau(t)]\}$, where $\tau(t)$ is the delay due to the time required for propagation. The delay $\tau(t)$ is

$$\tau(t) = 2R(t)/c, \quad R^2(t) = R_o^2 + (vt)^2 \tag{1}$$

with suitable choice of the time origin, as is clear from Figure 2. Using the binomial expansion,

$$R(t) \approx R_o + v^2t^2/2R_o \tag{2}$$

assuming that the signal is received over a small angle. Then the phase modulation due to the Doppler effect caused by the relative motion is

$$\phi(t) = -\omega_o \left(\frac{2}{c}\right)\left(R_o + \frac{v^2t^2}{2R_o}\right)$$

$$= -\left[\frac{4\pi R_o}{\lambda} + \frac{2\pi v^2}{\lambda R_o} t^2\right], \quad |t| \leq \tfrac{1}{2}T \tag{3}$$

where $\lambda = 2\pi c/\omega_o$ is the wavelength of the radiated wave and T is the length of time over which we receive the azimuth history from the single scatterer. Then the Doppler frequency shift is

$$\omega_D = -\frac{4\pi v^2}{\lambda R_o} t \qquad |t| < \tfrac{1}{2}T \tag{4}$$

Such a modulation, known as "linear FM," is common in radar work. It is also called a "chirp" pulse. The frequency shift is actually twice what one would expect from the Doppler effect until one considers the signal's two-way trip, from antenna to target to antenna.

The pulsing of the transmitted signal, which is necessary to achieve range resolution, has the effect of sampling the azimuth modulation. The approximate Doppler bandwidth is, from (4),

$$\Omega = \frac{4\pi v^2 T}{\lambda R_o} \tag{5}$$

(the maximum frequency is half this); therefore to avoid aliasing errors, the sampling rate, or pulse repetition frequency (PRF), must be at least this great (the pulse duration or width determines range resolution). This conflicts with the requirement for a large "unambiguous" range interval, which is that interval such that the return from one pulse does not

begin to arrive before the return from the preceding pulse has been completely received. The antenna can be designed to illuminate preferentially the unambiguous range interval; however, this cannot be done perfectly. So it is seen that a fundamental system design problem of SAR is that the requirement for good azimuth resolution conflicts with the requirement for large range coverage. In order to have a usefully large unambiguous range interval, the PRF must not be too great; in practice, this means that there will necessarily be some azimuth signal energy aliased [5] .

There are several heuristic ways of estimating the azimuth resolution that can be achieved by SAR. One way is to calculate the apparent beamwidth at the ground of a signal radiated from an antenna the length of the synthetic antenna. Another is to appeal to Fourier analysis. Each resolution element in the azimuth direction has a unique Doppler shift associated with it. It seems intuitively clear that if T, the time over which an object is observed, is very short, two objects which are very close together cannot be resolved, that separating them becomes easier as T increases, and that for $T \longrightarrow \infty$ objects arbitrarily close together can be distinguished. (Since T is proportional to the width of the beam, which is approximately inversely proportional to the length of the antenna, this would imply that making the antenna shorter improves azimuth resolution--the opposite of the length dependence of resolution without SAR processing. This is actually the case.) If a time-varying signal is observed over an interval of length T, then uncorrelated estimates of its spectrum can be made at intervals $\Delta\omega = 2\pi/T$ in the frequency domain [11]. (This really follows from the sampling theorem [12].) Thus the bandwidth $\Omega$ given by (5) is divided into N intervals

$$N = \frac{\Omega}{\Delta\omega} = \left(\frac{4\pi v^2 T}{\lambda R_o}\right)\left(\frac{T}{2\pi}\right) = \frac{2v^2T^2}{\lambda R_o} \qquad (6)$$

The maximum frequency is N/2 times the basic increment $\Delta\omega$. Such a set of discrete spectral estimates is the discrete Fourier transform of a time series of N samples covering the interval of length T [11,12]. This corresponds to dividing the (length) interval x=vT into N subintervals of length $\Delta x = x/N$, which can be regarded as a measure of the resolution length in the present context. From (6)

$$\Delta x = \frac{x}{N} = (x)\left(\frac{\lambda R_o}{2x^2}\right) = \frac{\lambda R_o}{2x} \qquad (7)$$

The length x=vT is the length subtended at the ground by the radiated beam, approximately $\lambda R_o/D_h$, where $D_h$ is the length of the antenna. So the azimuth resolution $\rho_a = \Delta x$ is

$$\rho_a = \frac{\lambda R_o}{2(\lambda R_o/D_h)} = \frac{D_h}{2} \qquad (8)$$

Equation (8) is actually the azimuth 3db resolution [5]; it is the velocity of the radar divided by the Doppler bandwidth in Hz (rather than in radians per second, as expressed by (5)).

The required PRF can easily be obtained now. The return signal at any time contains contributions from all points illuminated by the radar beam, therefore the spectrum contains all the frequencies given by (4). The highest frequency in the spectrum is

$$f_{max} = \frac{v^2 T}{\lambda R_o} \tag{9}$$

Therefore, the required sampling rate or pulse repetition frequency to avoid aliasing is twice this value,

$$PRF = \frac{2v^2 T}{\lambda R_o} \tag{10}$$

The time between samples is the reciprocal of the PRF. Making use of $x = vT = \lambda R_o / D_h$, we find

$$\text{time between samples} = \frac{R_o}{2v(\lambda R_o / D_h)} = \frac{D_h/2}{v} \tag{11}$$

Since v is the velocity of the platform carrying the radar, this is the time required to move a distance equal to half the length of the antenna, which (8) tells us is the resolution length. This conclusion is in satisfactory agreement with the intuitive feeling that the spacing of samples must be at least as fine as the achievable resolution.

The formula (8) for the maximum achievable azimuth resolution is quite interesting. As has already been pointed out, the dependence of the resolution on the length of the physical (rather than synthetic) antenna is the inverse of that for a long real antenna. Also, resolution is independent of range or wavelength, or indeed any parameters other than the length of the antenna. Speaking strictly from the standpoint of resolution, the shorter the antenna the better. However, it has been shown that the requirement for good azimuth resolution conflicts with the requirement for large range coverage, so a compromise must be made. Harger [5] shows that the ratio of the unambiguous slant range interval to the azimuth resolution is a constant fixed by vehicle velocity. Roughly, the time required to sample a slant range interval $\Delta R$ is $2\Delta R/c$ (the factor of 2 arises because the pulse must go out and come back), and the time required to traverse the resolution distance $\rho_a$ is $\rho_a/v$. Equating these times gives

$$\frac{2\Delta R}{\rho_a} = \frac{c}{v} \tag{12}$$

The slant range interval that can be mapped, in units of the resolution length, is a number inversely proportional to vehicle velocity.

## B. Data Rate for Orbital Payloads

The foregoing analysis is sufficient to provide some data rate estimates. The magnitude of the data rate is of fundamental importance, since it influences data storage and transmission requirements, and the possible means for processing the data. The relevant equations from the preceding section are (8), giving the maximum theoretical resolution, (10) and (11), for the required pulse repetition frequency (PRF), and (12), giving the maximum unambiguous slant range interval. A consideration of the geometry involved is the only remaining element needed to calculate upper limits on the data rate.

The theory in Section II.A concerned itself with the return from a single point target a fixed distance from the ground track of the platform (aircraft, satellite, etc.) carrying the radar. It is now necessary to consider the signal reflected from an entire two-dimensional ground scene. It will be assumed that the resolution lengths are the same in the range (across-track) and azimuth (along-track) directions.

Figure 3 shows a cross-section of the imaging geometry, that relevant to a single pulse. The direction of motion of the radar-carrying vehicle is normal to the plane of the figure. The two sides of the triangle adjacent to the angle $\beta_V$ differ in length by $\Delta R$. The maximum permissible value of $\Delta R$ is that given by Equation (12). The third side of the triangle is $\Delta R_g$, the ground range interval corresponding to the slant-range interval $\Delta R$. (In principle, the cross-track resolution may be made as fine as desired. Two points a distance d apart can be resolved if the pulse duration is short enough so that the reflection from the nearer point is completely received before the beginning of the return from the farther point arrives at the antenna. Pulse compression techniques are also frequently used. So the resolution requirement mentioned above is a condition on the pulse width, hence on the radar system bandwidth--and, consequently, on the data rate.) $R_m$ is the mean slant range to the illuminated terrain.

The angle $\beta_V$ subtended at the radar antenna by the ground swath $\Delta R_g$ is given by [5]

$$(2h \cos \gamma_o) \sin\tfrac{1}{2}\beta_V - \tfrac{1}{2}\Delta R \cos \beta_V = -\tfrac{1}{2}\Delta R \cos 2\gamma_o \qquad (13)$$

where h is the altitude and $\gamma_o$ is the depression or "look" angle below the local horizontal. Harger solves this equation in the small-angle approximation to find the lower limit on the corresponding antenna dimension, the "vertical aperture width"[5]. The exact solution of

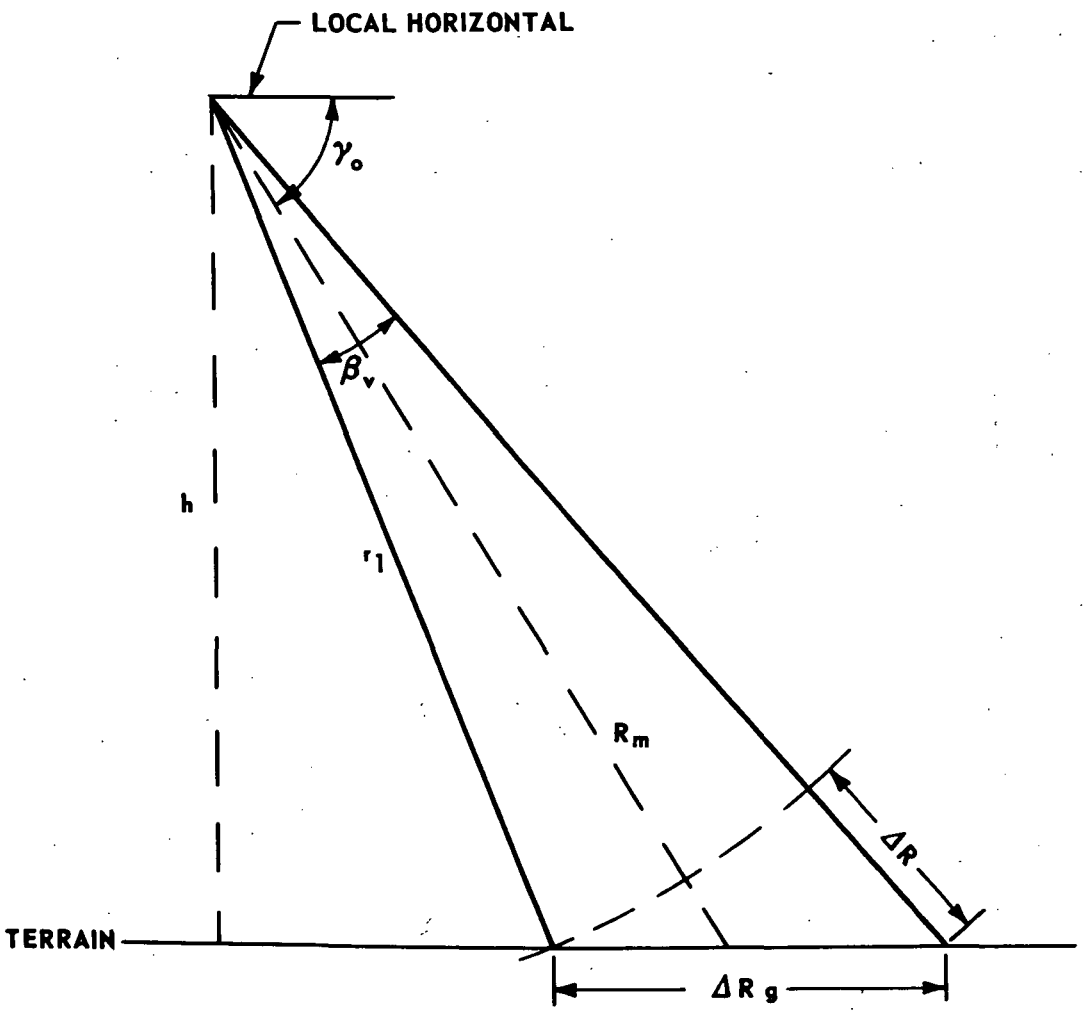


FIGURE 3. SYNTHETIC APERTURE RADAR CROSS-TRACK GEOMETRY

Equation (13) is

$$\sin \tfrac{1}{2}\beta_v = \frac{-h \cos \gamma_o + \sqrt{(h \cos \gamma_o)^2 + (\Delta R \sin \gamma_o)^2}}{\Delta R} \qquad (14)$$

It should be noted that Equations (13) and (14) are independent of $\Delta R_g$. $\Delta R_g$ can be found from $\beta_v$, h, $\gamma_o$, and $\Delta R$ by means of the law of cosines.

When $\Delta R_g$ is divided by the resolution length, it gives the number of samples each pulse must be divided into. This number, multiplied by the PRF (the number of pulses per second), gives the data rate. Alternatively, it is conventional to call the collection of corresponding samples from each received pulse one "range bin." The return in each range bin may be regarded as a sampled (at the PRF) azimuth "channel." So the product of the PRF and the number of range bins is the data rate. When the swath width is that corresponding to the maximum unambiguous slant range interval $\Delta R$, given by (12), the maximum data rate is obtained.

Figure 4 illustrates the orbital case. These curves were obtained following the arguments given above, assuming circular Earth orbits. The antenna was taken to be 4.5 meters long, leading to a resolution length of 2.25 meters. The parameter labeling the curves is the depression angle $\gamma_o$, ranging in 5-degree steps from $30^o$ to $60^o$.

One thing that is immediately noticeable is that the curves quickly approach asymptotic values for the data rate, independent of the altitude. Qualitatively, this is because the maximum swath width Rg increases slightly with altitude for a fixed $\gamma_o$ (this is a second-order effect, not seen in the small-angle approximation), while the circular orbital velocity--hence the PRF--decreases with altitude. For example, for $\gamma_o = 45^o$ the swath width is 63.05 km and the velocity is 7.56 km/sec assuming an altitude of 600 km, while for an orbit at an altitude of 1800 km the swath width is 68.31 km and the velocity is 6.98 km/sec.

An approximate analysis shows that the maximum data rate is, very nearly,

$$\text{maximum data rate} = \frac{c}{D_h \cos \gamma_o} \qquad (15)$$

Equation (15) does actually give the asymptotic values approached in Figure 4. It is interesting that this number does not depend on the range, even though the number of resolution cells (of linear dimension $D_h/2$) contained within the physical antenna beam does. Equation (15) also shows that, at one particular altitude, the data rate will be independent of the velocity v. (For instance, if the orbit is not circular, the data rate at one altitude will be the same as for a circular orbit,

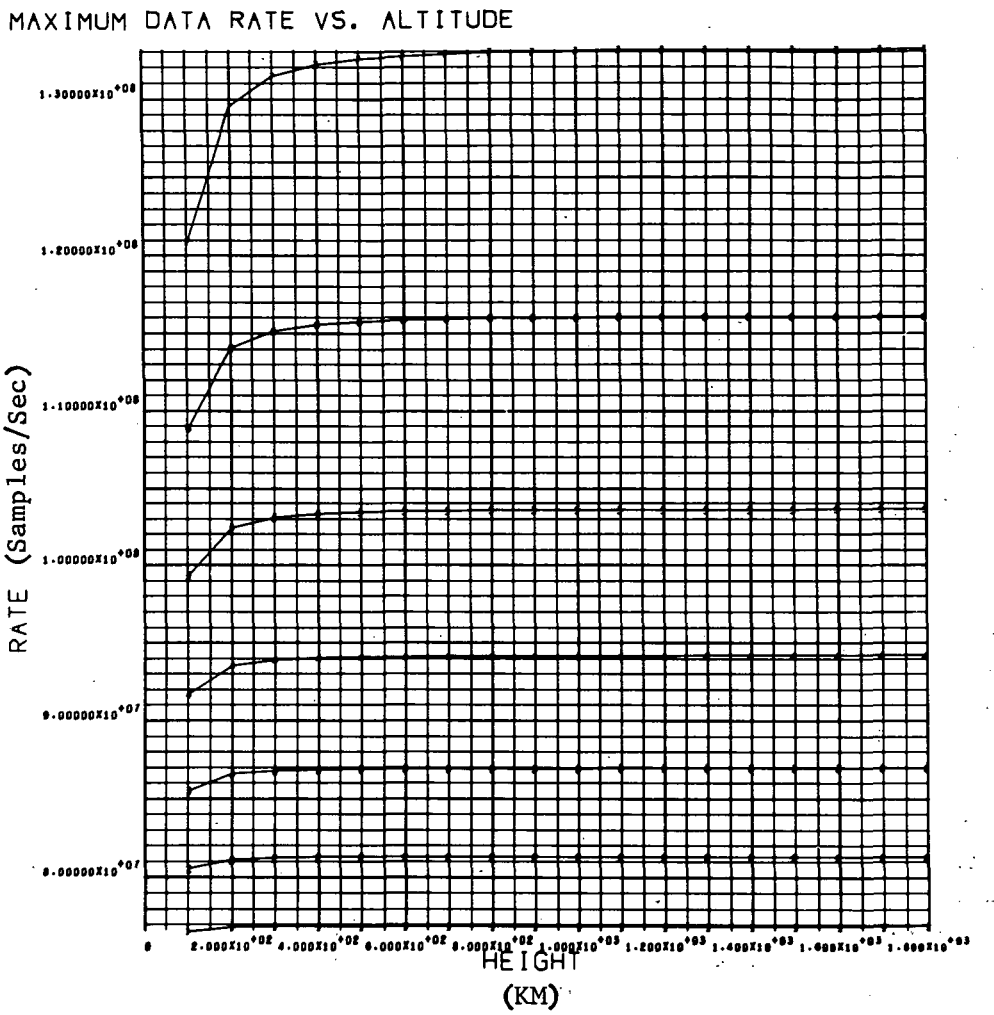


| Symbol | | $\gamma_0$ |
|---|---|---|
| 1 | ... | 30° |
| 2 | ... | 35° |
| 3 | ... | 40° |
| 4 | ... | 45° |
| 5 | ... | 50° |
| 6 | ... | 55° |
| 7 | ... | 60° |

Figure 4. Maximum Data Rate vs. Altitude for SAR in Circular Earth Orbit

although in general the velocity will be different--and it has been seen that the data rate in the orbital case is nearly independent of the altitude.) Also, if the PRF is increased from the value given by Equation (10), the achievable swath width is decreased by the same factor, leaving the data rate unchanged.

The curves shown in Figure 4 give maximum data rates both because they have been calculated for the very fine resolution inherent in the data (dictated by the signal's bandwidth) and because the maximum umambiguous swath width has been assumed. It has been seen that this swath width increases somewhat with altitude. If one carries out the calculations for a constant swath width, the data rate declines slightly with increasing altitude, in proportion with the orbital velocity. In practice, one would probably not attempt to achieve the maximum possible swath width, since this would very likely lead to problems with aliasing. The curves of Figure 4 show data rate upper bounds for all configurations of the system.

Some consideration will now be given to the handling of all this data. The processing may be done either on the ground or (if possible) on board. The extremely large data rate may preclude real-time transmission of the data to the ground as it is acquired, even if there is a receiving station in view. (Studies have shown that 5-bit words may be adequate to represent the data [9].) So some type of on-board storage will be required. (It will be seen that some type of storage is a part of any processing method.) One medium that is well suited for rapid and compact storage of great volumes of data is photographic film. Film storage is actually used for some airborne SAR systems [5,6]. The radar receiver output is used to intensity-modulate a cathode ray tube, the electron beam of which is swept in synchronism with the returning pulses. Successive range traces are recorded side by side on a film, which moves past at a speed proportional to that of the aircraft. The format of the film is shown in Figure 5.

Equation (11) shows that, assuming orbital speed and an antenna a few meters in length, the PRF is several thousand pulses per second. Making a reasonable estimate for data packing density of the order of hundreds of lines per cm for the CRT-film combination, it is clear that a substantial amount of film is used in storing the data received in a fairly short time. Similar conclusions are reached for other storage media, such as magnetic tape, disc, etc.

It appears that transmission of the raw data to the ground in real-time may be impractical. Storage of a large quantity of data is also not practical. Recording of data to be played back at a slower rate, thereby requiring a narrower-bandwidth telemetry link, can only be done to a limited extent, because of its storage requirement.

The basic difficulty is the high resolution inherent in the data, equivalently expressed in terms of its wide bandwidth. If it were possible to degrade the resolution of the data in real time, by some form of

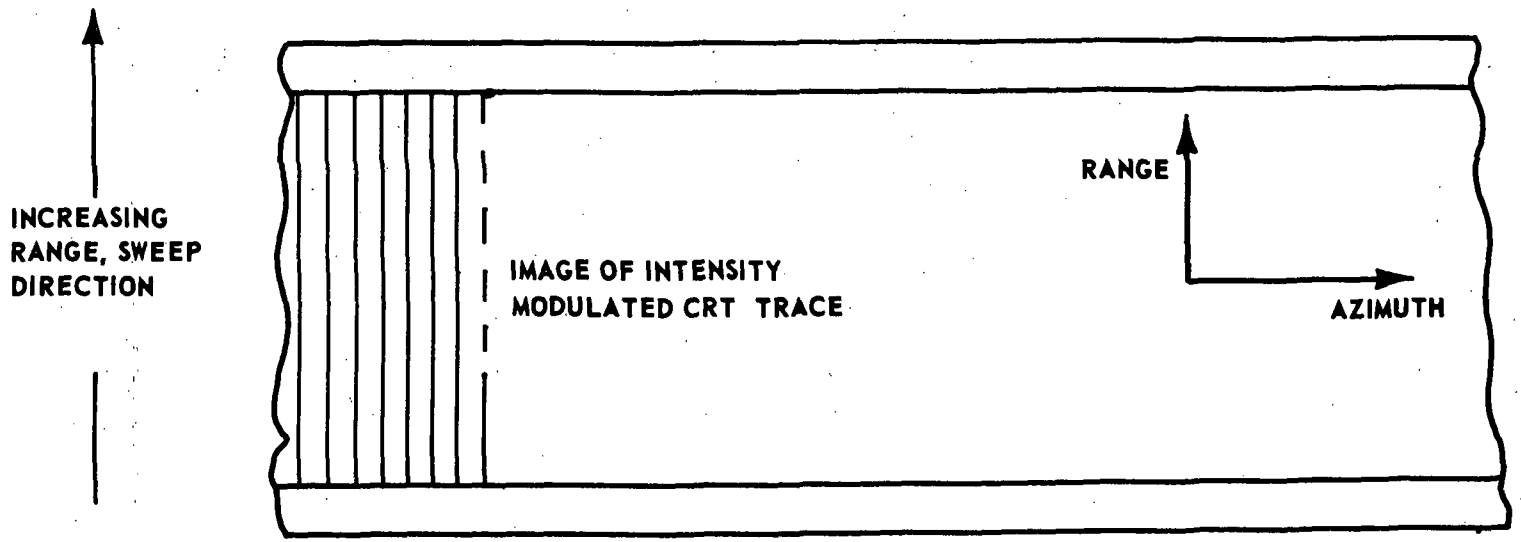


FIGURE 5. RADAR DATA FILM FORMAT

processing, the resulting reduced-resolution imagery could be transmitted in real time over a (relatively) narrow-band telemetry link. Such a procedure might effectively remove any restriction on the amount of time a satellite-borne SAR system could be operated.

A numerical example may be helpful. Since the results are essentially independent of altitude, any convenient altitude will do. The Skylab altitude, 435 km, will be used. The circular orbital velocity for this altitude is 7.65 km/sec. So 7.65 km is the along-track distance covered in 1 second; this is 3400 resolution lengths (pulses) with a 4.5 m antenna. If the depression angle is $45^{o}$ the maximum unambiguous swath width is 62.26 km, or 27670 resolution lengths. So the total number of picture elements (pixels) in the corresponding image is $3400 \times 27670 = 94.06 \times 10^{6}$. Since this is the amount of data received in 1 second, this number is the data rate. If, as stated above, 5-bit words are adequate, $470.3 \times 10^{6}$ bits/second is the required capacity for a real-time telemetry channel.

This value is so high that it is clearly advisable to consider means of reducing it. A resolution of 2.25 m is far better than is actually needed for most applications. (Noise, nonlinearities, and other errors would prevent its achievement in any case.) If the resolution is reduced to 25 m, the "1-second picture" is 306 resolution lengths long and 2490 wide; the data rate is $0.762 \times 10^{6}$ samples/second or $3.81 \times 10^{6}$ bits/second. If a swath width less than the maximum is used, the data rate is further reduced.

The reduction just described is for the final data rate, after processing. This is not the same as the data rate into the processor. The bandwidth (hence the data rate) in the "range channel" can be reduced, for instance by increasing the pulse width. However, in a single range bin, the azimuth Doppler bandwidth is determined simply by the width of the antenna beam. The sampling rate in the "azimuth channel"--the PRF--must be large enough to adequately represent a signal with this bandwidth; the magnitude is given by Equations (10) and (11). For the example given above, the data rate into the processor (for 25 m resolution) is $8.466 \times 10^{6}$ samples/second, equivalently $42.33 \times 10^{6}$ bits/second. The reduction to the final rate of $0.762 \times 10^{6}$ samples/second is achieved effectively by sampling the <u>output</u> of each azimuth channel (range bin) in the processor.

In general, degradation of the resolution by a factor Q decreases the data rate into the processor by the same factor. The number of resolution elements in the image, and the data rate out of the processor, is reduced by $Q^{2}$. The latter quantity is shown in Figure 6, which plots data rate (final) vs. resolution for the same values of $\gamma_{o}$ as in Figure 4. The curves were computed for the Skylab altitude, although Figure 4 indicates the results should also be valid for other (particularly higher) altitudes. The data rates in Figure 6 are also maximum, in the sense that they were computed for the maximum unambiguous swath width. It is seen that, for a resolution of 25 m, the data rate is near (generally under) $10^{6}$ samples/second for all the depression angles considered.

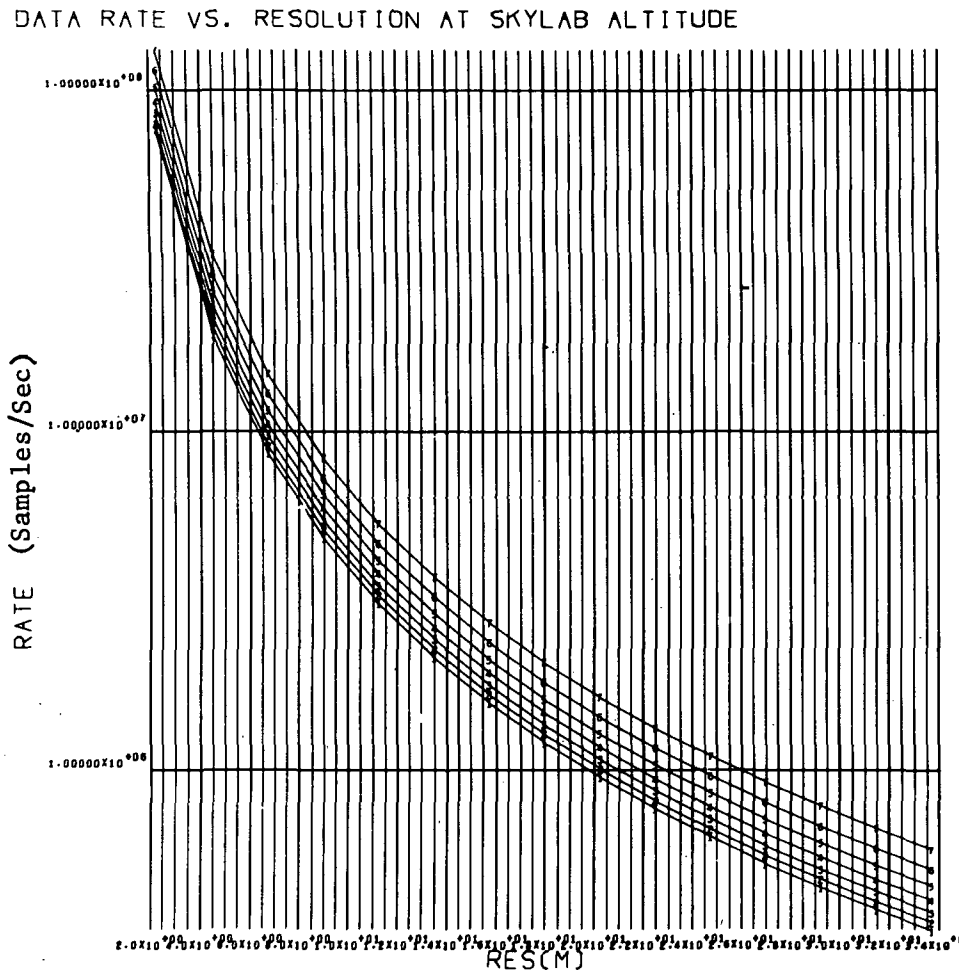


| Symbol | | $\gamma_0$ |
|---|---|---|
| 1 | ... | 30° |
| 2 | ... | 35° |
| 3 | ... | 40° |
| 4 | ... | 45° |
| 5 | ... | 50° |
| 6 | ... | 55° |
| 7 | ... | 60° |

Figure 6. Maximum SAR Data Rate vs. Resolution at Skylab Altitude

## C. Processing Techniques

One may consider processing the raw data acquired by a synthetic aperture radar on a satellite either on board on on the ground. If on-board processing is employed, conceivably it could be real-time or delayed, slower than real time. Some of the implications of real-time on-board processing, if it should be found possible, have been discussed. In this case, of course, film may not be used for intermediate storage. In any of the other instances, film storage is a possibility. The reasons for its use in current airborne SAR systems must be considered.

If film is the storage medium, it makes sense to consider doing the entire processing using optical elements. It is possible to construct a form of optical analog computer, using coherent light (e.g., a laser), which can do the job [4]. The basic operation, mathematically the same as pulse compression, can be done by a lens [7]. In fact, it could be done in range and azimuth simultaneously by optical means (rather than doing the range compression separately in the radar receiver). And there are other apparent advantages to optical processing. The processing in azimuth, which is a convolution with the impulse response of the matched filter, may equally well be thought of as a correlation with a reference function, the response of the system to a point target. The correlation in each range bin is different; the processing is range-dependent. Such a multichannel requirement can be readily met by an optical system. Optical processing systems are discussed in later sections of this report.

In Section IV it will be seen that the SAR optical processor consists of film transports and lenses, and a source of coherent light. The fact that the processing can be done by lenses (i.e., the reference function has the properties of a lens) carries a very interesting implication, for a lens does not create images but only transports an image to a new position (e.g., from infinity to a nearby plane). Then the fine-resolution image must exist even if the lenses are removed. Cutrona et al [4], Harger [5], and Rihaczek [6] show that the radar data film is an array of one-dimensional holograms or Fresnel zone plates in azimuth. (That they are sampled is unimportant, since we have assumed that the PRF is high enough to satisfy the requirements of the sampling theorem.) The optical processor is a very elegant solution to the SAR processing problem. In Section IV it will be seen how simple the optical processor is. Also, there is a striking similarity between the coherent radar system that acquires the data and the coherently illuminated processor that converts the data to a radar image; the optical processor carries out its calculation by physical operations that very closely mimic the actual generation of the radar data from the terrain.

Despite the aforementioned advantages, there are several disadvantages to using film recording and optical processing in an orbiting satellite application. One of these is logistical. The Blue Book [14] specifies an optical recorder in which 70 mm film is driven at the rate of 15 cm/sec. This equivalent to about 30 ft/min. An earlier edition of the Blue Book

described 70 mm cartridges containing 4000 feet of film, weighing about 60 pounds. This would be enough film for about 133 minutes of data. (These figures are consistent with weight-length data in the new Blue Book.) Now, one of the proposed uses of the synthetic aperture radar system mentioned in the Blue Book is to collect data for use in worldwide land use mapping. It is easy to see that this application could use up film very quickly. Since it may be desired to obtain measurements on the same regions with different polarizations, the consumption of film per unit of land area could be very high. In addition to the film itself, film processing equipment and chemicals may be needed to avoid the risk of transporting undeveloped film to the ground and losing large quantities of data accidentally.

Another possible disadvantage is in the operation of an optical processor. This instrument may be needed on board whether or not film recording of the data is used. Prof. R. K. Moore of the University of Kansas [15] maintains that it would require less film to record the original data on tape and use a CRT display of the data as input to an on-board optical processor, than to simply record the data on film and process it on the ground. The optical processor requires a vibration-free environment, careful handling, and precise adjustment. Its operation might require an astronaut to be specially trained.

Other problems can be envisioned (e.g., lens aberration, film grain, nonuniform film emulsions, etc.); it is clearly worth assessing the possibility of processing by some other means. Then the best combination of techniques for the mission could be chosen. Digital processing is a natural candidate. Harger [5], who gives the matter only cursory attention, concludes that digital processing is impossible. Gerchberg [9], who considers the problem carefully and in detail, feels that digital processing is quite possible using a special-purpose computer. It turns out, remarkably, that speed is not the basic problem. Analog-to-digital conversion, and storage and power requirements, cause the greatest difficulty. Digital processing would permit great flexibility, including using a method (called "subaperture processing" by Gerchberg [9]) for preventing the graininess that occurs in an image produced by coherent illumination. Processing for reduced resolution could reduce the data rate sufficiently to permit real-time telemetry of the final image to the ground. Because of the nature of the operations performed, it may be possible to use the "special-purpose" SAR processor in other applications. Research in this area may yield results in apparently unrelated fields.

## SECTION III. MATHEMATICAL THEORY OF SAR DATA PROCESSING

### A. Summary of Previous Results

In this section the mathematics of the processing to attain improved azimuth resolution is discussed. The order of magnitude of the data rate has been obtained, and this number's influence on the choice of the physical realization of the processor was discussed in the last section. The nature of the processing will now be explored.

For convenience, some pertinent equations derived previously are reproduced here. If a point target on the ground is assumed to be illuminated by a monochromatic electromagnetic wave of frequency $\omega_o$, then the phase modulation of the reflected signal received by the radar antenna, due to the relative motion between the scatterer and the antenna, is

$$\phi(t) = -\left[\frac{4\pi R_o}{\lambda} + \frac{2\pi v^2}{\lambda R_o} t^2\right], \quad |t| < \tfrac{1}{2}T \tag{16}$$

where

$R_o$ = component of radius vector from radar to target normal to direction of relative motion

$\lambda$ = wavelength of radiated beam

$v$ = relative velocity

$t$ = time

$T$ = length of time over which the target is in the beam (and reflected signal is received)

Equation (16) describes a <u>linearly frequency modulated</u> (linear FM) pulse. The Doppler bandwidth of this pulse is

$$\Omega = \frac{4\pi v^2 T}{\lambda R_o} \text{ radians} \tag{17}$$

(This statement will be considered more carefully in the next sections.)

The azimuth (along-track) resolution that, in principle, can be achieved by the synthetic aperture radar (SAR) processing is

$$\rho_a = D_h/2 \tag{18}$$

where $D_h$ is the length of the antenna in the along-track direction. The minimum pulse repetition frequency required to adequately sample the signal in the along-track direction is

$$PRF = \frac{2v^2T}{\lambda R_o} \tag{19}$$

The time between azimuth samples is the reciprocal of the PRF. Making use of the kinematical and geometrical relationships involved in the problem, the result is

$$\text{time between samples} = \frac{D_h/2}{v} \tag{20}$$

The slant range (along the radius vector) interval that can be unambiguously mapped, in units of the resolution length, is a number inversely proportional to vehicle velocity:

$$\frac{2\Delta R}{\rho_a} = \frac{c}{v} \tag{21}$$

where c is the speed of light. It has been seen that this establishes an upper limit on the quantity of calculations in the processing.

In the remainder of this section, some special properties of the linear FM signal are discussed, and it is shown how these properties make possible the processing to improve azimuth (along-track) resolution. The mathematical operations involved in the SAR processing are considered. Also, it is shown that the total signal processing may be considered to involve independent range and azimuth "channels" (it is the latter that is referred to as "SAR processing"). The groundwork is laid for the detailed discussion of digital processing of the signal.

## B. The Received Signal

The spectral characteristics of the linear FM signal have been considered by several authors, among them Harger [5] and Gerchberg [9]. These references show that one of the most useful parameters in the study of the SAR signal and its processing is the time-bandwidth product (TBP) of the signal. Strictly speaking, the bandwidth of a signal should be some measure of the nonzero extent of the signal's spectrum. Since, in general, the spectrum of a signal is not identically zero outside a particular range, "bandwidth" must be interpreted as the frequency range over which the Fourier transform of the signal attains "significant" values, such that outside this range the spectral magnitude is "negligible."

A concept which is intuitively appealing is that of instantaneous frequency: The time derivative of the phase of a sinusoidally varying

signal. The phase of the linear FM signal of interest here is given by (16). The instantaneous frequency (given by Equation (4)) is seen to be a linearly varying function of time; thus the name "linear FM." Equation (17), the bandwidth, is seen to be identical with the difference of instantaneous frequencies at $t = -T/2$ and $t = +T/2$. That this actually gives the bandwidth is an important characteristic of the SAR signal.

The (linear FM or "chirp") signal whose phase is given by (16) has finite duration. The exact value depends on the way in which one defines duration; however, the signal vanishes outside $-T/2 < t < T/2$, so the duration is "nominally" T. A waveform of finite duration, in general, has associated with it a finite bandwidth containing most of the signal's energy, and the time-bandwidth product has a minimum value of the order of unity (depending on how time and bandwidth are defined). The expression of this relationship is termed by Papoulis [12] the uncertainty principle; it is entirely analogous to the uncertainty principle in quantum theory.

Gerchberg [9] considers the hypothesis that, by processing a waveform of large TBP, it may be possible to reduce the waveform's duration or its bandwidth by the inverse of its bandwidth or duration, respectively, or even to reduce both simultaneously. An examination of the details of the proof of the uncertainty principle reveals two important facts:

1. The minimum bandwidth pulse (among all pulses with the same amplitude dependence) has no nonlinear phase term $\phi(t)$ in its modulation; and

2. The minimum rms signal duration for a given amplitude spectrum is achieved when the associated phase function $\theta(f)$ in the frequency domain is linear or constant.

The conclusion is that passage of the signal through a filter that removes the nonlinear phase of the waveform's spectrum minimizes the time-bandwidth product of the output signal, and the duration of the output signal is less than that of the input signal by the TBP of the latter. The two questions which must now be considered are what the precise mathematical form of the filter is and how the filtering can be achieved--that is, how the signal is processed.

## C. Matched Filtering and the Linear FM Signal

In the foregoing discussion, essentially the impulse response of a radar--its response to a point target--was discussed. It would seem desirable to have the processing of this return, to form an image of the point target, produce as narrow a pulse as possible. Suppose the impulse response $f(t)$ has Fourier transform $F(\omega) = A(\omega)e^{i\theta(\omega)}$, where A and $\theta$ are each real functions. Then the ideal filter would appear to be an

inverse filter, one whose frequency-domain response is

$$G(\omega) = 1/F(\omega) = A^{-1}(\omega)e^{-i\theta(\omega)} \tag{22}$$

When the input to such a filter is $f(t)$, its output is a constant in the frequency domain, and a Dirac delta function (impulse) in the time domain.

Thus, it appears that a synthetic aperture radar could locate a point target with no error. This sort of result is never possible with physical systems, and the reason is usually the presence of random noise. Neglecting random noise *is* the main defect in the above argument. The spectrum $F(\omega)$ of any physical signal $f(t)$ approaches zero in magnitude at large frequencies, so the gain of the inverse filter $G(\omega)$ must become indefinitely large at large frequencies. This may be impossible to achieve with a real filter, but, even if it were, it would not be desirable. The noise component that is present along with the signal has a spectrum which extends over all frequencies; so in the output from an ideal inverse filter, the signal would be swamped by noise.

A modification of the inverse filter is needed that, while keeping the output signal component as close to an impulse as possible, suppresses the noise outside the signal spectral band. Since the spectral phase of random noise is random, there is nothing to be gained by modifying $\theta(\omega)$ in (22). One amplitude function which is large at frequencies where the signal is large compared to the noise, and small where the S/N is small, is $A(\omega)$ itself. Therefore, a reasonable choice for the filter seems to be one with the characteristic

$$H(\omega) = A(\omega)e^{-i\theta(\omega)} = F^*(\omega) \tag{23}$$

$H(\omega)$ is a matched filter [13] for the signal with spectrum $F(\omega)$. Harger [5] presents extensive arguments to show that a good processing scheme for SAR is one employing a matched filter.

It will be pedagogically easier to approach the SAR signal and its processing in stages. First consider the transform relationship

$$s_1(t) = e^{-ikt^2} \longleftrightarrow S_1(f) = \sqrt{\frac{\pi}{k}}\, e^{i\pi f^2/k}\, e^{-i\pi/4} \tag{24}$$

The double-headed arrow is used to indicate that $s_1(t)$ and $S_1(f)$ are a Fourier transform pair, and $f = \omega/2\pi$ is frequency.

The infinite time-bandwidth product linear FM signal corresponding to (16) is

$$s_2(t) = \exp\left[i\left(2\pi f_o t - \frac{2\pi}{\lambda R_o} v^2 t^2 + \phi_n\right)\right] \tag{25}$$

where $f_o$ is the carrier frequency and $\phi_n$ is an arbitrary phase angle, involving the phase of the transmitted signal, the round-trip propagation delay, the shift in phase due to the electrical properties of the target, and possibly other factors. Making use of well-known properties of the Fourier transform [12], it can be seen from (24) that

$$s_2(t) \longleftrightarrow S_2(f) = \frac{1}{v} \sqrt{\frac{\lambda R_o}{2}} \exp\left[ i \frac{\pi \lambda R_o}{2v^2} (f-f_o)^2 \right] \exp\left[ i(-\frac{\pi}{4} + \phi_n) \right] \quad (26)$$

Two symmetries between the time and frequency domains of the infinite TBP linear FM signal may immediately be seen from (26):

1. In both domains the amplitude is constant.

2. In both domains there is a quadratic phase factor.

Since it is plausible that what is true of an infinite TBP signal is at least approximately true of a similar large TBP signal, the study of the waveform (25) will be continued.

The spectrum of a frequency-modulated signal is quite complex, in general. Since the frequency modulation is the shift of the instantaneous frequency (defined in the preceding section) away from the carrier frequency, one feels that instantaneous frequency should be a meaningful parameter in the study of FM signals. Rihaczek [6] introduces the device of assuming that an arbitrary signal is the result of passing a signal with a zero-phase spectrum of the proper shape through an all-pass filter with the desired spectral phase function. He finds that, if the zero-phase spectrum at the filter input is subdivided into spectral bands over which the filter phase is linear, the energy of each band will appear delayed by the <u>group delay</u> $\tau_g(f)$ at the filter output, represented by rf fluctuations of instantaneous frequency $f_i=f$, the center frequency of the band. The definition of group delay is

$$\tau_g(f) = -\frac{1}{2\pi} \frac{d\theta(f)}{df} \quad (27)$$

where $\theta(f)$ is the spectral phase function. Group delay is seen to be just the dual (in the Fourier transform sense) of instantaneous frequency. The pulse containing the energy of a particular band lasts for approximately $1/\Delta F$, where $\Delta F$ is the width of the band. The above approximation is good to the extent that the phase function can be assumed linear over the band.

So, in some cases, instantaneous frequency can be used to describe the spectrum of a signal. Parseval's theorem [12] shows how the energy

of a signal is divided among its frequency components, but it does not say anything about time-ordering. However, if the group delay is a monotonic function of f, so a given value of $\tau_g(f)$ is associated with only one frequency, then the above argument shows that the frequency f of the spectrum becomes the instantaneous frequency $f_i(t)$ of the signal at a time equal to the group delay. Formally,

$$f_i(t) = f \quad \text{for} \quad t = \tau_g \tag{28}$$

or

$$\frac{d\phi(t)}{dt} = 2\pi f \quad \text{for} \quad t = \tau_g \tag{29}$$

where $\phi(t)$ is the signal's phase function (in the time domain).

Next, considering the inverse problem, Rihaczek shows that, if the (temporal) phase of a signal is linear near $t=t_1$, the energy within the original time "band" at $t=t_1$ is concentrated at $f=f_1$, which means that $t_1$ plays the part of group delay for a frequency $f=f_i$.

$$\tau_g(f) = t \quad \text{for} \quad f = f_i \tag{30}$$

or

$$\frac{d\theta(f)}{df} = -2\pi t \quad \text{for} \quad f = f_i \tag{31}$$

Equations (29) and (31) are a link between the phases in the time and frequency domains. Formally inverting (28) and (30), and making the indicated substitutions, yields

$$\tau_g(f) = f_i^{-1}(f) \tag{32}$$

$$f_i(t) = \tau_g^{-1}(t) \tag{33}$$

which show that instantaneous frequency and group delay are inverse functions of each other.

When these considerations are applied to the linear FM waveform, some particularly simple results are obtained. One of the key properties of this signal is its symmetry in time and frequency. From (25), the instantaneous frequency of the modulation is linear in time,

$$f_i(t) = -\frac{k}{\pi} t \tag{34}$$

where the quadratic phase term in (25) has been written $e^{-ikt^2}$, $k = \frac{2\pi v^2}{\lambda R_o}$. From equations (33) and (28), it can be seen that the group delay is

$$\tau_g(f) = -\frac{\pi}{k} f \tag{35}$$

(This result could also have been obtained from (26).) One motivation for developing the foregoing arguments was the hope that they could be used to adapt (26) to give the spectrum of a finite time-bandwidth linear FM signal. Let the complex envelope of this (finite TBP) signal be

$$s(t) = a(t) e^{i\phi_i} \; e^{-ikt^2} \tag{36}$$

where a(t) is the real envelope of the pulse. The spectrum should be, approximately,

$$S(f) = \sqrt{\frac{\pi}{k}} \; e^{-i\pi/4} \; a(-\tfrac{\pi f}{k}) \; e^{i\phi_i} \; e^{ik(\frac{\pi f}{k})^2} \tag{37}$$

Now let us return to considering synthetic aperture radar. Assuming an (idealized) antenna beam with constant gain over its extent in the along-track direction, and disregarding the slight amplitude change in the return signal due to the changing slant range as the beam is swept by the point target, that signal is

$$s(t) = A \; \text{rect} \; (\tfrac{t}{T}) \; e^{i\phi_o} \; e^{-ikt^2} \tag{38}$$

where rect $(\frac{t}{T})$ is the rectangle function:

$$\text{rect} \; (\tfrac{t}{T}) = \begin{cases} 1 & \text{for} \quad |t| < \frac{T}{2} \\ 0 & \text{for} \quad |t| > \frac{T}{2} \end{cases} \tag{39}$$

The exact spectrum of (38) is

$$S(f) = A \exp\left[i\pi(TB)\left(\frac{f}{B}\right)^2\right] e^{i\phi_o} \left\{ C\left[\sqrt{2TB}\left(\frac{f}{B} + \frac{1}{2}\right)\right] - C\left[\sqrt{2TB}\left(\frac{f}{B} - \frac{1}{2}\right)\right] - iS\left[\sqrt{2TB}\left(\frac{f}{B} + \frac{1}{2}\right)\right] + iS\left[\sqrt{2TB}\left(\frac{f}{B} - \frac{1}{2}\right)\right]\right\} \quad (40)$$

where the nominal bandwidth B is (cf. Equation (17))

$$B = \frac{k}{\pi}(t_{end} - t_{start}) = \frac{k}{\pi} T \quad (41)$$

and C(t) and S(t) are the Fresnel integrals. Graphs in References 6 and 9 show how well the amplitude of the sum of Fresnel integrals approximates a rectangle and how well the phase of this sum approximates $\pi/4$. The agreement improves with increasing TB, and the approximation is acceptable when TB $\gtrsim$ 10.

Because of the relationship between phase in one domain (time or frequency) and extent in the other, and because group delay depends on frequency in the same way that instantaneous frequency depends on time for the large TBP linear FM signal, one might expect the envelopes in the two domains to have similar shapes in general, not only for rectangular envelopes. Gerchberg [9] considers the second derivatives of the phase functions and, in doing so, establishes this result.

The linear FM signal is an example of a pulse compression waveform [5,6,9]. A commonly used radar signal (not only for SAR) is a periodic sequence of pulses that are phase modulated with a quadratic function of time--i.e., linear FM--with the aim of "compressing" the pulses to enhance resolution. Thus a synthetic aperture radar, whose point target response (in the azimuth or "sweep" direction) is a linear FM waveform, may use pulses which are themselves linearly frequency modulated in order to enhance cross-track resolution. The processing of SAR returns may amount to a two-dimensional pulse compression.

Four central points pertaining to the processing of large time-bandwidth product pulses which have been obtained are the following:

1. There is a minimum time-bandwidth product for a pulsed signal.

2. For a given waveform amplitude distribution in the time domain, any nonlinear phase function in time will increase the nominal and the rms bandwidth of the signal.

3. For a given waveform amplitude distribution in the frequency domain, any nonlinear phase function in frequency will increase the nominal and the rms time duration of the signal.

4. For linear swept FM pulse compression signals (time-bandwidth products > 10) the signal envelope in one domain will mimic the signal envelope in the inverse (transform) domain. The signal phase will be quadratic in both domains as well.

It is possible to "compress" the signal in time and achieve the minimum TBP by removing the nonlinear phase of the signal's spectrum with a matched filter (see Equation (23)). Some intuitive feeling for the effect of matched filtering can be obtained by examining Equations (26) and (35). Removal of the nonlinear phase could be thought of as compressing the signal in the time domain by forcing all the frequency components to have the same group delay.

Before considering possible methods of performing the processing, a few more observations will be made. Because of the envelope-mimicking property of the linear FM transform pair, the amplitude spectrum of the signal (38) is itself a rectangle function, of extent proportional to T. After the nonlinear spectral phase is removed by the matched filter, the spectrum (of the matched filter output) is that of a sinc function--$\sin \pi x/\pi x$. The wider the extent in the frequency domain--proportional to T--the narrower is the principal lobe of the sinc function. Since T is increased by making the radar antenna shorter, thereby increasing its beamwidth, a primary result of Section II, that resolution length is proportional to antenna length, has been derived in another way.

In addition to the central peak, the sinc function has sidelobes. It then follows that two targets that are separated in time by the interval between the peak of the main lobe and that of the first sidelobe of the matched filter response may be interpreted as a single target, especially if one target's reflection coefficient is much greater in magnitude than the other's. This is another aspect of the radar ambiguity problem that was mentioned previously. This problem will not be considered in any detail here; it is studied at length in the literature [5,6,9].

One may wish to reduce the ambiguous response of the matched filter to signals outside the main response lobe by some form of additional filtering. There is an extensive literature on optimum aperture weighting. The cost of sidelobe reduction is an increase in the width of the main lobe, i.e., decreased target resolution. Because of the envelope-mimicking property of the linear FM waveform, the filtering for sidelobe reduction may be done either in the time or the frequency domain. The considerations of this paragraph are discussed in Reference 9 and much more extensively in Reference 6.

## SECTION IV. OPTICAL AND DIGITAL SAR SIGNAL PROCESSING

Sections I and II of this report are mainly descriptive. They introduce synthetic aperture radar, discuss the synthetic aperture principle and derive some basic results concerning resolution, signal characteristics, and data rate. Bounds on the data rate for the orbital case are obtained, and possible methods of performing the synthetic aperture processing are sketched. Section III is a detailed exposition of the mathematical theory of SAR data processing. It is seen that the algorithm is cross-correlation of the signal in each range bin with an appropriate reference function. This is equivalent to mathematically simulating a long array antenna--or synthetic aperture--by storing the received data, properly weighting (amplitude and phase) the returns from sequential locations of the physical antenna, and coherently summing them.

This section will present a more detailed investigation of possible processing methods than was given previously. It will be seen that the necessary phase shifting is that required to compensate for the difference in path lengths from a point on the ground to successive locations of the antenna--the situation is similar to focusing by a lens. The optical analogy provides useful insight into SAR processing.

The two basic methods discussed in this section are coherent optical processing and digital processing. The theory of coherent optical processing will be developed, and it will be shown how the necessary operations can be performed by such a system; this is the state-of-the-art method. The requirements for digital processing, and the conceptual basis of several potential approaches to the design of a real-time SAR digital processor will be discussed.

First, the SAR optical processor will be considered. The basic physical principles, and some details of optical processing in general, are reviewed in Appendices A and B.

### A. Optical Processing of Synthetic Aperture Radar Signals

1. The Radar Signal. The principles discussed in Appendices A and B will now be applied to the processing of synthetic aperture radar signals. Typically, the return signals are synchronously demodulated and used to intensity-modulate a cathode-ray tube electron beam, the beam being swept vertically during the time interval of interest after each transmitted pulse. The traces are recorded on a film drawn past the screen with horizontal speed $v_f$. If x is used to denote the coordinate along the film (horizontally) and y is the coordinate across the film, the recording consists of the returns from each successive pulse, placed side by side. On the film, x is related (proportional) to the along-track

or azimuth coordinate of the target scene, and y is related to the cross-track or range coordinate. This format is shown in Figure 5. If the film is properly exposed and developed, the amplitude transmission function is given by

$$t(x,y_1) = t_b + \chi \sum_n \left| \vec{\sigma}_n(x_n, r_1) \right|$$

$$\times \cos\left[ 2\pi f_x x - \frac{4\pi r_1}{\lambda_r} - \frac{2\pi}{\lambda_r r_1} \left( \frac{v_a}{v_f} x - x_n \right)^2 + \phi_n \right] \quad (42)$$

along a line $y=y_1$ on the film [21]. This is a composite of the elementary signals described by Equations (16) and (38). In this expression $t_b$ and $\chi$ are constants which permit the recording of a bipolar video signal as a transmission function between 0 and 1, and the sum is over the returns from all the point targets at slant range $r_1$, corresponding to $y_1$ on the film. The quantity $\vec{\sigma}_n$ is a complex amplitude factor for the reflected (and received) signal from the nth point target, $f_x$ is the spatial-frequency analog of the residual carrier frequency after demodulation, $\lambda_r$ is the wavelength of the radar carrier, $v_a$ is the speed of the platform carrying the radar, $v_f$ is the horizontal velocity of the signal film during recording, and $\phi_n$ is the phase associated with $\vec{\sigma}_n$. (Strictly speaking, each point target return should be multiplied by a rectangle function which is nonzero only over the interval during which the target is in the antenna beam or, more generally, by the antenna gain pattern. However, inclusion of these factors would only have a complicating effect on this discussion.)

2. Coherent Optical Correlation. The processing which must be performed consists of correlating the recorded signal in each range bin with a "reference function," equivalent to the return from a single point target [27]. The multichannel cross-correlation operation can be performed fairly easily with a coherent optical processor. The three elementary mathematical operations needed for cross-correlation are multiplication, integration, and displacement of one function relative to the other; the optical techniques for doing these operations are discussed in Appendix B. Figure 7 shows such a processor. Imaging of the transparency r (the reference function) onto g (the signal, recorded as a photographic transparency) produces the multiplication. The Fourier-transforming property of lenses is utilized to perform the integration. The signal g is placed in the front focal plane of lens $L_3$, and r is imaged onto g. Then the Fourier transform of the product rg appears in the back focal plane of $L_3$. If our observation is confined to the axial point in this plane, the Fourier transform becomes a simple integration. Thus a pinhole is placed on axis and the illumination in the pinhole is continuously photographed as the signal record moves through the aperture.

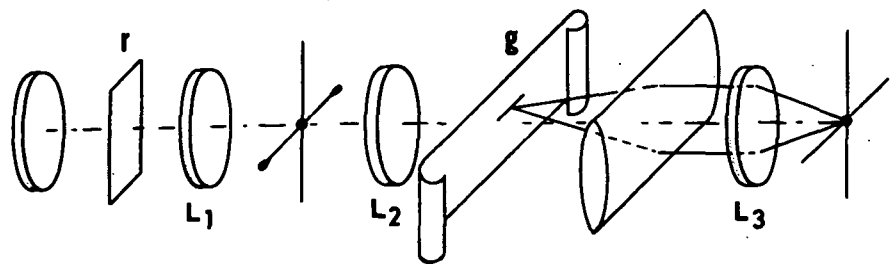


FIGURE 7. A COHERENT OPTICAL MULTICHANNEL CROSS-CORRELATOR (FROM REFERENCE 27)

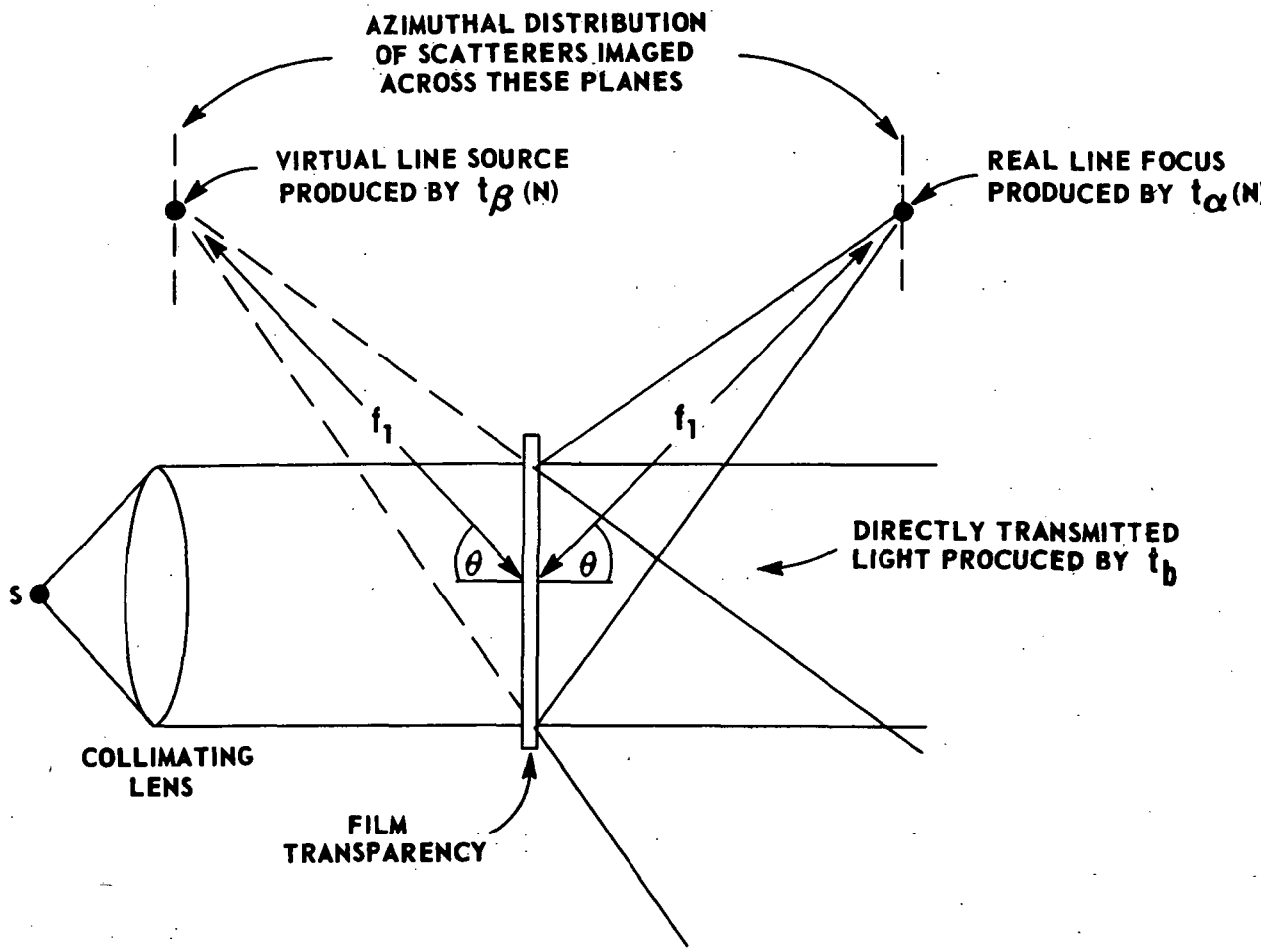


FIGURE 8. LIGHT TRANSMITTED BY THE LINE $y = y_1$ OF THE FILM TRANSPARENCY (FROM REFERENCE 21)

This is one form of optical correlator. However, upon closer examination, some problems arise. As mentioned in Appendix B, both the signal and reference function must be written about a bias or gray level, since film density is restricted to positive values. Let $r_o$ and $g_o$ be the signal and reference functions, respectively, and let $\circledast$ stand for the operation of cross-correlation. The consequence is that the optical processor calculates $(r_b + r_o) \circledast (g_b + g_o)$ instead of $r_o \circledast g_o$, where $r_b$ and $g_b$ are the required bias terms. The three extraneous terms must be prevented from interfering with the desired result.

3. The SAR Optical Processor. The fact that lenses produce Fourier transforms in coherent optical processors can be used to solve this problem. The spatial-frequency spectrum of $r_b + r_o$ is displayed at the back focal plane of lens $L_1$. Since $r_b$ is a constant gray level, its spectrum is a bright spot on axis, while $r_o$, having no zero-frequency component (because of the "carrier" $f_x$), is displayed as two distributions of light symmetrically placed about the axis. So a stop on axis--in effect, a high-pass filter--removes $r_b$, consequently removing two terms. (One of those two, $r_b \circledast g_b$, would have been the largest of the four.) The third extraneous term, $r_o \circledast g_b$, vanishes because $r_o$ and $g_b$ have non-overlapping spectra.

The solution of this problem still leaves another important one. There is a severely large light attenuation loss in this system. About half the incident light is absorbed by the reference-function transparency, and most of the transmitted light is removed by the zero-frequency stop in the back focal plane of lens $L_1$. Perhaps only 0.001% of the light incident on $r_o$ reaches the output slit [27].

Correction of this shortcoming is possible, using a different approach to the optical processing. Field amplitudes, rather than intensities, are dealt with in coherent optical systems. Well-defined phase relationships exist between the fields in different parts of coherent systems. So it is meaningful to think of adjusting signal phases as well as amplitudes (this is alluded to in Appendix B). The reference function $r_o$ is, effectively, one term in the summation of Equation (42). Neglecting the (arbitrary) constant phase term, the reference function is (proportional to)

$$r_o = \cos(2\pi f_x x - \phi)$$

$$= \tfrac{1}{2} \exp\left[i(2\pi f_x x - \phi)\right] + \tfrac{1}{2} \exp\left[-i(2\pi f_x x - \phi)\right] \quad (43)$$

where $\phi$ is the quadratic term. (The bias $r_b$, which is not wanted anyway, has not been written.)

Expanding the cosine in terms of complex exponentials emphasizes that the representation of the reference function as a real transparency contains

a redundancy; its spectrum has conjugate sidebands. Inspection of the two terms in the argument points the way to the solution of the problem. The first term represents a linearly increasing phase shift--that is, its effect is simply to bend the light rays a constant amount and change the direction of propagation of the wavefronts. It is clearly not needed. This leaves only the second term. The reference function which has been arrived at is purely a phase-adjustment function; if it can be realized, the large light attenuation due to absorption by the reference-function transparency would be completely eliminated. (Also, since there is no longer a bias term, the light lost by filtering out this term also would not occur.)

A variable phase shift can be produced by a lens. Since the refractive index of glass is different from that of air, different parts of the incident wavefront have their phases retarded by different amounts, depending on the thickness of the lens. Only the proper form of the lens (or lenses) now needs to be determined.

It has been seen that the mathematics of the necessary SAR processing is easily formulated in terms of complex functions. It was shown in Section III that the desired processing in azimuth consists of removal of a nonlinear phase. This is the same result that has been obtained here in a different way.

From the form of Equation (42), it appears that the required phase shift of the lens is a quadratic function of x. In Appendix B it was shown that, aside for a constant phase delay, the multiplicative effect of a spherical lens on a normally incident plane wave--the amplitude transmission function of the lens--is

$$t(x, y) = \exp\left[-i \frac{\pi}{\lambda f} (x^2 + y^2)\right] \tag{44}$$

in the paraxial approximation [21]. Here f is the focal length of the lens. For a cylindrical lens (one that is a portion of a right circular cylinder), the transmission function is similar to (44), only the factor $(x^2 + y^2)$ is replaced by $x^2$.

It is seen that this form appears in Equation (42). Aside from the bias term $t_b$, the transmission function of the radar signal film along a line $y=y_1$ is a sum of cosine terms, one for each point scatterer on the ground at the corresponding slant range. Consider the term for one point scatterer, with index n=N. The cosine may be written in terms of complex exponentials, leading to two terms. One of them is

$$t_\alpha^{(N)}(x, y_1) = \frac{\chi}{2}\, \sigma'_N(x_N, y_1) \exp(i2\pi f_x x)$$

$$\times \exp\left[-i\frac{2\pi}{\lambda_r r_1}\left(\frac{v_a}{v_f}\right)^2\left(x - \frac{v_f}{v_a}\, x_N\right)^2\right] \quad (45)$$

The first exponential factor, like the first term in each exponential of Equation (43), simply introduces a tilt in the phase front of this component of transmitted light. The angle of tilt is given by the relation

$$\sin\theta = \lambda_o f_x \quad (46)$$

where $\lambda_o$ is the wavelength of the illuminating light. Comparing the second factor of Equation (45) with Equation (44), it is seen that this factor behaves like a positive cylindrical lens with focal length

$$f_1 = \tfrac{1}{2}\,\frac{\lambda r}{\lambda o}\left(\frac{v_f}{v_a}\right)^2 r_1 \quad (47)$$

and with the lens axis located at

$$x = \frac{v_f}{v_a}\, x_N \quad (48)$$

The other term in the expansion of the signal film transmission function in terms of complex functions, which may be called $t_\beta^{(N)}(x, y_1)$, is the complex conjugate of Equation (45). The first exponential factor produces a wavefront tilt of $-\theta$, where $\theta$ is given by Equation (46). The other exponential factor is the transmission function of a negative cylindrical lens, also centered at the coordinate x given by Equation (48), and with the same focal length $f_1$, as given by Equation (46). Figure 8 shows the effect of the three terms in the expansion just discussed. The bias term $t_b$ gives rise to directly transmitted light, $t_\alpha^{(N)}$ yields a real image behind the transparency, and $t_\beta^{(N)}$ produces a virtual image in front of the film.

At this point it appears that the signal film transparency is capable of forming an image by itself. In fact, the signal film is an array of one-dimensional holograms [27]. However, the image formed directly is defective in several ways. Examination of Equation (47) shows that the focal length is proportional to the range of origin of the reflected signal. (The equivalent lens is conical, not cylindrical.) If many point scatterers are present at range $r_1$, each generates its own pair of real and virtual line foci. The relative azimuthal positions

of the scatterers determine the relative positions of the centers of the lenslike structures on the film, and therefore are preserved in the relative positions of the corresponding line foci. However, because of the range dependence of $f_1$, the lens of azimuth focus is a tilted plane, corresponding to the tilt of the ground relative to the incident radar beam. There is one such plane on each side of the film, a real image and a virtual image.

Furthermore, the signal film itself is the focal plane in the range dimension. Therefore, the images are defocused in range at the tilted planes of azimuth focus. The operations which must be performed to produce the final image are erection of the plane of azimuth focus into coincidence with it.

Figure 9 shows a combination of lenses that achieves this result. A positive conical lens, with focal length depending on the range coordinate (consequently on the y coordinate) according to Equation (47) is placed directly behind the signal film. Its effect is to erect the plane of virtual azimuth focus and move it to infinity. A cylindrical lens placed as shown one focal length from the signal film creates a virtual image of the y-dimension structure at infinity. The x and y images now coincide, and are brough back from infinity to form a real image by a spherical lens placed one focal length from the final image plane $P_2$. The final image is sharply focused in both range and azimuth [21,27].

To use the system shown in Figure 9 to perform the processing, a coherent light source (e.g., a laser) provides the illumination. The signal film and the final image film are both driven horizontally at the appropriate speeds, and the image is recorded through a properly placed slit. Extraneous light is blocked from the image film. More details are discussed in Reference 27. It should be noted that the residual carrier frequency, recorded as a spatial frequency $f_x$, makes possible the separation of the different components of the recorded signal. Without $f_x$ the real and virtual foci would not have been deflected at angles $\theta$ and $-\theta$ relative to the directly transmitted light. Without such deflections, the virtual line focus, for example, could not be viewed without interference from the real line focus and the directly transmitted light due to the bias. This "offset frequency" optical technique was developed by E. N. Leith, and is also a feature of the Leith-Upatnieks hologram, the most widely used type [21].

## B. Digital Processing of Synthetic Aperture Radar Signals

1. Possibility of Digital Processing. The possibility of digital processing for SAR has received surprisingly little attention in the literature. Harger, after making a reluctant effort to estimate the requirements, concluded that real-time digital processing was impossible [5]. (Harger assumed that optical processing would be acceptable

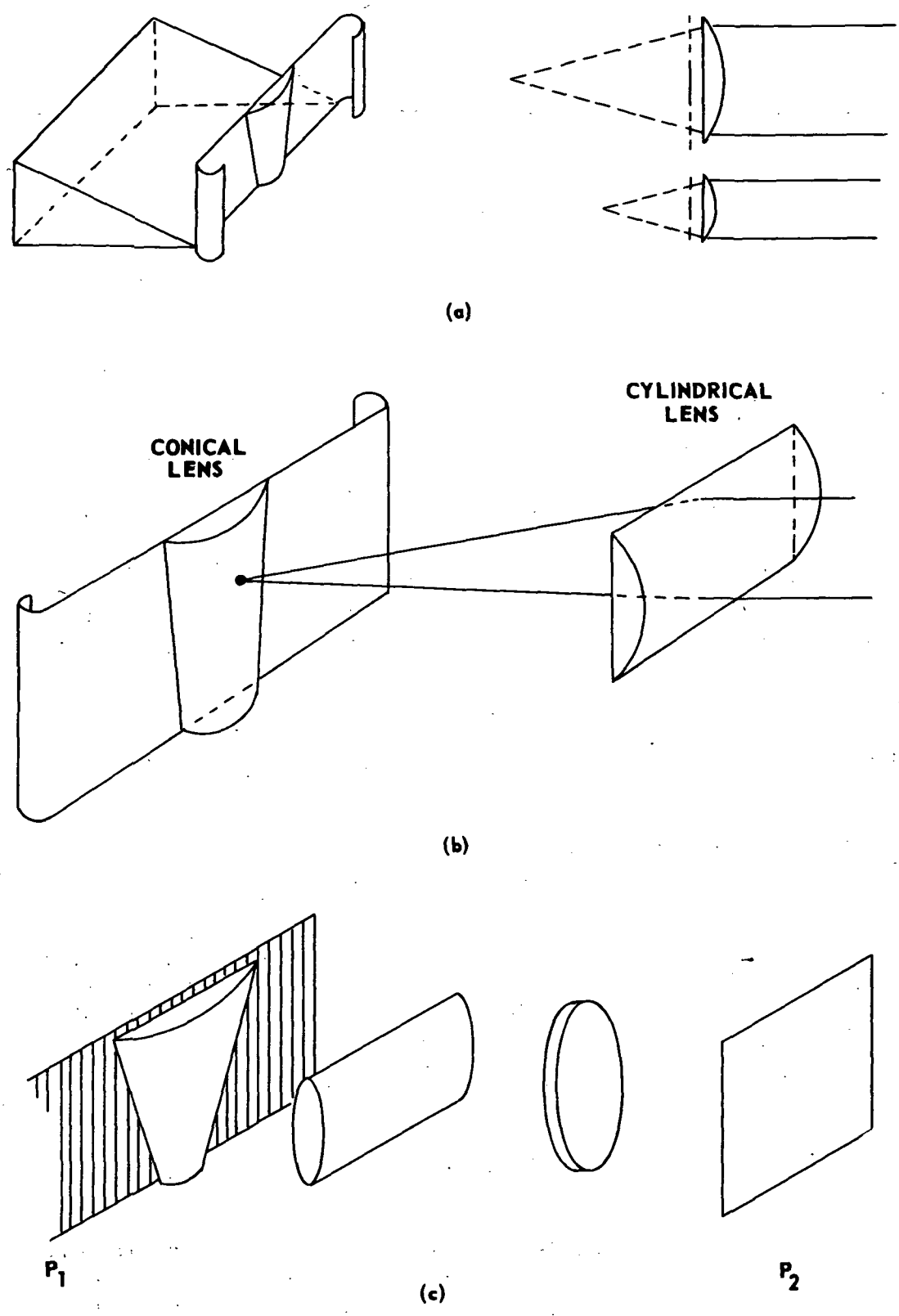


**FIGURE 9. DEVELOPMENT OF AN ANAMORPHIC LENS SYSTEM FOR COMPENSATION OF THE RADAR IMAGE (FROM REFERENCE 27)**

if processing in real time was not a requirement.) However, Gerchberg, who conducted a much more extensive study of the possibility, was more optimistic [9]. His estimate (made in 1970) was that, making reasonable assumptions about the rate of development of computer technology, by 1975 a real-time onboard digital processor for a satellite-borne SAR system would be marginally feasible.

A considerable amount of the early work on synthetic aperture radar, and on the coherent optical processing technique for SAR signals, was done at the University of Michigan, in the same laboratory where much of the pioneering work in holography and other optical methods was performed. Because of this combination of circumstances, and because the coherent optical processing method produces satisfactory results with relatively uncomplicated equipment, one may speculate that electronic approaches to SAR processing have been given less attention than would otherwise have been the case--without disparaging the work that was done at Michigan. Gerchberg's study, and a remark by Leith [27], indicate that non-optical processing techniques may be feasible, possibly even working in real time. For some types of missions the advantages of digital processing (vs. the difficulties associated with optical processing) may outweigh the problems of developing a new type of computer.

In Gerchberg's report, a sketch of a processor design is presented [9]. There is very little detail and his use of terms like "cycle time" is not identical with common usage in the computer field. Also, he doesn't consider processing speed (for individual operations), transfer rates, etc., in sufficient detail. And it may be argued that the organization of the processor and the implementation of the algorithm are not as efficient as they could be, using modern techniques. So Gerchberg's analysis must be approached cautiously. On the other hand, it is the only detailed study of digital processing applied to synthetic aperture radar in the open literature (as known to the present writer), so it is interesting at least for that reason. It is not the purpose of this report to design a processor, but rather to present discussion concerning the feasibility of various techniques. Keeping in mind its limitations, Gerchberg's report may be used at least to obtain first guesses (perhaps upper limits) for storage capacity, processing speeds, etc., and as a basis for comparison with other approaches to digital processing of SAR signals. Gerchberg wrote his report basically as a radar engineer rather than a computer designer, so it provides a useful point of view.

2. Basic Processing. The processing algorithm consists of a multichannel cross-correlation. The signal in each range bin is correlated with a reference function, equivalent to the return signal from a point target at that range. The reference function involves a range-dependent parameter, so (ideally) it is different for each range bin. The basic algorithm is illustrated in Figure 10. The mathematical details were worked out in Section III.

Some properties of the ideal (i.e., unmodified) algorithm can be seen easily. Leaving the signal on a "residual" carrier (offset frequency) was

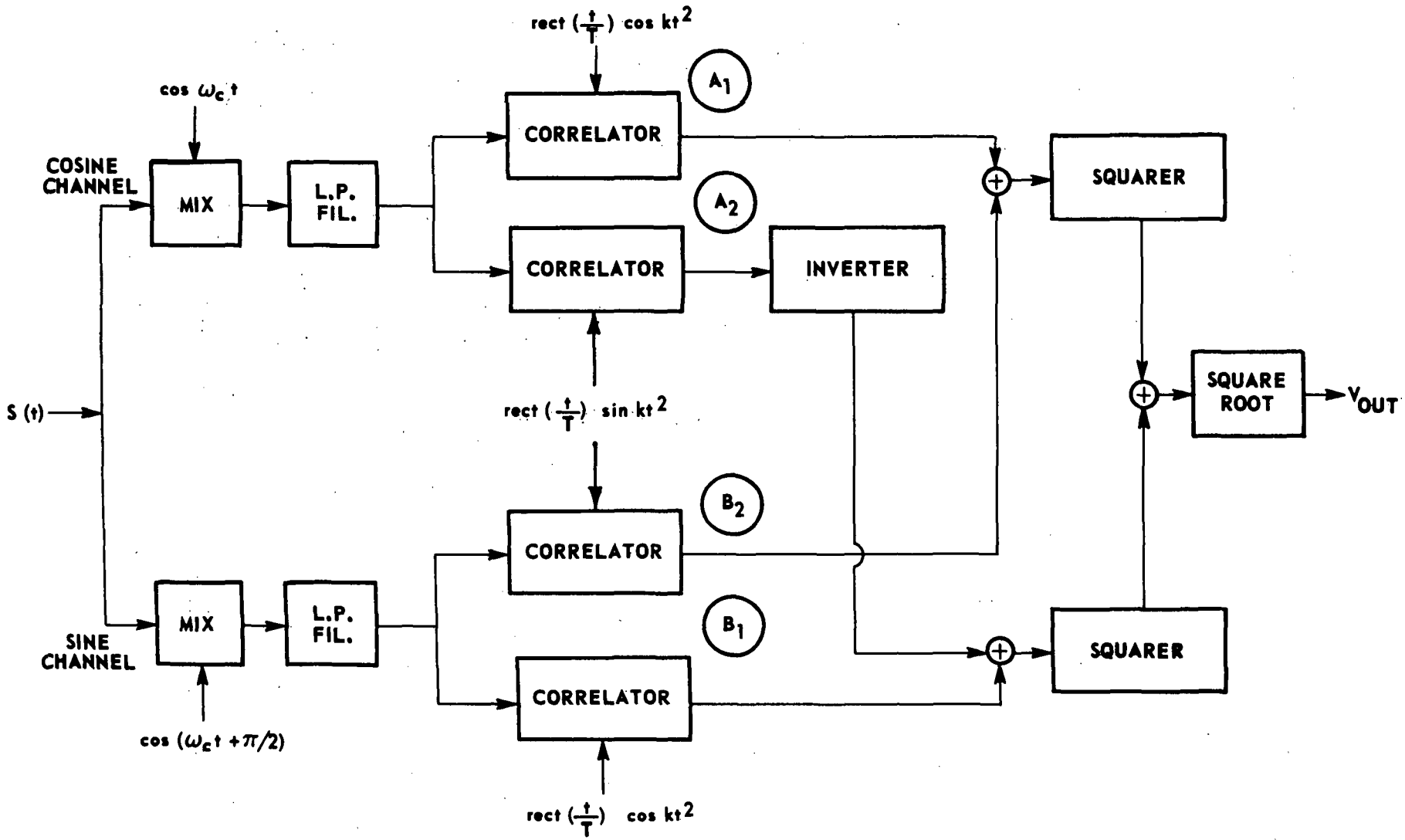


FIGURE 10. ALGORITHM EMPLOYED WITH QUADRATURE DETECTION

found to be very useful when optical processing is employed. However, it is not necessary for digital processing. With zero offset, the PRF of the radar system does not need to be higher than the Doppler bandwidth, B 9 . Then, if T is the length of time a point target is in the radar beam, the time-bandwidth product TB is equal to the number of pulses which must be processed together.

Gerchberg shows that, for processing by an active correlator, quadrature detection is required [9]. A simple plausibility argument that illustrates the reason is the following: For zero offset frequency, and bandwidth B, the highest frequency in the signal's spectrum is B/2. The signal is observed over an interval of length T, so it can be expressed in a Fourier series whose frequency increment is 1/T. Then the number of frequencies involved in the series, N, satisfies

$$N(1/T) = B/2 \implies N = (TB)/2 \tag{49}$$

In order to use all the information contained in the original TB signal samples, there must be two terms--sine and cosine--per frequency. Equivalently, both amplitude and phase information are needed. Failure to use both results in the output amplitude's being sensitive to the arbitrary phase of the signal (see Equation (38)). Again, Figure 10 shows the exact method of implementation.

3. Variations on Fundamental Algorithm. A few variations on the basic processing algorithm will be considered next. A reasonable measure of the quality of the results is required in order to assess the different methods. Although most of the discussion up to this point has concerned itself with the imaging of point targets, it is necessary to consider the properties of the superposition of a large number of such point images. While military uses of radar are frequently concerned with the locations of isolated "point targets," for earth resources applications of imaging radar it is actually the ground "clutter" which is of primary interest [28]. Under some simple assumptions, it is easy to show that a reasonable model of a single extended terrain category (e.g., water, or forest, or wheat fields) as a radar target is such that the voltage reflection coefficients over an area are statistically distributed. Specifically, they are Rayleigh distributed in amplitude, with mean proportional to the square root of the differential scattering cross section, and uniformly distributed in phase [9]. The variance in intensity of radar return strength represents uncertainty. So the ratio of image mean to standard deviation (M/STD) provides a measure of image quality.

Imagery produced using the straightforward algorithm described previously have a rather low value of this quantity, leading to the well-known "radar scintillation" effect (speckling or graininess, characteristic of imagery produced using coherent illumination). The changes in the M/STD ratio due to using some of the variations described next will be mentioned. Analytical calculations are difficult to perform, but the various methods can be studied quantitatively using the simulator described in Section V.

The mathematical form of the image of a point target can be found fairly easily. (See the discussion following Equation (41), Section III.C.) It is proportional to a sinc (sin x/x) function [27]. In addition to a large central peak, the sinc function has sidelobes. These sidelobes give the appearance of small (in intensity) point targets near the main point. At the expense of some close-target resolution, these spurious responses can be reduced by using a weighted reference function. This can be implemented very easily--perhaps with a library of weighting functions--using digital processing. The effects of different weighting functions can be explored most readily using the simulator referred to previously.

The theoretical need for quadrature processing has been discussed. However, inspection of Figure 10 makes non-quadrature detection appear very attractive, assuming that acceptable imagery can be produced in this way. A great saving in storage, processing hardware, and the number of operations that must be performed results from using only the channel marked $A_1$ in Figure 10. It can be shown that resolution is not affected; the intensity of a single image point depends on the phase of the target voltage reflection coefficient, and the M/STD is reduced by about 3 dB.

Another processing variation consists of modifying the reference function by substituting $\sin kt^2/|\sin kt^2|$ and $\cos kt^2/|\cos kt^2|$ for $\sin kt^2$ and $\cos kt^2$, respectively. That is, the new reference function takes on the values $\pm 1$ only. This method was first described by Moore and Rouse, who pointed out a simple way of realizing it electronically [10]. Mathematically, the modified reference function is a Fresnel zone plate. There is little image degradation due to zone plate processing; a slightly higher "clutter" level is the main difference.

The simplest special case of zone plate processing consists of only using the central Fresnel zone. This is simply accumulation of the signal without phase adjustment, over the longest interval for which this is permissible. It is known as "unfocused processing" [3]. The principal effect, since the bandwidth of the reference function is reduced (TB = 2 for unfocused processing), is to make the resolution considerably poorer. Also, the sidelobes are numerous and high, leading to a noisy image. For the numerical example at Skylab altitude presented in Section II.B., the resolution with unfocused processing is of the order of 70 m. (This is still considerably better than the along-track beamwidth, a few km.)

In general, it is possible to degrade the resolution of the image (and decrease the amount of calculation) by shortening the reference function. In effect, this throws away the high-frequency information in the signal. The image quality, as measured by M/STD, is practically unaffected by this. However, there is a method of trading resolution for M/STD, and improving the image gray-tone quality--yet with fewer mathematical operations than are required for the basic algorithm. Since, as was pointed out in Section II.B., the theoretical resolution may be much higher than is actually needed, this may be a very desirable option.

If the resolution of a high-resolution but grainy image is high enough, the viewer may view it from a sufficient distance that the apparent graininess (and the resolution) is reduced. The viewer's eyes may be thought of as performing an averaging function, or post-detection integration. Although the resolution is reduced, all the information is used. A method of degrading the resolution of SAR imagery by reducing the reference function bandwidth, without losing the high-frequency information in the signal, is to break the full reference function into several shorter pieces, perform the SAR processing separately with each, and sum the results. The discussion in Section III.C. shows that each piece, or subaperture, of the reference function is matched to a different part of the signal's spectrum, so the procedure described here is a form of averaging in Doppler bandwidth. Images achieved with subapertures whose principal lobes do not embrace the same range of Doppler frequencies in the return signal are images of ground targets from a given statistical population which are decorrelated, so they may be summed to increase the M/STD of the final image. If N non-overlapping subapertures are used, encompassing the entire length of the reference function, the image M/STD is enhanced by the factor $\sqrt{N}$, while the length of a resolution element is increased by the factor N [9].

4. A Proposed Real-Time SAR Digital Processor. In 1970 Gerchberg studied the requirements and presented design details for a real-time on-board (spacecraft) SAR digital processor, which he felt could be built in 1975, embodying several of the ideas just discussed [9]. The analysis considered details affecting accuracy, and compromises to reduce the size of the processor, so as to produce imagery with specified characteristics (resolution and M/STD). An interesting conclusion is that processor speed is not a big problem, but that the amount of storage required--especially the quantity of power consumed--is a key factor.

The analysis will not be repeated in great detail here, but the principal points will be mentioned. A basic assumption is that a resolution length greater than the theoretical "nominal" value is acceptable. It has been seen that this can be achieved by reducing the length of the reference function. The required amount of storage is correspondingly reduced. The storage requirement can be further reduced, along with the size and complexity of the processor, by employing non-quadrature processing. This leads to a 3 dB reduction in the M/STD ratio. This ratio can be increased by using subaperture processing. It will be seen that this does not affect the size of main storage, but requires the addition of another, much slower, memory unit. So the processor studied by Gerchberg is one that performs non-quadrature subaperture processing in real time, yielding an image with specified resolution and M/STD. (Full-focused non-quadrature processing--using a single "subaperture", of length equal to the full reference function length--is a special case.)

When subaperture processing is used, with the full reference function divided into N contiguous non-overlapping segments, the resolution is degraded by a factor N--the resolution length becomes N "nominal" resolution lengths. For the degenerate case of using only one of the N subapertures

there is no improvement in M/STD. If G ($G \leq N$) subapertures are used, the M/STD ratio is enhanced by the factor $\sqrt{G}$. As will be seen, the amount of storage depends on the value of G, so in general it is best to use the smallest value of G that will provide the required M/STD.

The structure of Gerchberg's processor can be obtained from the equation describing subaperture processing. In very compact notation, the Ith output $\Omega_I$ is

$$\Omega_I = \sum_{K=0}^{G-1} \left| R_K * S_{(KL + IN)} \right| , \qquad L = TB/N \tag{50}$$

In this equation, N is the maximum number of non-overlapping contiguous subapertures; G is the number of subapertures used; $R_M * S_N$ stands for the sum of products involving the Mth piece of the reference function $R_M$ and starting with the Nth signal point, $S_N$,

$$R_M * S_N = \sum_{i=0}^{L-1} R_{Mi} S_{N+i} \tag{51}$$

L is the length of one subaperture in nominal reference lengths or signal samples, and all subscripts take on successive integral values beginning with 0. Equation (50) implicitly contains the degradation in resolution, calculating only every Nth point on the image line.

In each range bin, the processor employs two levels of storage. The first, called the "working store", contains the latest L points. The correlation process is performed against these L numbers by multiplying each of them by the appropriate reference function point, and accumulating the products in a register. Each time a term of the form R * S is completed, it is transferred to the appropriate cumulative adder in the second level of storage, the "averaging store". From Equations (50) and (51), G sums of products R * S, each involving L accesses of working storage, must be performed before the next N points come into the input buffer. (At this time, the contents of working--or primary--storage are replaced by a new set of samples whose subscripts are incremented by N.) Since the sampling rate is the pulse repetition frequency, B, this requires the primary storage to be no slower than $N^2/(B^2TG)$ seconds per access.

Also it is seen from Equation (50) that L = TB/N signal points are generated by the radar before the next subaperture contributes to the Ith image point, $\Omega_I$. Since an R * S term (subaperture output) is generated every N signal points, $TB/N^2$ subaperture outputs are generated before another point is added to a given location in the averaging store. Since there are G subapertures, $(TB/N^2)G$ locations are required in the averaging

store for continuous operation. The averaging store is accessed one-Lth as often as the working storage, leading to an access time of N/BG seconds.

Gerchberg also describes strategy for reducing the word-length requirement in the averaging store, and considers some sources of error, but the principal ideas are given above. Since the image lines for each range bin are independent of one another, he considers that they may all be processed independently, in parallel. Gerchberg's processor is actually a collection of parallel processors, one for each range bin. Gerchberg's report contains a table collecting the formulas relevant to specifying processor requirements. It provides information on the tradeoffs available between processor size and speed, image resolution, and image M/STD.

An idea of the magnitudes of the numbers involved can be obtained from a numerical example. One presented by Gerchberg will be repeated here. He considered a radar in an orbiting satellite at an altitude of 600 n.mi., traveling (roughly) 7 km/sec, imaging a ground swath 40 km wide. The antenna length was taken to be 4 m, leading to a nominal resolution length of 2 m, and the radar carrier frequency is 10 GHz. Some quantities that can be derived from this are: $T = 1.377$ seconds, $B = 3500$ Hz, $TB = 4820$. The desired image parameters are: resolution = 30 m, M/STD = $\sqrt{18}$ .

To obtain the desired resolution, the resolution degradation factor, N, is 15. Then the length of a subaperture is $L = TB/N = 321$ data samples. Using the fact that the inherent M/STD ratio for a homogeneous class of targets is 5.61 dB, it is found that, with non-quadrature subaperture processing, $G = 10$ of the possible 15 subapertures produce the desired M/STD. With 30-meter resolution, there are 1334 range bins. Computer simulations indicate that 5-bit words are adequate for the working storage and the analysis shows that 9-bit words suffice for the averaging store.

The working store needs to be $L = 321$ words long at 5 bits per word, or 1605 bits in each range bin. The size of the averaging store must be $(TB/N^2)G = 214$ words, each 9 bits long, or 1926 bits per range bin. The total amount of storage required, for all 1334 range bins, is about 4.71 megabits.

There is a considerable difference in speed between the two levels of storage. In the working storage, the required access time is $N^2/(B^2TG) = 1.3$ $\mu$sec. In the averaging store, however, the requirement is only $N/BG = 0.43$ milliseconds. The averaging store specifications, 2.57 megabits with an access time of 0.43 milliseconds, sound rather easy to meet. However, it must be recalled that Gerchberg's design calls for organizing this into 1334 parallel, independent banks of storage. Making an educated guess based on then-current design trends, he assumed that the entire storage requirement could be managed with Large Scale Integrated (LSI) memory chips with access times of 100 nanoseconds and power dissipations of 10 microwatts per bit, assumed to be feasible by 1975.

The other significant specifications in this example were: for the radar, PRF = 3500 Hz (B), pulse duration = 0.1 n sec., peak pulse power = 170 kw, and average transmitter power = 60 watts; and for the processor, power required (including cooling) = 200 watts, volume = 5 cu.ft., and weight = 60 pounds.

Are these numbers reasonable? With the organization assumed, processor speed is not a significant problem. Analog-to-digital converters with speeds in the required range are currently being built. The most severe requirement is for the large amount of storage, and the power to operate it, and the parallel problem of dissipating the heat produced. A figure quoted by Gerchberg was for the Texas Instruments 16-bit memory chip No. SN5481, with a power dissipation of 275 milliwatts. A 4.71 megabit memory made of these circuits would require over 80 kilowatts.

With regard to the accuracy of Gerchberg's 1975 projections, it is interesting to follow up one bit of proposed development. Gerchberg reported (in 1970) that Texas Instruments would produce a memory chip in late 1971 with the following characteristics: 4000 fully addressed bits on a one square inch chip, dissipating 1.6 watts, and with an access time of 0.5 $\mu$sec. That Texas Instruments project actually did produce memory chips in two models: 2 kbit, 150 n sec. access time, and 16 kbit, 1.5 $\mu$sec access time, both with power requirements per bit as good as was projected [29]. It was estimated that, today, a metallic oxide semiconductor (MOS) memory could be built containing 2000 bits per package, with 0.5 $\mu$sec access time, dissipating 25-50 $\mu$watt/bit, and that Gerchberg's estimate of what would be feasible by 1975 was quite reasonable [29].

5. Alternate Approaches. The processor whose design was sketched in the preceding section offered one approach to performing the calculations, and one (not very precisely defined) approach to processor organization. The design was straightforward, and the specifications, though formidable, may be possible to meet. However, there are a number of more sophisticated techniques, both of algorithm design and processor organization, that may lead to a considerably more efficient processor.

It is almost certain that today the most common method of calculating correlation functions and convolutions on a digital computer is by means of the fast Fourier transform (FFT) [11]. There is an extensive literature on the FFT. Some of its relevant properties will be summarized here, omitting the mathematical derivations. The FFT is a highly efficient method of computing the discrete Fourier transform, which is a transform in its own right, possessing many properties paralleling those of the (continuous) Fourier integral transform or the Fourier series. One of these is the behavior under a shift of origin, leading to a method of calculating discrete convolutions or correlation functions simply by multiplication in the transform domain (plus a complex conjugation for correlation functions). The FFT algorithm is so efficient that, except for short sequences, calculation of the correlation or convolution in this way requires fewer mathematical operations than using an algorithm based directly on the definition. This leads to both greater speed and

greater accuracy--the latter because there is less roundoff error with a smaller number of operations.

The SAR processing algorithm is an example of a relatively common type of digital filtering, where the reference function (fixed length) is much shorter than the function to be filtered (arbitrary length). A convenient way of handling this case is by the method called "sectioning of the record" by Cooley et al [11], or "select-save" by Helms [30]. This is a computationally efficient way of filtering an essentially infinitely long signal with a much shorter (impulse response) filter, by breaking the signal into overlapping sections and performing a convolution section by section. (The term "convolution" will be used interchangeably with "correlation" here, since the two operations are practically identical in the frequency domain. The SAR matched filtering operation has been described both as correlation with the return from a point target, and as convolution with a filter whose transfer function is the complex conjugate of the Fourier transform of the point target return--Equation (23).) Although FFT subroutines are commonly restricted to sequences whose lengths are powers of two, the select-save method can use such a subroutine without requiring that the number of points in either the signal or the filter sequence be a power of two.

In the last section, it was pointed out that the reduction in resolution permitted "sampling" the output line, with a corresponding reduction in calculation. A property of the FFT permits a similar reduction in resolution, with fewer computations required [31]. Also, there are techniques for performing the FFT calculation more efficiently when the sequence is real rather than complex [11]--as is the case when non-quadrature processing is used. Another property of the FFT algorithm is that, in its basic form, the results are produced in "scrambled" order, and must be "shuffled" to put them into correct order [11]. However, in computing correlations or convolutions, both transformed sequences are in the same scrambled order, so they can be multiplied without unscrambling and then inverse-transformed to yield the final result. The inverse transformation restores the correct order. Singleton discusses several of these FFT properties as they relate to digital filtering [32].

The preceding discussion of the FFT was primarily software-related. There are hardware implementations of the FFT; that may be the most sensible approach in a special-purpose processor. Before discussing hardwired FFT processors specifically, however, some advanced types of general computer architecture will be described. Two new approaches to computer design are pipeline structure and parallel processing.

The pipeline arrangement is highly efficient when the same set of operations must be performed repeatedly on well-ordered data sets. Examples are the vector dot-product calculation and matrix multiplication. The pipeline concept consists of breaking an operation into its distinct steps and arranging them in "pipe" fashion. For example, on a fundamental level, an operation like a floating point addition has several steps, such as justification (a shift of the mantissa of one of the two numbers, so

both have the same exponent), addition, and normalization (putting the result into normalized floating point form). (These are in addition to retrieval and storage.) Figure 11 shows a pipeline that performs an operation consisting of three separate and distinct steps. The operation takes a total time T to perform, the sum of the times for each of the stages. But if the steps are separate and distinct, as assumed, operands may be entered into the pipe so that all three steps are performed simultaneously, on different operands. If the process is such that a large number of identical operations are required in sequence, on a long series of operands, than the average operation time is substantially reduced. When the pipe is completely filled, the average time required for the operation illustrated in Figure 11 is $(t_A + t_B + t_C)/3$.

An example of a pipeline processor is the Texas Instruments ASC computer. Its arithmetic unit is constructed from a number of "sections," each of which can perform a separate arithmetic or logical operation in the same manner as the steps in Figure 11. The time required to accomplish the function of each section is 50 nanoseconds. So with well-ordered data sets, once the "pipe" is filled, results appear every 50 nsec.

The parallel processing concept involves operating a number of conventional type processors simultaneously, under the control of a single central control unit. The ILLIAC IV, the fourth generation in a line of advanced computers designed and developed at the University of Illinois, is an example of a parallel computer [33]. Its processing structure is illustrated in Figure 12. (The original design of ILLIAC IV consisted of four "quadrants"; Figure 12 shows one quadrant, which is what has been built so far.) Each processing element (PE) can perform a wide range of arithmetic and logical operations. Each processing element memory has a capacity of 2048 64-bit numbers (the processing elements are capable of breaking each word into independent shorter words). The routing network permits several types of data transfers and interconnections between PE's.

The philosophy of parallel computing is that speed can be gained by performing many operations simultaneously. In principle, there is no limit to the effective computer speed, assuming a sufficient number of parallel elements. However, as in the case of pipeline processing, a problem must be properly structured to make full use of the potential speed increase. (Another practical limitation to parallel processing is that a system containing very many components is subject to frequent hardware failures.) In the ILLIAC IV, since the single central controller cannot issue different instructions at the same time, the maximum speed of processing occurs when all 64 processing elements can execute the same instruction simultaneously. Programs must be organized differently for a parallel computer than for a serial machine. For example, some things (such as division of each element of an array by a constant) done sequentially, in a loop, on a conventional computer would be done simultaneously on a parallel processor. Gerchberg's processor [9] overcomes the fundamental limitation described by Harger [5] by processing each range bin separately, in parallel. Harger considered strictly serial processing.

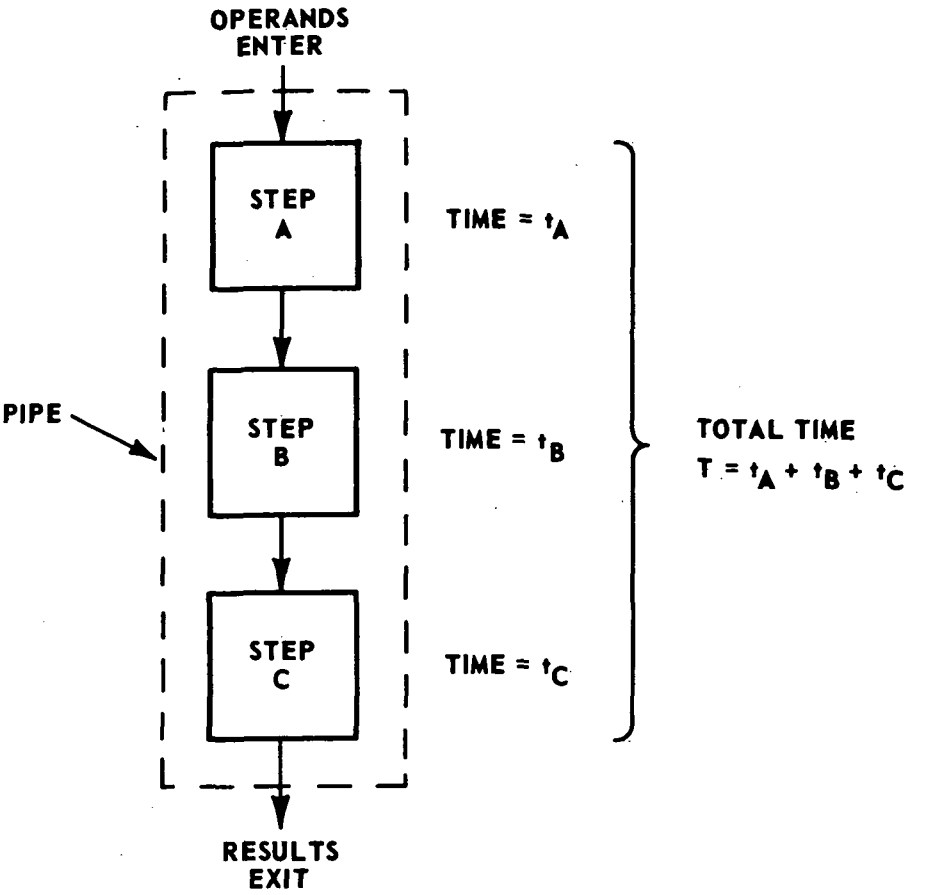


FIGURE 11. PIPELINE PROCESSOR CONCEPT

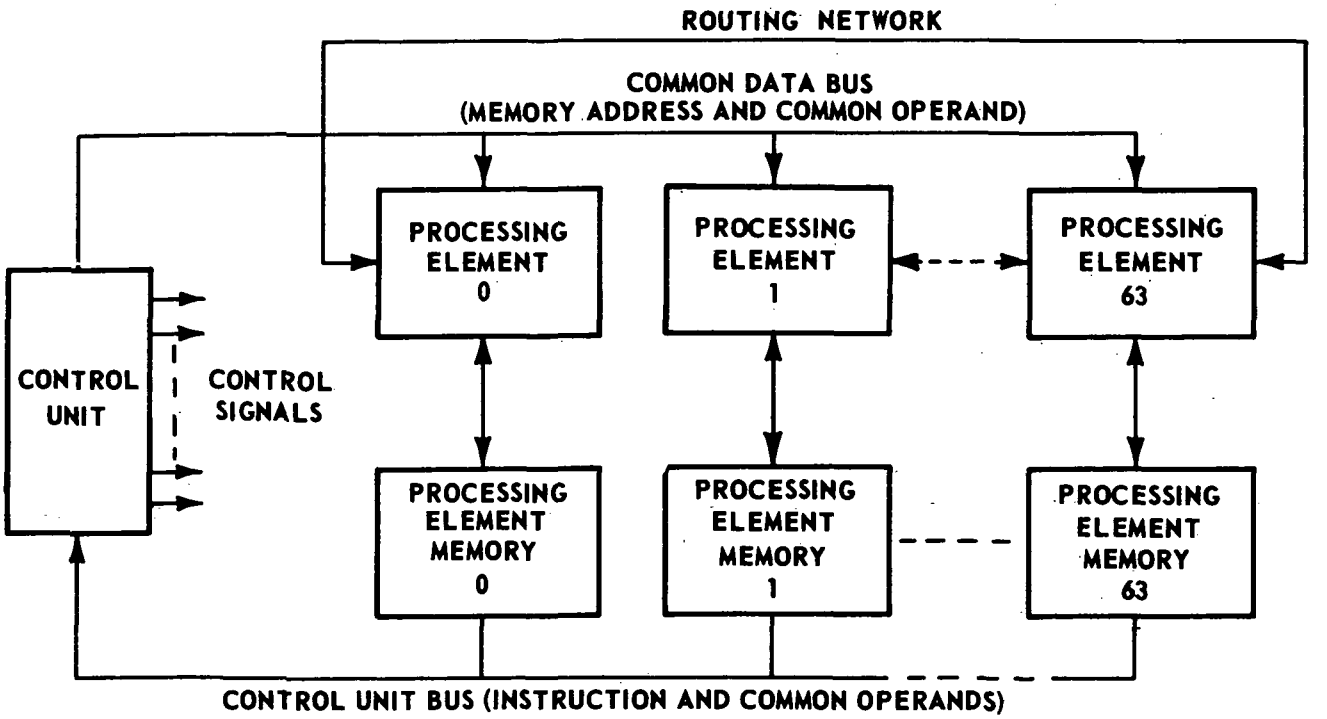


FIGURE 12. PARALLEL STRUCTURE OF ILLIAC IV

The question of which type of processor--pipeline or parallel--is faster cannot be answered in general, independently of the problem to be solved. Skill in setting up the problem and programming is also a factor. For certain problems, not well suited to either pipelining or parallel processing, conventional modern computers may even be faster. For the right type of problems, expectation of an order-of-magnitude increase in speed for parallel or pipeline processing is not unreasonable. Experience in writing parallel algorithms may lead to significant improvements in speed, compared to the present situation. One example of an algorithm written for parallel processing is Pease's version of the fast Fourier transform [34].

It is only a small step further to consider combining pipeline and parallel processing. For example, Gerchberg's proposed processor is parallel, but little detail is specified for the processor for each range bin [9]. The required operation is eminently well suited to pipelining, so the processor could be a parallel combination of pipeline computers. Proper design might lead to a highly efficient processor.

This is a simple example of the possibilities in extrapolating from the basic ideas of parallel and pipeline computing. In certain cases, taking advantage of special properties of algorithms, other interesting designs are possible. Groginsky and Works described a remarkable organization of a special-purpose processor for calculating the fast Fourier transform (a radar signal processor, in fact) [35]. Since it has been seen that the FFT may be of great value in the SAR processing, it is worth examining this design in some detail.

The FFT algorithm calculates the discrete Fourier transform,

$$F(j) = \sum_{k=0}^{N-1} X(k)W^{-jk}, \quad j = 0, 1, \ldots, N-1 \tag{52}$$

where X is the original sequence, F is the transform, N is the number of points, and W is the principal Nth root of unity, $W = \exp(2\pi i/N)$. Equation (52) represents $N^2$ complex multiply-add operations.

The FFT algorithm results from the recognition that Equation (52) can be reformulated more economically as a recursive calculation, involving shorter-length transforms, when the number of points N is factorable. The fast Fourier transform results when N is decomposed into its prime factors. The simplest and most commonly used version is for N a power of 2; that is the version that will be discussed here.

To obtain the algorithm, one writes j and k as binary numbers, e.g., $j = j_{n-1}(N/2) + \ldots + j_1(2) + j_0$, where $n = \log_2 N$, and each $j_i$ may take the value 0 or 1. This is abbreviated $j = (j_{n-1}, \ldots, j_1, j_0)$. Several

different versions of the FFT result from different algebraic manipulations of the resulting equation. The version to be discussed here is the Cooley-Tukey algorithm. The general member of the set of recursive equations making up the Cooley-Tukey FFT algorithm is [36]

$$A_P(j_0, j_1, \cdots j_{P-1}, k_{n-P-1}, \cdots, k_0)$$

$$= \sum_{k_{n-P}=0}^{1} A_{P-1}(j_0, j_1, \cdots, j_{P-2}, k_{n-P}, \cdots, k_0) \qquad (53)$$

$$\times \; W^{-(j_{P-1}2^{P-1} + \cdots + j_1 2 + j_0)k_{n-P}(\frac{N}{2^P})}$$

$A_0$ is the original array, X, and $A_n$ is the discrete Fourier transform. It should be noted that the final stage, P=n, has the $j_i$ in reverse order; that is, the transform is calculated in "bit-reversed" or "reverse binary" order. Figure 13 illustrates the logic of the algorithm. Each stage calculates a set of two-point transforms, combining results from the preceding stage as shown. The "scrambled" order of the final result is indicated. Equation (53) represents $2N\log_2 N$ complex operations, but the first term involves multiplication by $W^0=1$, and some symmetries of W reduce the amount of calculation even more.

Because the calculation is recursive--because each stage only needs the data generated by the preceding stage--Equation (53) is a natural pipeline algorithm. There are some additional symmetries and properties of the algorithm that were made use of by Groginsky and Works in constructing a pipeline processor, the mth stage (counting backwards from n-1) of which is shown in Figure 14. The "rotation vector" referred to there is the proper sequence of powers of W. In each stage, blocks of $2^m$ data samples alternately enter the delay line and arithmetic unit. When a data block fills the delay line, control is switched to the arithmetic unit. The arithmetic unit processes two data samples at a time, one from the data input and one from the delay line; the rotation vector comes from a read-only memory. Of the two outputs produced, one goes to the next stage and the other into the delay line. The next time control is switched to the delay line, the $2^m$ computed samples in the delay line are forwarded to the next stage, while new data enters the delay line. This rather tricky mode of operation is illustrated by Figure 15, for N=16. Time increases going down the page. An ellipis in the "OUT" column indicates that input data are entering the delay line. Inspection of Figures 13-15 together should make clear how this processor works.

The Groginsky-Works FFT processor is very elegant as described so far. But further examination of Equation (53) leads to another extremely

(a) N = 8

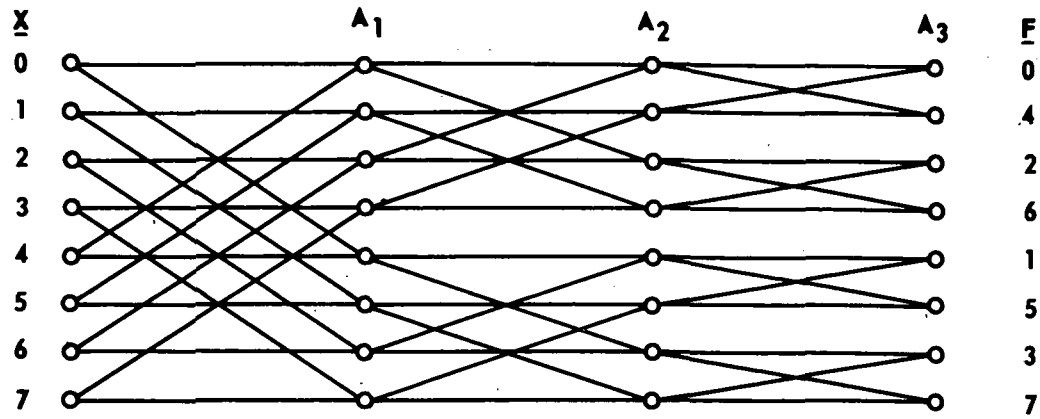


(b) N = 16

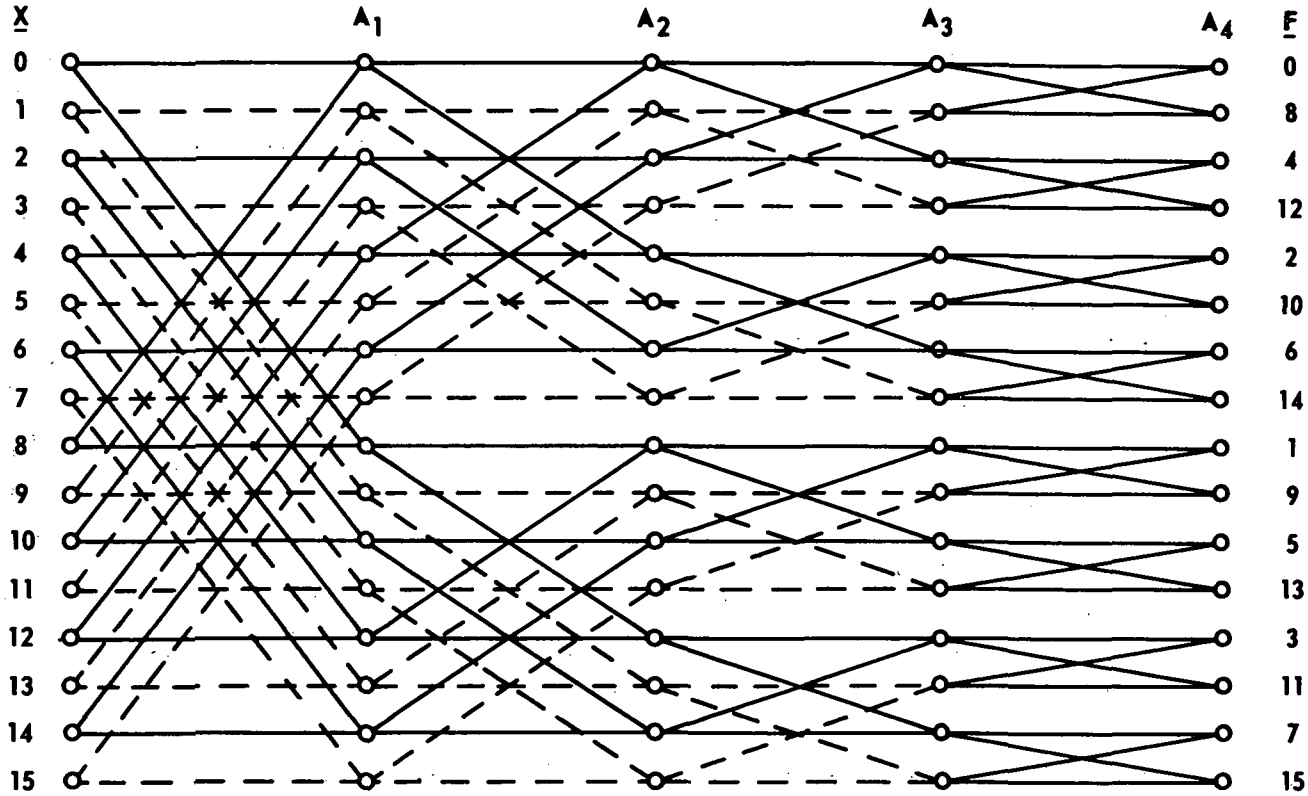


FIGURE 13. SIGNAL FLOW GRAPH FOR COOLEY–TUKEY ALGORITHM
(a) N = 8 (b) N = 16

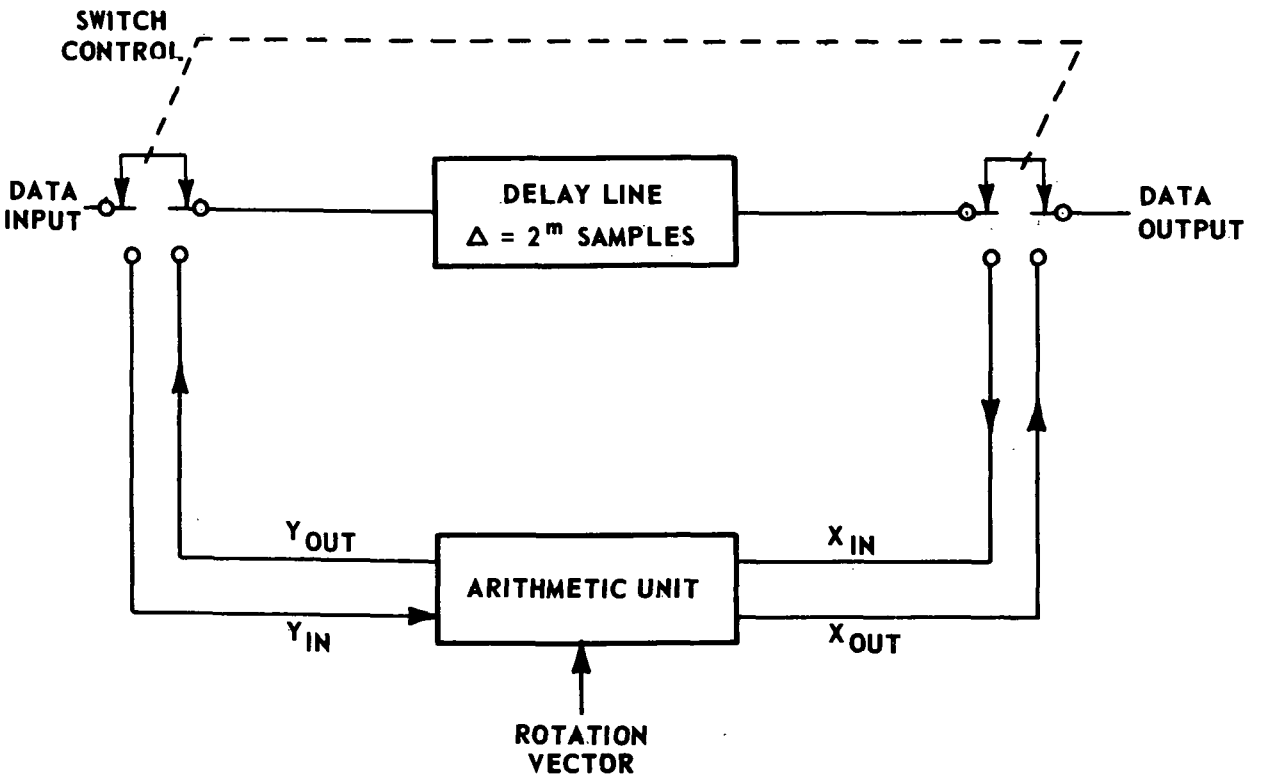


FIGURE 14. PIPELINE FFT m MODULE (FROM REFERENCE 35)

| STAGE 3 DELAY $2^3$=8 | | | STAGE 2 DELAY $2^2$=4 | | | STAGE 1 DELAY $2^1$=2 | | | STAGE 0 DELAY $2^0$=1 | | | OUTPUT |
|---|---|---|---|---|---|---|---|---|---|---|---|---|
| IN | OUT | | IN | OUT | | IN | OUT | | IN | OUT | | |
| | Next Stage | Delay Line | | Next Stage | Delay Line | | Next Stage | Delay Line | | Next Stage | Delay Line | |
| X(0) | --- | --- | | | | | | | | | | |
| X(1) | --- | --- | | | | | | | | | | |
| X(2) | --- | --- | | Filling | | | | | | | | |
| X(3) | --- | --- | | | | | | | | | | |
| X(4) | --- | --- | | | | | | | | | | |
| X(5) | --- | --- | | | | | of | | | | | |
| X(6) | --- | --- | | | | | | | | | | |
| X(7) | --- | --- | | | | | | | | | | |
| X(8) | A1(0) | A1(8) | A1(0) | --- | --- | | | | | Pipeline | | |
| X(9) | A1(1) | A1(9) | A1(1) | --- | --- | | | | | | | |
| X(10) | A1(2) | A1(10) | A1(2) | --- | --- | | | | | | | |
| X(11) | A1(3) | A1(11) | A1(3) | --- | --- | | | | | | | |
| X(12) | A1(4) | A1(12) | A1(4) | A2(0) | A2(4) | A2(0) | --- | --- | | | | |
| X(13) | A1(5) | A1(13) | A1(5) | A2(1) | A2(5) | A2(1) | --- | --- | | | | |
| X(14) | A1(6) | A1(14) | A1(6) | A2(2) | A2(6) | A2(2) | A3(0) | A3(2) | A3(0) | --- | --- | |
| X(15) | A1(7) | A1(15) | A1(7) | A2(3) | A2(7) | A2(3) | A3(1) | A3(3) | A3(1) | A4(0) | A4(1) | F(0) |
| X(16) | --- | --- | A1(8) | --- | --- | A2(4) | --- | --- | A3(2) | --- | --- | F(8) |
| X(17) | --- | --- | A1(9) | --- | --- | A2(5) | --- | --- | A3(3) | A4(2) | A4(3) | F(4) |
| X(18) | --- | --- | A1(10) | --- | --- | A2(6) | A3(4) | A3(6) | A3(4) | --- | --- | F(12) |
| X(19) | --- | --- | A1(11) | --- | --- | A2(7) | A3(5) | A3(7) | A3(5) | A4(4) | A4(5) | F(2) |
| X(20) | --- | --- | A1(12) | A2(8) | A2(12) | A2(8) | --- | --- | A3(6) | --- | --- | F(10) |
| X(21) | --- | --- | A1(13) | A2(9) | A2(13) | A2(9) | --- | --- | A3(7) | A4(6) | A4(7) | F(6) |
| X(22) | --- | --- | A1(14) | A2(10) | A2(14) | A2(10) | A3(8) | A3(10) | A3(8) | --- | --- | F(14) |
| X(23) | --- | --- | A1(15) | A2(11) | A2(15) | A2(11) | A3(9) | A3(11) | A3(9) | A4(8) | A4(9) | F(1) |
| X(24) | A1(16) | A1(24) | A1(16) | --- | --- | A2(12) | --- | --- | A3(10) | --- | --- | F(9) |
| X(25) | A1(17) | A1(25) | A1(17) | --- | --- | A2(13) | --- | --- | A3(11) | A4(10) | A4(11) | F(5) |
| X(26) | A1(18) | A1(26) | A1(18) | --- | --- | A2(14) | A3(12) | A3(14) | A3(12) | --- | --- | F(13) |
| X(27) | A1(19) | A1(27) | A1(19) | --- | --- | A2(15) | A3(13) | A3(15) | A3(13) | A4(12) | A4(13) | F(3) |
| X(28) | A1(20) | A1(28) | A1(20) | A2(16) | A2(20) | A2(16) | --- | --- | A3(14) | --- | --- | F(11) |
| X(29) | A1(21) | A1(29) | A1(21) | A2(17) | A2(21) | A2(17) | --- | --- | A3(15) | A4(14) | A4(15) | F(7) |
| X(30) | A1(22) | A1(30) | A1(22) | A2(18) | A2(22) | A2(18) | A3(16) | A3(18) | A3(16) | --- | --- | F(15) |
| X(31) | A1(23) | A1(31) | A1(23) | A2(19) | A2(23) | A2(19) | A3(17) | A3(19) | A3(17) | A4(16) | A4(17) | F(16) |
| X(32) | --- | --- | A1(24) | --- | --- | A2(20) | --- | --- | A3(18) | --- | --- | F(24) |
| X(33) | --- | --- | A1(25) | --- | --- | A2(21) | --- | --- | A3(19) | A4(18) | A4(19) | F(20) |
| X(34) | --- | --- | A1(26) | --- | --- | A2(22) | A3(20) | A3(22) | A3(20) | --- | --- | F(28) |
| . | | | | | | | | | | | | . |
| . | | | | | | | | | | | | . |
| . | | | | | | | | | | | | . |

Figure 15. FFT Pipeline Processor Flow Diagram, N=16

useful property. After a small amount of manipulation, the output of the next-to-the-last stage can be written

$$A_{n-1}(j_0, j_1, \ldots, j_{n-2}, k_0) =$$

$$\sum_{k_1=0}^{1} A_{n-2}(j_0, j_1, \ldots, j_{n-3}, k_1, k_0) \tag{54}$$

$$\times \; W_{N/2}^{-(j_{n-2}2^{n-2} + \ldots + j_1 2 + j_0)k_1}$$

In this equation $W_{N/2} = W^2 = \exp(2 \times 2\pi i/N) = \exp\left[2\pi i/(N/2)\right]$. It would be the correct W to use for a sequence of N/2 points. Inspection of Equation (54) shows that, indeed, for $k_0=0$ the (N/2)-point discrete Fourier transform of the even-indexed X values is calculated, while $k_0=1$ gives the (N/2)-point transform of the odd-indexed X values. Comparison of Figures 13(a) and 13(b) should illustrate this property; the stage in Figure 13(b) labeled $A_3$ gives two independent 8-point transforms, interleaved.

This special case shows the procedure to follow in the general case. By working with Equation (53), it can be seen that $A_p$ can be interpreted as $M = N/2^P$ independent L-point transforms, $L=2^P$, interleaved or multiplexed as described above. These statements are also true of the processor, since it is a mechanization of Equation (53). The output appears in the same channel sequence as the original data. The same spectral component of each channel of data is calculated before the frequency is changed. This arrangement is ideal for pulsed radar (such as SAR) or sonar, where the data for a number of range bins are received before the next samples for each range bin arrive. Figure 16 shows the operation of the processor of Figure 15 in performing 8-point transforms on two interleaved data channels.

A "breadboard" real-time FFT processor to provide spectral analysis for a tracking pulse-Doppler radar was built, using this design [35]. It was composed of nine processing modules (as in Figure 14), a synchronizer, A-D converter, and display. The processing modules employed a total of 2600 TTL integrated circuits for switching and arithmetic functions, and a total of five hundred 200-bit MOSFET shift registers for delay. The machine simultaneously processed eight channels, at a sample rate of 16K complex samples per second per channel, with a transform length of 512 complex samples and a quantization of 24 bits per complex sample. Therefore, the throughput rate was 128K samples per second, or over three million bits per second.

| | Stage 3 DELAY $2^3$=8 | | Stage 2 DELAY $2^2$=4 | | | Stage 1 DELAY $2^1$=2 | | | OUTPUT | |
|---|---|---|---|---|---|---|---|---|---|---|
| IN | OUT | | IN | OUT | | IN | OUT | | | |
| | Next Stage | Delay Line | | Next Stage | Delay Line | | Next Stage | Delay Line | Channel 1 | Channel 2 |
| X(0) | --- | --- | | | | | | | | |
| Y(0) | --- | --- | | Filling | | | | | | |
| X(1) | --- | --- | | | | | | | | |
| Y(1) | --- | --- | | | | | | | | |
| X(2) | --- | --- | | | | | of | | | |
| Y(2) | --- | --- | | | | | | | | |
| X(3) | --- | --- | | | | | | | | |
| Y(3) | --- | --- | | | | | | | | |
| X(4) | A1(0) | A1(4) | A1(0) | --- | --- | | | | Pipeline | |
| Y(4) | B1(0) | B1(4) | B1(0) | --- | --- | | | | | |
| X(5) | A1(1) | A1(5) | A1(1) | --- | --- | | | | | |
| Y(5) | B1(1) | B1(5) | B1(1) | --- | --- | | | | | |
| X(6) | A1(2) | A1(6) | A1(2) | A2(0) | A2(2) | A2(0) | --- | --- | | |
| Y(6) | B1(2) | B1(6) | B1(2) | B2(0) | B2(2) | B2(0) | --- | --- | | |
| X(7) | A1(3) | A1(7) | A1(3) | A2(1) | A2(3) | A2(1) | A3(0) | A3(1) | F(0) | |
| Y(7) | B1(3) | B1(7) | B1(3) | B2(1) | B2(3) | B2(1) | B3(0) | B3(1) | | G(0) |
| X(8) | --- | --- | A1(4) | --- | --- | A2(2) | --- | --- | F(4) | |
| Y(8) | --- | --- | B1(4) | --- | --- | B2(2) | --- | --- | | G(4) |
| X(9) | --- | --- | A1(5) | --- | --- | A2(3) | A3(2) | A3(3) | F(2) | |
| Y(9) | --- | --- | B1(5) | --- | --- | B2(3) | B3(2) | B3(3) | | G(2) |
| X(10) | --- | --- | A1(6) | A2(4) | A2(6) | A2(4) | --- | --- | F(6) | |
| Y(10) | --- | --- | B1(6) | B2(4) | B2(6) | B2(4) | --- | --- | | G(6) |
| X(11) | --- | --- | A1(7) | A2(5) | A2(7) | A2(5) | A3(4) | A3(5) | F(1) | |
| Y(11) | --- | --- | B1(7) | B2(5) | B2(7) | B2(5) | B3(4) | B3(5) | | G(1) |
| X(12) | A1(8) | A1(12) | A1(8) | --- | --- | A2(6) | --- | --- | F(5) | |
| Y(12) | B1(8) | B1(12) | B1(8) | --- | --- | B2(6) | --- | --- | | G(5) |
| X(13) | A1(9) | A1(13) | A1(9) | --- | --- | A2(7) | A3(6) | A3(7) | F(3) | |
| Y(13) | B1(9) | B1(13) | B1(9) | --- | --- | B2(7) | B3(6) | B3(7) | | G(3) |
| X(14) | A1(10) | A1(14) | A1(10) | A2(8) | A2(10) | A2(8) | --- | --- | F(7) | |
| Y(14) | B1(10) | B1(14) | B1(10) | B2(8) | B2(10) | B2(8) | --- | --- | | G(7) |
| X(15) | A1(11) | A1(15) | A1(11) | A2(9) | A2(11) | A2(9) | A3(8) | A3(9) | F(8) | |
| Y(15) | B1(11) | B1(15) | B1(11) | B2(9) | B2(11) | B2(9) | B3(8) | B3(9) | | G(8) |
| X(16) | --- | --- | A1(12) | --- | --- | A2(10) | --- | --- | F(12) | |
| Y(16) | --- | --- | B1(12) | --- | --- | B2(10) | --- | --- | | G(12) |
| X(17) | --- | --- | A1(13) | --- | --- | A2(11) | A3(10) | A3(11) | F(10) | |
| | | | | | | | | | . | |
| | | | | | | | | | . | |
| | | | | | | | | | . | |

Figure 16. FFT Pipeline Diagram, 2 Interleaved Channels, N=8 Each

A design of this type shows some promise for the SAR processing case. The scrambled order of the output is no drawback, it has been seen. A rate of 16K samples per second per channel is greater than is needed; in the example cited in Section IV.B.4, the PRF was 3.5K samples per second. Therefore, with minimal modifications, the Groginsky-Works processor could perform 128-point transforms on 32 data channels in real time, using two fewer stages than the processor described above. Forty-two such processors would be sufficient to perform forward transforms for 1334 range bins; forty-two more could inverse-transform the products with reference function spectra, to provide the final results. Such an organization would involve 84 separate processors, plus the circuitry for performing multiplications, instead of the 1334 processors in Gerchberg's design.

And the specifications of the processor described in the Groginsky-Works 1969 article are certainly not the ultimate. These authors noted that only the words entering the arithmetic unit from the delay lines require multiplication by rotation vectors; consequently, some of the delay time could be employed in performing the multiplications. They then considered the advantages of using pipeline multipliers for this purpose, and concluded: "A pipeline FFT processor employing pipeline multipliers could have a throughput rate limited only by the speed of available adders. This speed is presently in excess of 100 million bits per second." [35]

The processor just described is one example of a hardware FFT machine. Other designs are possible; some examples will simply be mentioned, without detailed analysis. Zukin and Wong [37] described an all-digital signal processor for a high PRF radar, that works in real time and replaced larger, heavier, and more expensive analog equipment. The processor includes an analog-digital converter that performs 585,144 eight-bit conversions/second. Pease [38] described a partially parallelized real-time FFT processor, employing some of the ideas of his earlier article [34]. The design goal was for a processor able to handle one complex datum every few hundred nanoseconds. Access time is overlapped with process time, so efficient use is made of relatively slow memories, while the arithmetic units are used with almost 100 percent efficiency.

To summarize: The conventional method of SAR processing is by means of a coherent optical system, as described in Section IV.A. In Section IV.B, the possibility of employing digital techniques was raised. The basic processing algorithm was described, and some of its details were contrasted with those for the optical method. Some variations on the basic algorithm were also discussed. One proposed on-board real-time SAR digital processor was described in detail; its specifications were found to probably be realizable within a few years. The last part of Section IV.B discussed other approaches, both software- and hardware-related. The use of the fast Fourier transform in making the processing more efficient was indicated. Three hardware FFT processors that have already been built were described, one in considerable detail. Their specifications indicate what was possible in the late 1960's. Knowledge of the rate of development in the field, as exemplified by the remarks in Section IV.B.4, gives a reasonable idea of what will be possible in a few years.

# SECTION V. SYNTHETIC APERTURE RADAR SYSTEM SIMULATOR

## A. Introduction

1. Experiment Simulator Concept. In general, the value of a computer simulation of a complex system is that it permits testing a variety of configurations, under many sets of conditions. Aside from this flexibility, a computer simulation affords a way of studying a system that may be too expensive, difficult, or dangerous to thoroughly test directly. There is no other way to realistically "flight test" a spaceborne instrument without actually flying it aboard a space vehicle. A simulator is a tool in the intelligent design of valuable data-gathering systems to be used during expensive space missions.

For the particular case of scientific instruments on satellites, a computer simulation can provide a realistic test environment for the exercise of concepts in scientific data management, as well as providing design criteria and requirements specifications for the equipment and for processing algorithms. Some specific ways in which a simulator can be used are:

1) Synthetic data can be generated to substitute for data which are physically unattainable--for example, because the instrument has not yet been flown in space.

2) The existence of data-sensitive errors in experiment software can be identified, and the corrections to these errors fully tested.

3) The equipment and the software can be tested over the entire range of the data parameters, to arrive at a suitable design to carry out the desired experiment plan.

A simulation of a complete synthetic aperture radar system is described in subsequent parts of this Section. Some examples are shown, to give an idea of the usefulness this simulator might have in preparing to use SAR as a satellite-borne remote sensor. The simulator is capable of providing information on image quality, and can be used to study possible tradeoffs between image quality and processor complexity. This is one of the design tradeoffs that must be investigated in payload planning.

2. Overall Concept of Simulator. The term "synthetic aperture" refers to mathematical operations applied to the signal in such a way that the image map is affected in the along-track dimension only. The total processing consists of similar operations applied separately to the fractions of the return signal from each slant range. So the simulator works with one "range bin" at a time. The complete simulator consists of four functional subdivisions:

1) A target model and provision for both internal target generation and input of external targets.

2) A radar system module, with flexibility in the choice of parameters of the transmitter, antenna and receiver.

3) A preprocessor/processor system, capable of simulating any degree of focusing, as well as certain techniques for reducing image graininess and decreasing storage requirements. Simulation of digital processors with a wide range of word lengths is possible.

4) Provisions for assessing system performance. These include statistical analyses at various points, tabulations of essentially every variable in the program, plots, and hard-copy image output.

This simulation is based on one developed by Gerchberg for use in a study of the feasibility of digital techniques for processing SAR data [9].

## B. Structure of Simulator

SAR processing reduces the time-bandwidth product of the received azimuth signal from a value T times B to unity and, in so doing, reduces the azimuth resolution length by the same factor, from the length of the region illuminated by the radiated beam to the final resolution length.

The radar antenna is characterized by its two-way pattern, which has a shape (gain as a function of position) and a beamwidth. From the foregoing, the length of ground scene illuminated by the antenna beam is TB times the resolution length. So the length of a resolution cell is a natural basic unit of measurement, whose use provides considerable dimensional simplification. Section II.A showed that the azimuth resolution length $\rho_a$ and the antenna length $D_h$ are related by

$$\rho_a = D_h/2 \tag{55}$$

Therefore, the above discussion shows that several system parameters are lumped together by

$$N = TB = (\lambda R/D_h)/(D_h/2) = 2\lambda R/D_h^2 \tag{56}$$

where N is the number of resolution cells encompassed by the antenna beam in the along-track direction, $\lambda$ is the wavelength of the radiated signal, and R is the slant range to the range bin being considered.

In the next section, it will be shown that a reasonable target model consists of a linear array of equally spaced point scatterers, at least one per resolution cell. Therefore, the distance between point targets is a natural "sub-unit". The minimum required pulse repetition frequency (PRF) to avoid aliasing is one pulse per time interval in which the radar antenna moves a distance equal to the length of a resolution element. The simulation avoids a fixed PRF and achieves slightly more flexibility by expressing the PRF in terms of the number of point target intervals between pulses. Thus the vehicle velocity is taken out, and time units are expressed in terms of equivalent distance units. The simulator combines essentially all dimensional units into the number of resolution cells encompassed by the antenna beam, the number of point targets per resolution cell, and the number of point targets incremented between pulses.

Figure 17 is a system diagram of the simulator.

1. Target Model and Data Representation. The pulsing of the transmitted signal causes each received azimuth history to be a sampled signal. It would appear that a target model which is an array of equally spaced points, such that the spacing between target points is no greater than the spacing between pulses, is adequate. This supposition is verified by Moore and Thomann [28]. It can be shown that a reasonable model of terrain as a radar target is a grouping of point scatterers whose voltage reflection coefficient amplitudes are Rayleigh distributed and whose voltage reflection coefficient phases are uniformly distributed between $-\pi$ and $\pi$. Assuming such a model, the SAR system obtains one sample per range bin with each pulse. If the radar effectively observes each resolution cell once in passing, it obtains one sample from a Rayleigh distribution (in amplitude). This is because the scattered waves from every point of the resolution cell add up to produce a resultant interference pattern which may consist of many lobes. Since the direction of incidence for the radar wave is seldom normal to the mean surface, the main lobe is usually away from the radar antenna and the backscatter is made up of minor lobes. Thus, a sample might come from a strong lobe, or it might come from a null between lobes. This causes a "speckling" effect observed on coherent radar images. In the model, targets which comprise a single terrain category are assumed to have a mean amplitude of reflection coefficient which is proportional to the square root of the differential scattering cross section of the target category; the points have their amplitudes Rayleigh distributed and their phases uniformly distributed [9,28].

The simulator has the ability both to generate several types of target lines and to input targets from external sources. The internally generated targets are, in effect, test patterns. The external target option gives the user considerable flexibility in inputting targets or actual radar receiver output signals to the simulator.

a. Internally-generated targets. The CYCLE pattern is designed for checking the frequency response of the processor, and is also used

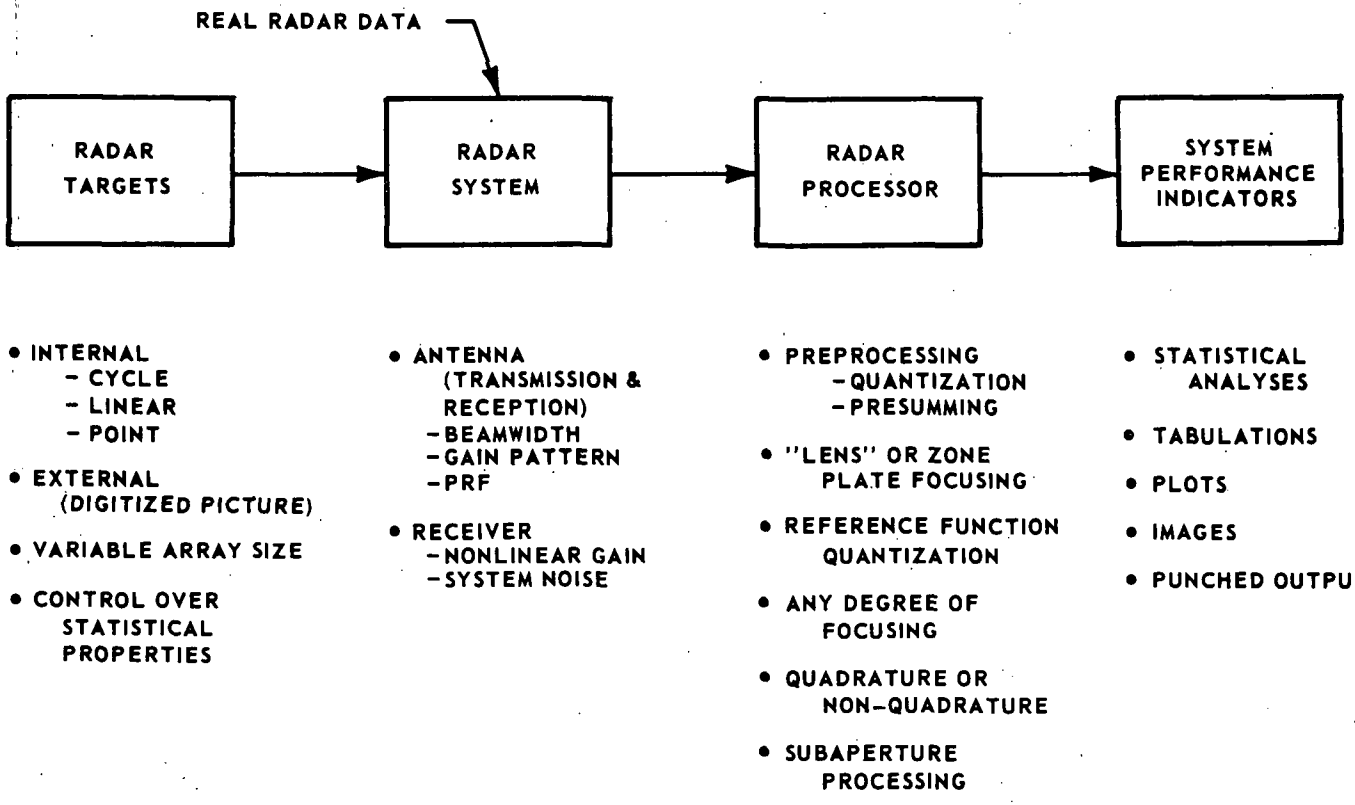


FIGURE 17. SYNTHETIC APERTURE RADAR SIMULATOR SYSTEM DIAGRAM

for measuring the image signal to noise ratio of the image of a class of targets arising from a single statistical population. The CYCLE pattern is a target line consisting of a series of highs and lows (of mean target reflection coefficient amplitudes) of equal size, with varying frequency. The basic pattern has a certain number of point targets with high amplitude, followed by an equal number of points with low amplitude. There are a certain number of cycles of this frequency, followed by an equal number of cycles with one more point in each half cycle, and so on, until the maximum period is reached. The user specifies the high and low amplitudes, the minimum and maximum number of points per half cycle, and the approximate number of points; the program (generally) increases the total number of targets in the line so there are the same number of cycles of each period. The amplitudes are either constant, equal to the user-supplied values, or "statistical", in which case they are Rayleigh-distributed pseudo-random numbers with means of 1.25 times the user-supplied constants. The target voltage reflection coefficient phases may (independently of the choice for the amplitudes) be chosen equal to a specified constant, or uniformly distributed between $-\pi$ and $\pi$.

As an example, suppose a target line of approximately 100 targets is called for, with periods ranging from 3 per half cycle to 5 per half cycle. The resulting line will have five cycles each consisting of 3 "high" point targets and 3 "low" point targets, followed by five cycles of 4 "high" point targets and 4 "low" targets, then five cycles of 5 "highs" and 5 "lows" each. The total number of points in the target line would be 120, automatically increased by the program from the user-supplied approximate value of 100.

If the same number is specified for both the "high" and "low" amplitudes, the program automatically performs a statistical analysis of targets, returns, and image lines in the manner described in a later section of this report. If the target reflection coefficient amplitudes and phases are both statistically chosen, this feature provides a statistical analysis of the performance of the system being modeled against targets drawn from a particular population.

The LINEAR pattern is designed to help measure some of the effects of nonlinear system operation. It consists of a target array with linearly increasing reflection coefficient amplitudes. The amplitudes are deterministic; the reflection coefficient phases may be either all equal to a specified constant, or chosen from a uniform distribution.

The POINT target option simulates a point, or delta function, target reflection coefficient amplitude. Therefore, it is a very useful analytic tool, essentially allowing the impulse response of the simulated system to be measured. Also, the option is a valuable aid in illustrating the theory. Both the amplitude and phase of the (single nonzero) target reflection coefficient may be constant or statistically chosen. The latter option is especially helpful for investigations of phase-sensitive (e.g., not involving quadrature detection) processors.

The simulator also contains a tape storage option, which allows the saving of targets and returns on an intermediate storage file. Therefore, it is possible to test a host of receiver-processor combinations on a given target configuration at a considerable saving in computer time. Because of this partitioning, the simulation up to the input to the radar receiver only needs to be carried out once in such a study.

Section V.C includes examples of each of the internally generated target types which illustrate the foregoing discussion.

b. Externally input targets. A tape containing arbitrary image data (e.g., a digitized representation of a picture produced by a scanning microdensitometer) may be used as basic target input data. The simulation program multiplies each number (amplitude) by a pseudo-random number drawn from a Rayleigh distribution with a mean of 1.25 and variance of 0.43 and supplies a phase for each point uniformly distributed between $-\pi$ and $\pi$. In this way the data are transformed into a form more nearly resembling actual radar data.

This option extends the flexibility of the simulator considerably. If the source of data is an actual radar image, digitized and treated as described above, the simulation becomes remarkably realistic. Because of this input option, the range of target types which may be used becomes virtually unbounded.

The tape storage option described in the preceding section is available for externally input targets as well as for those which are internally generated. This option makes it possible (by producing a tape in the proper format) to use actual radar receiver output as input data to the simulation.

2. Radar System. The radar system modeled by the simulator is shown schematically in Figure 18. The transmitter is characterized by its operating frequency or wavelength, the pulse repetition frequency (PRF), and the pulse modulation (both amplitude--pulse width--and phase, e.g., "chirp" modulation). It was already shown how the wavelength of the transmitted signal and the PRF are absorbed into the units used in the program (see Equation (56) and the discussion following it). And since the simulation only considers a single range bin, features of the pulse modulation are irrelevant. Therefore, the characteristics of the radar transmitter are handled very simply by the simulator. The antenna and receiver, however, involve considerably more.

a. Antenna and construction of received signal. As was pointed out previously, the "size" of the antenna--the length on the ground encompassed by the nonzero extent of the antenna beam--measured in "nominal" resolution cell lengths, is the time-bandwidth product TB. More precisely, an antenna pattern of uniform gain and the same beamwidth as the actual antenna would provide a return signal from a point target which is a chirp (linear FM) signal of duration T and bandwidth B. The

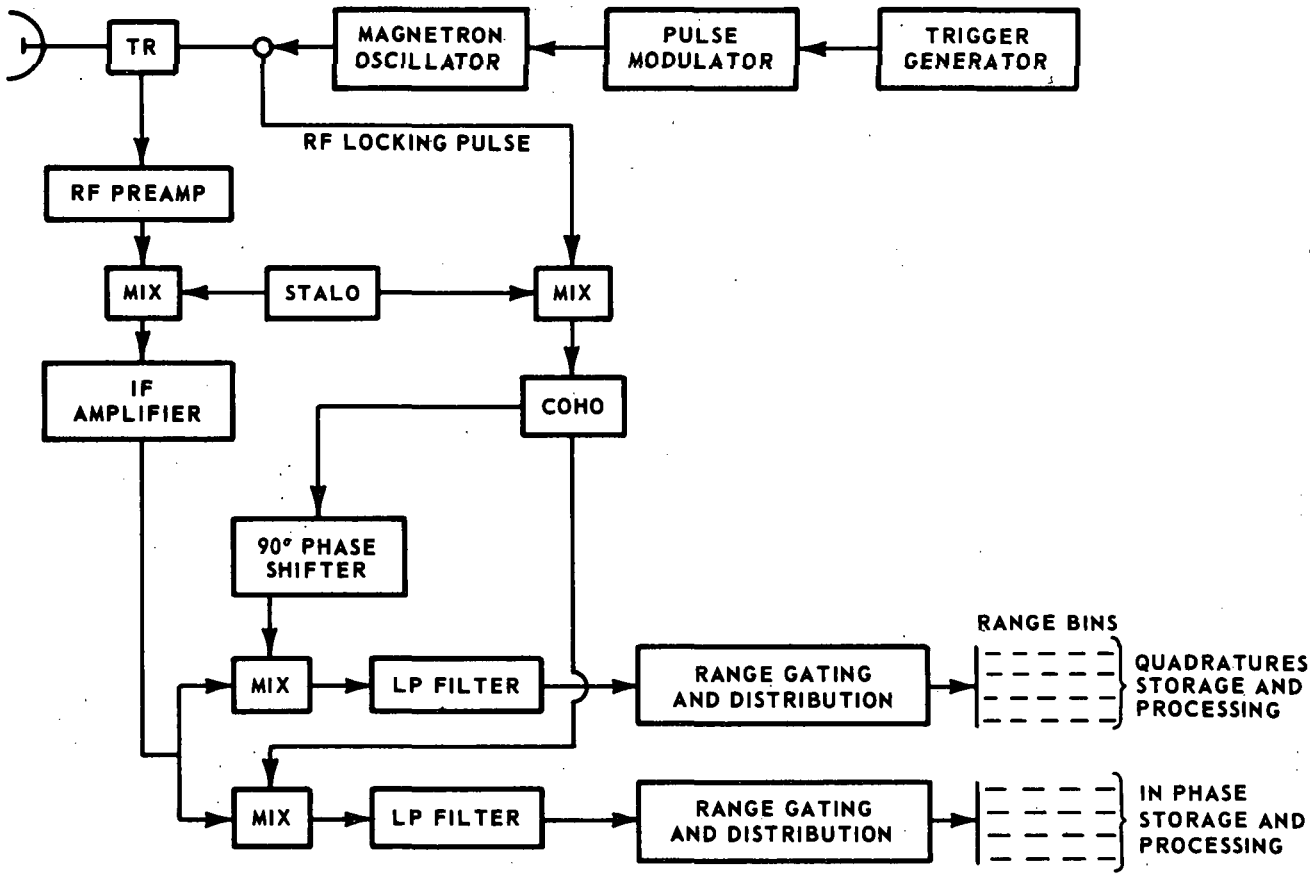


FIGURE 18. SCHEMATIC OF SAR SYSTEM SIMULATED (FROM REFERENCE 9)

resolution which can be attained is such that the number of resolution cells is equal to TB.

Therefore, the time-bandwidth product, and the number of target points per resolution cell, define (for the simulation) the length of the antenna--the number of point targets encompassed by the antenna beam. One return is generated for each position of the antenna beam containing at least one point target. The beam may be visualized as sweeping over the target array. The increment between returns (equivalent to the PRF), in terms of the distance between point targets, is specified as an input quantity.

The return at each position of the antenna is a sum over all the target points in the beam. The amplitude of each term is the product of the voltage reflection coefficient amplitude associated with the point and the relative magnitude of the two-way antenna pattern at that point. The phase of each term in the sum is the target reflection coefficient phase plus a phase factor due to the difference in two-way path lengths between the antenna and the different points on the ground. This may be expressed as a convolution.

To see this, let x be the position coordinate of the radar antenna in its line of motion, and let R(y) be the complex voltage reflection coefficient of a target point at along-track position y. If G(x-y) is the value (gain) of the antenna pattern at the point on the ground, when the antenna is at x, then the contribution from that point to the return signal is $R(y)\ G(x-y)\ \phi(x-y)$, where $\phi(x-y)$ is a phase factor which accounts for the two-way path length between the antenna and target. The total return signal from that range bin is then

$$S(x) = \int R(y)\ G(x-y)\ \phi(x-y)\ dy \qquad (57)$$

where the range of integration is over all points y at that slant range in the beam of the antenna, when the latter is at x. Since, by definition, the antenna gain vanishes outside the beam, the limits of the integral may be made infinite. Clearly, then, Equation (57) is a convolution integral. Although the fast Fourier transform has made it more practical in some cases, the calculation of a convolution on a computer is a time-consuming procedure. The great amount of computation required to generate the receiver output emphasizes the value of the intermediate storage option described previously.

The simulator provides a choice of several antenna patterns; more are easily added.

The antenna simulation also includes a possible Doppler mismatch in the system [5]. A mismatch in Doppler frequency could occur in several ways. For instance, the antenna might be boresighted slightly away from the normal to the vehicle's velocity vector. A similar effect could be

caused by the return signal's being mixed with a local oscillator signal at a slightly wrong frequency in performing the coherent detection. Reference 5 discusses the distortion caused by such errors.

b. Radar receiver. The simulation of the receiver includes both system noise and distortion due to gain which is a function of the amplitude of the received signal's voltage. The noise is taken to be narrow-band Gaussian additive noise and is added to the signal according to Rice's scheme [39]. After combination of the signal and the noise, a possibly nonlinear receiver gain characteristic is applied. The general form of the gain curve is a linear function of input voltage up to a breakpoint value and a logarithmic function above this value. Explicitly

$$\begin{aligned} \left|V_{OUT}\right| &= K\left|V_{IN}\right| && \text{for } \left|V_{IN}\right| \leq D \\ &= DK + P \log_{10}\left(\left|V_{IN}\right| - D + 1\right) && \text{for } \left|V_{IN}\right| > D \end{aligned} \tag{58}$$

If P=0, the receiver "limits" its output to DK (both variable). On the other hand, by making D=0 and P nonzero, a logarithmic receiver is simulated. If both D and P are nonzero, "soft limiting" is the result. Nonlinear characteristics of the data recording system may also be accounted for here [28].

3. Processor. The usual method of producing high-resolution images from SAR data is by means of coherent optical processing systems [5]. However, Gerchberg showed that digital processing, although difficult, is not impossible to perform [9]. In some cases, it is a worthwhile alternative to consider. This was discussed in previous sections, particularly Sections II.B, II.C, and IV.B.

Although this is a digital computer simulation, the processor simulated is not necessarily only a digital processor. Some configurations are explicitly digital processors, but in general the mathematical operations performed may be regarded as being performed by any type of processing system. Several processing variations may be simulated. Also, certain preprocessing operations may be performed.

Section V.C. contains examples illustrating several processing options.

a. Preprocessing modules. Quantization of the return signals may be performed. This is equivalent to digitizing the return signals into words of a specified number of bits. This may be done prior to storing the signals in a digital memory (which may or may not be part of a digital processor). One bit is reserved for the sign and the remaining bits represent the magnitude, making the total number of quantization levels $2^n$ for n-bit words.

Another preprocessing technique which reduces the storage required, although at the expense of degrading the resolution, is presumming. The simulation has the ability to sum series of returns of specified length prior to processing. That is, adjacent pairs, triples, etc., of return signal points can be added together. This reduces the required storage by a factor equal to the number of pulses summed.

b. Processing variations and options. The basic processing operation required to produce an image is correlation with a "reference function", the return which would be received from a point reflector at the same slant range, assuming a uniform (rectangular) antenna pattern. This is the same thing as matched filtering [5,9]. Figure 10 shows the processing algorithm. The procedure may be regarded as the correlation of two complex quantities, using both amplitude and phase information (in-phase and out-of-phase components). In an optical processor, this correlation with a quadratic phase function is performed by moving the signal (recorded on film) past a lens.

It is helpful to the imagination to think of the processing operation as that of focusing; in the simulation, the computer acts essentially as a digital lens. It is well known that the image of a point formed by a lens of finite size is a spot whose size is inversely proportional to the size of the aperture. In the SAR processing case, the maximum aperture length is the length of the return signal from a point target (proportional to the amount of time the target is in the beam). If optical processing is used, the aperture is actually a physical aperture whose extent is the length of the signal recorded on the film. This aperture size, therefore, determines the limiting resolution of the system. The simulator permits reduction of the length of the reference function--reduction of the size of the aperture--thereby correspondingly degrading the resolution and permitting any degree of focusing.

Still thinking intuitively, if the processing can be performed by a lens, it seems that it could also be done using a Fresnel zone plate. The rigorous mathematical confirmation of this supposition was given by Moore and Rouse, who also proposed a method of implementing this processing technique electronically [10]. The capability for "zone plate" processing exists in the simulator; every processor configuration may be simulated in the "regular" mode or in the "zone plate" mode.

In the "zone plate" mode, the reference function takes on two values: +1 and -1, altering sign in neighboring Fresnel zones. In effect, the reference function is quantized to two levels. It is also possible to quantize the reference function to any other number of levels (up to 36-bit representation), similar to the quantization described in the section on preprocessing. These quantization options make possible the simulation of a digital processor with any word length.

The SAR processing may be regarded as the synthesis of a very long array antenna, whose elements are the actual physical antenna at the positions it takes up every $(PRF)^{-1}$ seconds. The length of the synthetic

antenna is so great that the curvature of the (synthesized) wavefront received from a point reflector on the ground is significant. The "ideal" processing consists of adjusting the phase of the signal received by each element and summing the outputs. In the way the antenna is focused on each range bin. A simpler processing method is simply to sum the returns without affecting the relative phases. In this case, the length of the synthetic antenna is limited to that value such that the signals received by the end elements are not too far out of phase with respect to the center of the array. Specifically, only the first Fresnel zone can be used. This unfocused processing is "zone plate" processing with the length of the reference function equal to $\sqrt{2TB}$, in the units used in the simulator. Any other number of Fresnel zones, up to the maximum length, may be used, with either "zone plate" or regular reference functions. In short, as stated before, any degree of focusing, from full to none, may be simulated.

The magnitude of the data rate, and the associated storage requirement, were discussed in Section II; they were shown to be very large. Referring to Figure 10, a possible substantial saving can be seen. If only the portion of the processor shown as channel $A_1$--essentially, only using the real parts of the complex representations of the signal and reference function--would do the job, nearly 75 percent of the operations would be eliminated, the hardware required to implement the algorithm would be cut in half, and the storage required in the processor would be reduced by a factor of two. (Principally, electronic processing is being considered.) This was previously discussed in Section IV.B.3.

This "non-quadrature" processing is capable of doing the imaging, although the magnitude of the output is dependent on the phases of the target voltage reflection coefficients. The result is an image with equal resolution to that produced by the complete algorithm shown in Figure 10, but with a higher "clutter" level [9]. All of the processing options of the simulator can be performed using either quadrature or non-quadrature processing.

In the discussion of radar targets, it was pointed out that images produced by a SAR system have a speckled or grainy appearance. The apparent graininess of a photograph printed in a newspaper is reduced if the viewer looks at the photograph from a sufficient distance. There is a tradeoff between resolution and image quality if this is done. This observation suggested a technique for reducing the speckling of a radar image which was called "subaperture processing" by Gerchberg [9]. Simply degrading the resolution by shortening the reference function does not reduce radar image graininess. Subaperture processing, in effect, creates several synthetic aperture antennas, each with a wider along-track synthetic antenna beam than is possible with full focused processing but still much reduced in along-track width compared to the physical antenna's beam. Each of these beams is "squinted" within the width of the physical antenna's beam so that, in general, it is directed fore or aft of broadside to the physical antenna's beam. This is accomplished by using portions (which may or may not be overlapping) of the reference function in the

processing. The images from the separate subapertures are then averaged to form the final image, which has improved gray-tone quality and a linear resolution determined by the length of one subaperture. When it is recalled that the return from a point target is a linear FM signal, it can be seen that subaperture processing is a form of averaging in Doppler bandwidth. Moore and Thomann have also discussed averaging to improve radar image quality, and the worth of such techniques in geoscience applications [28].

Subaperture processing works with a smaller portion of the received signal at any one time. It can be shown that the processor storage and computation rate requirements are reduced when subaperture processing is used. Additional storage is required to perform the averaging. However, this can be extremely slow storage, which might be outside the primary processor, and involving a technology much less sophisticated than that required to perform the correlations. (Again, electronic processing is principally being considered here, although subaperture processing could be done optically.) A processing technique which can improve image quality (assuming the resulting linear resolution is adequate) while reducing computational requirements is an important consideration. The simulator has the capability to perform a generalized type of subaperture processing, in which the subapertures may be modified by weighting functions (i.e., not necessarily constant gain across a subaperture), and the subapertures may be averaged together with different weights.

In summary, the processor simulation contains several options which permit the representation of a great range of SAR processing configurations. The optimum full-focused processor algorithm may be simulated. The length of the reference function used in the processor may be reduced, decreasing the amount of computation required at the expense of resolution. "Zone plate" processing, which is relatively simple to implement electronically and produces results almost equal to the optimum algorithm, can be simulated. A digital processor working with essentially any word length can be studied with this simulator. By varying the number of bits per word and (primarily) the length of the reference function used in the correlations, any degree of focusing, from full to none, may be simulated. Non-quadrature processing, a method which in some cases produces acceptable results while reducing the amount of computation and storage required, can be used in combination with any other options. And the use of subaperture processing to reduce image graininess and improve gray-tone resolution may be studied using the simulator.

4. Output Options. The output provides both quantitative and visual measures of simulator performance, including processed image output in a form suitable for further post-processing (e.g., image enhancement). One type of output, already described, is the (intermediate) tape storage for targets and returns. The other forms of output will now be discussed in detail.

a. Tabulations. Certain tabulations are printed out automatically. At the user's request, essentially every number in the simulation

can be printed, clearly labeled as to what it is. This is not ordinarily necessary, but it provides a means of checking exactly what is going on, if there should be any doubt.

The automatically obtained printout begins with a listing of the specific configuration being simulated: details of the target arrays, PRF, antenna, receiver characteristics, type of processing and parameters involved, and certain other "bookkeeping" details of the simulation. The arrays printed are the target amplitude, the output from each subaperture, and the summation of all subaperture outputs to produce the final image (or just the image, if subaperture processing is not specified). If statistical analysis of the targets, returns, and/or image lines is called for, the results of the analysis are printed.

The optional tabulations include all the other arrays: antenna phase (relative phase shift due to the difference in two-way path length to different points on the ground), antenna pattern (gain), return signal before noise is added (unless a noise-free receiver has been specified). Also, these arrays are dumped at the end: the processor reference function (both channels), target phase and amplitude, return signal amplitude and phase, in-phase and out-of-phase receiver outputs, weighted (and quantized, if so specified) reference function (both channels), the final image, and the output of the last subaperture.

b. Plots. Plots can be obtained of the target line amplitude and phase, the return signal amplitude and phase, and the final image line. If the plot option is chosen when subaperture processing is performed, the output of each subaperture is also plotted.

c. Images. Images can be produced by processing data corresponding to a two-dimensional ground scene, one line at a time, and "stacking" the resulting output lines. This can be done in a variety of ways. The simulator has a punch option which allows the user to request that the target and/or image lines be punched out. The cards can then be used as input to a program which displays intensities. A tape containing both channels of receiver output and the image lines can also be written by the simulator. There is a post-processor program which serves as an interface to an Optronics System P-1500 Photowrite digital filmwriter (Optronics International, Inc., Chelmsford, Mass.). Images and/or simulated radar signal films can be produced.

d. Statistical analyses. Statistical analyses can be made of the target reflection coefficient amplitudes, radar return signals, and the image line generated by the processor. If subaperture processing is used, the output of each subaperture can be analyzed.

The quantities calculated are the mean, variance, covariance, and the ratio of the mean squared to the variance. In addition, a confidence interval is determined for each estimate, using a T statistic. The sampling intervals for the analyses can be specified by the user.

Apart from the general usefulness of statistical measurements, there are some specific applications. The method used to simulate receiver noise requires a knowledge of the mean value of received signal voltage at the antenna. The simulator has the proper calculations built in for the internally generated targets. However, for external targets, this value must be supplied. (A convenient way of running the simulator with external targets is to take advantage of the tape storage option described in the section on targets. The statistical analysis of returns can be performed in the run which creates the intermediate tape file. Then the processing, with many different receiver-processor combinations, may be done in a later run.) Also, the ratio of mean to standard deviation in the image of a single terrain category is a measure of the "speckling" present; a low value corresponds to a grainy image, while a larger value signifies improvement. The square of this ratio is calculated. When one considers space applications, it is clear that the length resolution of the image should be no better than is actually required, since this factor significantly affects the bandwidth of the telemetry link to transmit the image to the ground and the amount of on-board storage required (See Section II.B.) Therefore, the image mean/standard deviation ratio is an important figure of merit which shows the extent to which length resolution has been traded for gray-tone resolution by a given method of processing. It enables one to ensure that an algorithm under consideration does not degrade image gray-tone resolution to an unacceptable degree.

## C. Examples

Figures 19-23 illustrate some details of the simulation using internally generated target lines. The format is the same in each figure, three plots per page. The first two show the phase and amplitude, respectively, of the array of target points. The last plot on each page shows the corresponding image of the target line produced by the processor. Table 1 lists details of the simulator configuration in each case.

Figures 19 and 20 show the CYCLE and LINEAR target patterns, with the target phase set equal to zero for each point in both cases, and the image lines formed using the processing algorithm of Figure 10. Figures 21-23 all show the same radar system applied to a point target, but with different forms of processing. This series of figures illustrates the theory admirably. The return signal's amplitude is a square pulse, nonzero over the interval during which the point target intercepted the antenna beam; the return signal's phase is quadratic. (This discussion assumes the carrier has been removed.) This is the type of signal known as "linear FM", a pulse compression waveform. A property of this signal is that its spectrum has approximately the same form as the signal itself [5,9]. Figure 21 shows the result of perfect removal of the quadratic phase factor in the spectrum. The image line is the inverse Fourier transform of the function whose magnitude is a square pulse and whose phase is zero. It is a close replica of the target amplitude line. The nonzero target phase had no effect.

Table 1. Cases Portrayed in Figures 19-23

| Figure | Target Type | System Parameters | Processing |
|---|---|---|---|
| 19 | CYCLE, Phase=0 | 1 target/res. cell, pulse period=target spacing, flat antenna gain | full focused, quadrature, flat weighting function |
| 20 | LINEAR, Phase=0 | 6 targets/res. cell, pulse period every 3rd target, flat antenna gain | full focused, quadrature, flat weighting function |
| 21 | POINT, Phase=$-\pi/2$ | 5 targets/res. cell, pulse period every 2nd target, flat antenna gain | full focused, quadrature, flat weighting function |
| 22 | POINT, Phase=$-\pi/2$ | 5 targets/res. cell, pulse period every 2nd target, flat antenna gain | full zone plate, quadrature, flat weighting function |
| 23 | POINT, Phase=$-\pi/2$ | 5 targets/res. cell, pulse period every 2nd target, flat antenna gain | unfocused, quadrature, flat weighting function |

Figure 22 shows the result of zone plate processing. The behavior is similar to what Moore and Rouse predict [10]. The close target resolution is the same as in Figure 21, and the principal sidelobes are also virtually the same. Only the "clutter" levels are higher, leading one to believe that zone plate processing will produce a noisier image than the optimum algorithm. Figure 23 illustrates unfocused processing, which is simply accumulation of the return signal without phase compensation, where the number of terms in each sum (each output point) corresponds to the length of the first Fresnel zone. The along-track resolution is gross and the sidelobe level is high compared to the two preceding figures.

Figure 24 shows two simulated radar images, derived from an actual radar image used as a target, as described previously. The rectangular shapes are agricultural fields. The top image was produced using the algorithm shown in Figure 10, unmodified. The bottom image shows the effect of subaperture processing, using five non-overlapping subapertures encompassing the full length of the reference function. The top image has higher resolution, but it is very grainy. When viewed from a slight distance, the improved contrast of the bottom image is quite evident. The effect is particularly noticeable in the lighter areas.

Figure 25 continues the progression toward a specific processor simulation. The top image was produced similarly to the bottom image of

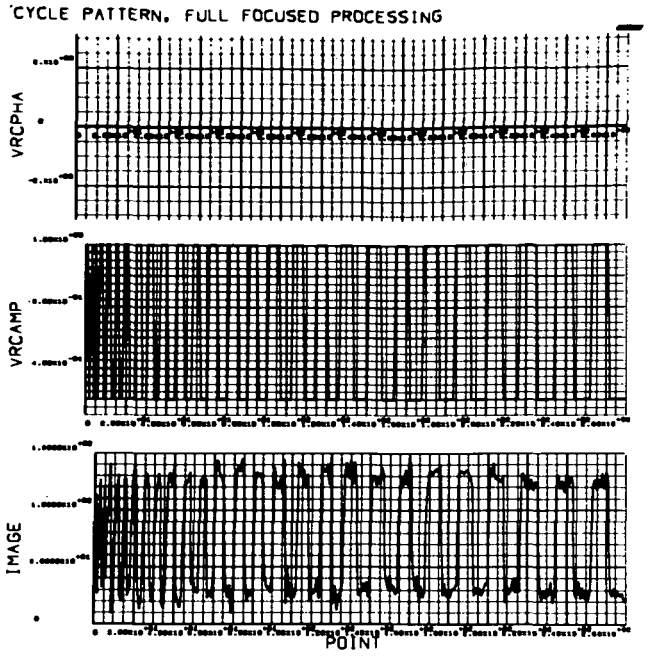


Figure 19. Cycle Target Pattern, Full Focused Processing

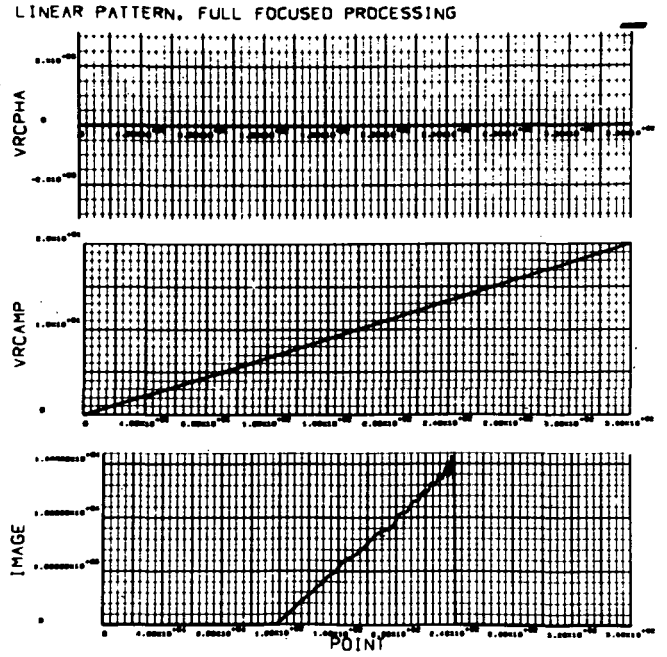


Figure 20. Linear Target Pattern, Full Focused Processing

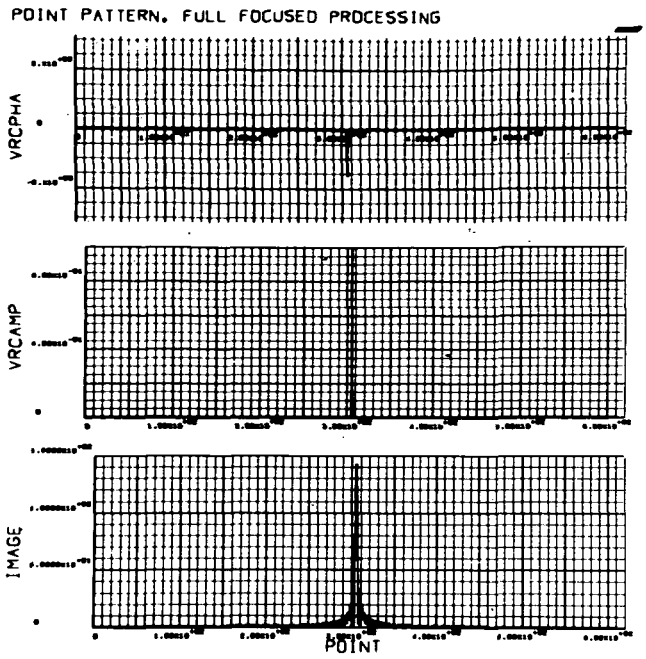


Figure 21. Point Target Pattern, Full Focused Processing

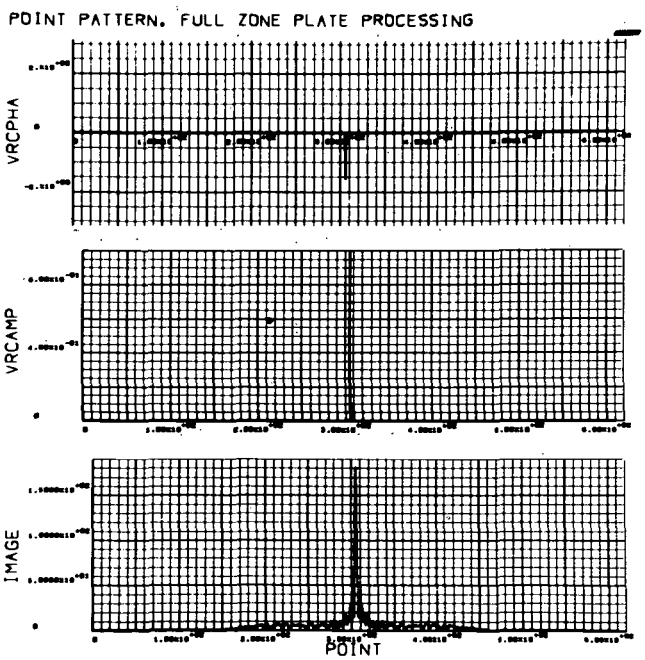


Figure 22. Point Target Pattern, Full Zone Plate Processing

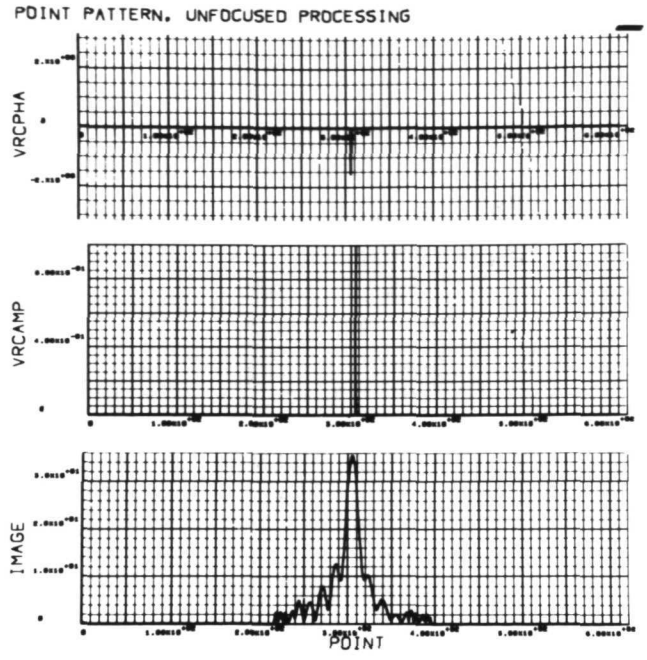


Figure 23. Point Target Pattern, Unfocused Processing

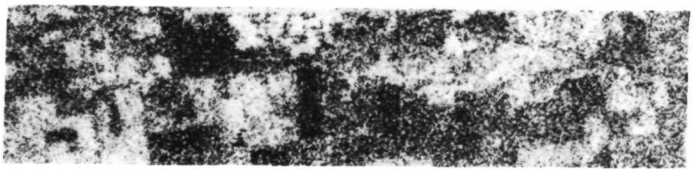

Unmodified Matched Filter Algorithm

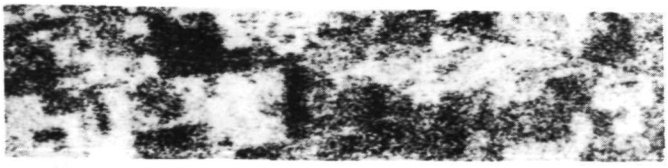

Subaperture Processing, Average of Five
Non-Overlapping Subapertures

Figure 24. Computer Generated SAR Images--Comparative Processing Study

Non-Quadrature Algorithm, Subaperture Processing

Same, as Produced by Digital Processor Utilizing Five-Bit Words

Figure 25. Computer Generated SAR Images--Continuation of Comparative Processing Study

Figure 24, except that non-quadrature processing was used. As pointed out previously, this could reduce the hardware and storage requirements for the processor, at the expense of a somewhat noisier image. It is noted that the image is still less noisy than that produced using the "optimum" algorithm. The bottom image in Figure 25 was processed by the same algorithm as the top image. However, a digital processor utilizing five-bit words was specifically simulated here. There was virtually no image degradation.

# SECTION VI. CONCLUSIONS

When the first pictures of the Earth from the perspective of space were published, the single fact that became apparent to the greatest number of people was the limited extent of what had often seemed infinite before--our environment. Other pictures showed that the rapid synoptic coverage of observations from space might provide the best method of obtaining information that would be of use in understanding and managing the world's resources, both natural and man-made.

Except for previous efforts on a small scale, the remote sensing of earth resources is a new field. An example of the sort of remote sensing that has been done for some time is aerial photography. The worth of this technique has been obvious, but the magnitude of a large-scale mapping job in a short time has been such as to make it uneconomical, except in certain special applications such as military reconnaissance, where the need outweighs the cost. Now, when the need for understanding our environment and the way we use it has become pressing, a new tool is available. The artificial satellite makes it possible to view large areas in short periods of time. For example, the Earth Resources Technology Satellite observes virtually the entire world once every eighteen days.

A new technology, remote sensing, is developing to meet the challenge. This multidisciplinary field brings together work in a number of formerly distinct areas. Previously known instruments are being refined and improved, and new ones are being developed. Concurrently, techniques for using the sensors and handling and interpreting the data they acquire are being worked on. A major new problem involves the management of the quantity, and rate, of data from satellite-borne remote sensors.

One instrument considered a valuable candidate for the remote sensing of earth resources is side-looking synthetic aperture radar. SAR has one of the highest data rates of all proposed remote sensors. This report deals with handling the data produced by this sensor, and getting it to the users rapidly without loss of significant information. Topics covered include the basic principles of SAR, estimation of the data rate for the Earth-orbital case, the detailed mathematical theory of the signal processing, discussions of processing techniques (both brief and detailed), and a description of a computer simulation of a complete SAR system, including processor. A major section of this report discusses the possibility of digital processing of the synthetic aperture radar signal.

The use of a coherent optical processing system to form an image from SAR data, recorded on film, has been a very elegant and satisfactory method in the past. However, the possibility of using synthetic aperture radar in certain specialized earth resources space missions changes the relative importance of various factors, and may dictate other means of storing and processing the data.

For example, if a synthetic aperture radar system is to be operated in an unattended mode on a free-flying Research Application Module (RAM), such things as "consumables", telemetry data rates, etc., become important considerations. Entirely different data storage and processing concepts may possess advantages in such an environment of partial or full automation. It may be desirable to make some processed data available to a principal investigator on the ground shortly after the acquisition of raw data in such an unattended, long-duration mission. Several levels of on-board automation, from very limited to total closed-loop control, are possible. For effective usage in the context of the total spacecraft system, it may be crucial that the SAR data be in a form which is computer-compatible.

The conventional technique for processing SAR data, described in the literature, is to use a CRT-film recorder combination to record the received signals, and then use the processed "signal film" as input to a coherent optical processor. Moore and Thomann discuss the difficulty caused by the nonlinearity and limited dynamic range of this type of recording system; they recommend the use of other methods for recording the data [28]. Magnetic tape recorders are felt to be preferable from the standpoints of cost and complexity. Other problems arise in a spaceborne system. It is likely that the users of the processed imagery will be on the ground. For long-term satellite missions, the problem of getting the data to the user may be formidable. The raw data rate is so great that it may not be practical to transmit it to the ground as it is acquired. Transporting exposed film to the ground risks accidental loss of the data. On the other hand, on-board photographic processing might create logistics problems, and the possibility of radiation fogging of exposed film during long-term storage must be considered. The operation of an optical processor presents its own problems, particularly if one comtemplates doing it by automatic machinery on an unmanned spacecraft.

This listing of potential areas is only illustrative; it is not meant to be complete. The point is that a tradeoff study is needed in preparation for actual missions, weighing costs against benefits for the various possible approaches. Optical techniques are being actively developed, and some of the limitations of current systems may be overcome in the next several years. However, if one considers applying new technology to the problem considered here, it is reasonable to evaluate possible electronic techniques as well. It should be noted that the second-generation data system proposed in the report of the National Academy of Sciences Woods Hole conference alluded to on-board digital processing of SAR data [8]. Gerchberg found that the concept of real-time digital processing of data obtained by a satellite-borne SAR system is tenable; he sketched the design of a "1975 SAR System with Real-Time Digital Processing" which applied an incoherent integration technique (subaperture processing) to trade excess bandwidth (hence resolution) for image quality, at the same time reducing the data rate [9]. Significant problems are concerned with fast analog-to-digital converters and high-density storage (particularly power requirements). Indications are that these problems are being solved.

A numerical example may help express some of the foregoing ideas in concrete terms. Preliminary estimates have indicated that imagery possessing a resolution of 25 m. would contain sufficient detail to be of value in contemporary research studies in several fields in which the use of SAR has been discussed: geology [40], the study of ice conditions [41] and the determination of sea ice drift [42], the detection of oil slicks [43], and other pollution and environmental studies [44]. Table 2 presents reasonable and representative parameters for an SAR system on an earth observations satellite. Assuming equal along-track and cross-track resolution lengths are desired, the data rate is $30.1 \times 10^6$ samples/sec for 2.25 m. resolution. The rate of hundreds of millions of bits per second required to transmit raw data from the satellite to the ground in real time is a key input to the tradeoff study referred to previously. At this data rate, storage could become a problem fairly quickly, too. If it were possible to process the raw data in real time and reduce the resolution from the possible value of 2.25 m. to the required value of 25 m., the data rate would be reduced to approximately $22 \times 10^4$ samples/sec.

Table 2. Representative SAR Design Details

| | |
|---|---|
| Orbital Altitude | 500 km. (270 n.mi.) |
| Orbital Speed | 7.62 km./sec. (4.11 kt.) |
| Swath Width | 20 km. (10.8 n.mi.) |
| Antenna Dimensions | 4.5 m. x 1.5 m. |
| Antenna Boresight Direction | $45^\circ$ from nadir |
| Radar Carrier Frequency | 10 GHz |
| Radar Carrier Wavelength | 3 cm. |
| Best Possible Azimuth Resolution | 2.25 m. |
| Minimum Required PRF | $3.39 \times 10^3$ pulses/sec. |

Alternatives to current storage and processing techniques should certainly be considered for satellite-borne synthetic aperture radar systems. The intent of the simulator (described in the foregoing section) was to make it possible to simulate the imaging performance of various radar systems against diverse targets. With its several performance-measuring features, including actual image output, it can be used for assessing the effectiveness of different radar/processor combinations. For example, a processing technique which reduces the amount of storage required, but severely degrades the image quality, is not a good solution to the design problems. A simulator could be used to study problems of this type. Various modular configurations could be considered for experimentation, permitting a hardware/software tradeoff between preprocessor

and processor elements, as well as determination of the most satisfactory form of the processing algorithm.

The problem of handling the data produced by SAR is complex. The raw data rate is so high that a very wideband channel would be required to transmit it directly to the ground. One approach would be to record the data and play it back more slowly for transmission to the ground. Practical bounds on storage capacity limit this technique. Film recording and optical processing are attractive methods for handling the large volume of data and doing the multichannel range-dependent processing. However, serious problems associated with this method have been indicated. The high data rate is due to the high resolution inherent in the data--higher than is actually needed. If real-time processing to obtain the desired resolution could be performed, the data rate would be cut by a factor of around 100, making telemetry that much more feasible. It appears that digital processing to achieve this is possible, but the problem of design of the processor is not trivial.

There is no clearly defined best method of solving the problem that is the subject of this report. It is necessary to choose the most practical compromise, the solution that produces the best results possible at the desired time, with allowable development cost. This report has attempted to gather a summary of the relevant topics into one place, to serve as a convenient starting point for future study.

## APPENDIX A

## FUNDAMENTAL OPTICAL PRINCIPLES

One of the basic ideas of physical optics is Huygens' principle [16]: If a light source is surrounded by a closed surface $\sigma$, the disturbance produced by the source can reach the region of space beyond $\sigma$ only by traversing this surface. Huygens' principle regards the disturbance in the outer region as caused by the disturbance at the surface $\sigma$; that is, the various points of the surface $\sigma$, when reached by the wave, become the origin of secondary waves, and the disturbance observed beyond the surface $\sigma$ results from the superposition of these secondary waves.

If one considers the light "disturbance" at a particular point P caused by the light source, or by several sources, Huygens' principle considers the disturbance at P as resulting from the superposition of secondary waves that proceed from a surface surrounding P. The function of the arbitrary surface in Huygens' principle is to divide space into two regions: one containing the light source or sources, and one containing the point at which the light disturbance is measured (or evaluated). Figure A1 illustrates the situation.

It was shown by Kirschhoff that Huygens' principle was an approximate form of a certain integral theorem, which expresses the solution of the homogeneous wave equation at an arbitrary point in the field in terms of the values of the solution and its first derivatives at all points on an arbitrary closed surface surrounding the point [17]. The formulation is in terms of a scalar field, which may be thought of as a single polarization component of an electromagnetic wave. Alternatively, it can be shown that, because of the very high frequencies of optical fields, in the majority of problems encountered in optics an approximate description in terms of a single complex scalar wave function is adequate [17].

For the purposes of this discussion, it is sufficient to consider monochromatic scalar waves. Then the time dependence may be separated out, reducing the scalar wave equation to the Helmholtz equation,

$$(\nabla^2 + k^2)\, E(x, y, z) = 0 \qquad \text{(A1)}$$

where $E(x, y, z)$ describes the spatial variation of the scalar waves, $k = 2\pi/\lambda = \omega/c$, and $\lambda$ and $\omega$ are the wavelength and angular frequency, respectively. By using Green's theorem, it may be shown that the field satisfying (A1) at the point $P = (x, y, z)$ is

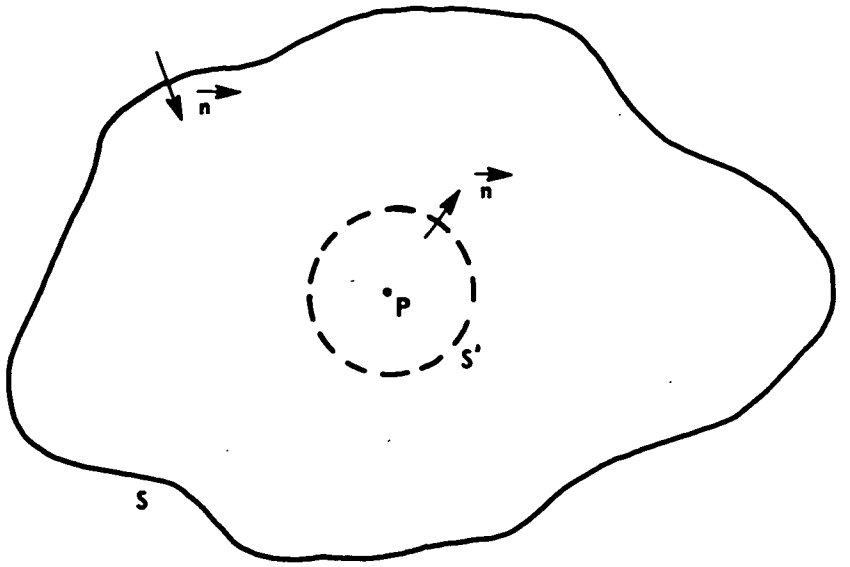


FIGURE A1. REGION OF INTEGRATION FOR KIRCHHOFF INTEGRAL

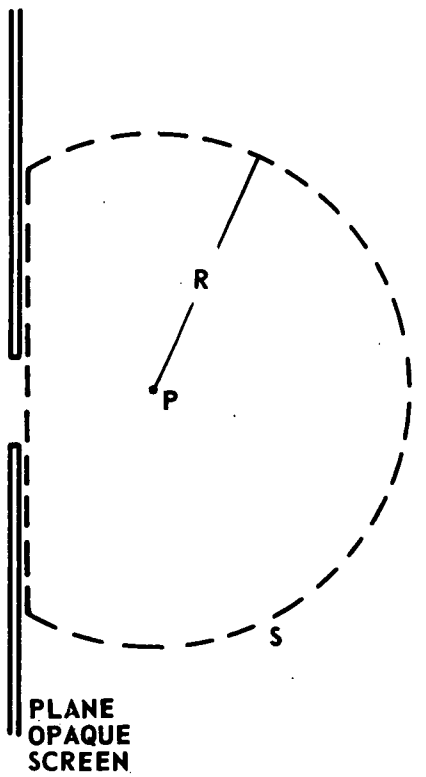


FIGURE A2. CONSTRUCTION FOR DERIVATION OF FRESNEL – KIRCHHOFF DIFFRACTION FORMULA

$$E(P) = \frac{1}{4\pi} \iint_S \left\{ E \frac{\partial}{\partial n} \left[ \exp(iks)/s \right] - \left[ \exp(iks)/s \right] \frac{\partial E}{\partial n} \right\} ds \quad \text{(A2)}$$

where S is a closed surface bounding a volume containing P, $\frac{\partial}{\partial n}$ denotes differentiation along the inward normal to S, and s denotes the distance from P to the point of integration [17].* Equation (A2), Kirchhoff's integral, may be put into a simpler and more useful form by means of Kirchhoff's approximation (Kirchhoff's boundary conditions) [17].

Consider a monochromatic wave propagated through an opening in a plane opaque screen which is normal to the x-axis, and assume that the linear dimensions of the aperture, although large compared to the wavelength, are small compared to the distances of the source and the point P from the screen. Let the surface S consist of the opening, a portion of the non-illuminated side of the screen, and a portion of a large sphere of radius R centered at the point P. Figure A2 illustrates the situation.

Kirchhoff's integral could be used to give the field at the point P = (x, y, z) assuming that the values of E and $\partial E/\partial n$ were known exactly everywhere on the surface S. In Kirchhoff's approximation it is assumed that:

1) E and $\partial E/\partial n$ have the same values within the aperture as they would have in the absence of the screen.

2) The field and its derivatives equal zero everywhere on the dark side of the screen.

3) The radius R of the sphere is taken sufficiently large that the contribution to Kirchhoff's integral from the sphere may be neglected.

With these assumptions, Equation (A2) becomes

$$E(x,y,z) = \frac{-ik}{4\pi} \iint \frac{\exp(ik\,|\vec{r} - \vec{r}'|)}{|\vec{r} - \vec{r}'|} E_{x'}(y',z') \frac{\left[1 + \cos \chi(\vec{r} - \vec{r}')\right]}{2} dy'dz' \quad \text{(A}$$

*When k=0, Equation (A1) reduces to Laplace's equation, and (A2) reduces to the formula from potential theory which expresses the potential in a source-free region as an integral involving the potential and its normal derivative over a surface (as in electrostatics) [18].

where the integration is over the aperture, $E_x'(y',z')$ is the value of the field in the aperture, and $X$ is the direction of propagation with respect to the x-axis.

Equation (A3), obtained by applying the Kirchhoff boundary conditions to Equation (A2), is known as the Fresnel-Kirchhoff diffraction formula. The assumptions in Kirchhoff's approximation can be shown to be rigorously inconsistent, although they are a very good approximation [21]. However, another derivation eliminating the inconsistencies of the Kirchhoff theory leads to a practically identical expression, the Rayleigh-Sommerfield diffraction formula [21]. In the approximation to be made next, there is no difference between the two expressions.

The last factor in the integrand of Equation (A3) is known as the "obliquity factor". If we restrict consideration to small angles with respect to the general direction of propagation, the obliquity factor may be set equal to unity with small error. Often this a perfectly reasonable assumption. In many cases of interest, the aperture will contain a photographic transparency, illuminated by a plane wave. The smallest practical resolvability of photographic film recording is of the order of 1000 line pairs/mm = $10^6$ line pairs/m. A diffraction grating with a line spacing d will scatter a wave through an angle $\lambda/d$ (in first order), where $\lambda$ is the wavelength. If $\lambda \approx 5000$ Angstroms $= 5 \times 10^{-7}$ m (visible light), the angle is $5 \times 10^{-7}/10^{-6} = 5 \times 10^{-1}$ radians for the line spacing given above. If the scattering is restricted to this angle or less, the approximation for the obliquity factor is valid.

Also, since it is assumed that the x-axis is approximately aligned with the scattering cone, the expansions of $|\vec{r} - \vec{r}'|$ can be simplified. The resulting simplified form of the Kirchhoff diffraction integral is

$$E_x(y,z) \approx \frac{-ik}{4\pi} \frac{\exp\left[ik(x-x')\right]}{(x-x')} \iint \exp\left[ik \frac{(y-y')^2 + (z-z')^2}{2(x-x')}\right] E_x'(y',z')dy'dz' \quad \text{(A4)}$$

where the notation $E_x(y,z)$ has been adopted to emphasize that we are considering the diffracted field in a plane x = constant, due to the field in the plane with x coordinate x', $x > x'$. It is seen from (A4) that the mathematical effect on the scalar field of propagation of the light wave in free space through a distance L is convolution of the initial field with an impulse response $\exp\left[ik(y'^2 + z'^2)/2L\right]$; the approximations made to obtain that result are not very restrictive.

If Equation (A4) is evaluated for very large values of x (Fraunhofer zone), a further simplification results. If the definition $R = |x - x'|$ is made, then the Fraunhofer zone is the region such that the largest value of $\left[k(y'^2 + z'^2)/2R\right]$ is much smaller than unity. In this region, the diffraction integral becomes

$$E_x(y,z) \approx \frac{-ik}{4\pi} \frac{\exp(ikR)}{R} \exp\left(ik \frac{y^2 + z^2}{2R}\right)$$

$$\times \iint \exp\left(-i \frac{ky}{R} y' - i \frac{kz}{R} z'\right) E_x'(y',z') \, dy'dz' \qquad (A5)$$

That is, in the Fraunhofer or far-field zone, the scalar field is given, within a quadratic phase factor, by the (scaled) two-dimensional Fourier transform of the aperture scalar field. For optical wavelengths and an aperture with linear dimensions of a few centimeters, the Fraunhofer zone begins several kilometers away.

## APPENDIX B

## OPTICAL PROCESSING

Equation (A5) of Appendix A showed that, under some rather mild restrictions, the optical field in the Fraunhofer or far-field zone, resulting from diffraction by an aperture, is essentially the two-dimensional Fourier transform of the field within the aperture. However, in a typical case involving optical wavelengths, the Fraunhofer zone begins several kilometers from the aperture. This is much too great a distance to make the Fourier transforming property of diffraction by an aperture useful in data processing devices. Also, the transform is spread over a wide area, and the intensity is very low.

It seems intuitively obvious, however, that it should be possible to bring the Fourier transform nearer by means of lenses. In fact, this is true [19]. It may be shown that a spherical lens with focal length f is equivalent to a transparency with transmission function

$$t = \exp\left[-i\,(k/2f)\,(x^2 + y^2)\right] \qquad \text{(B1)}$$

(aside from a constant phase delay)--that is, the incident field is multiplied by this factor [12,20]. For a spherical lens the focal length f is positive. In general, if f is positive the effect of the transmission function t is to transform a plane wave in front of the lens into a spherical wave (in the "paraxial" approximation) converging toward a point on the lens axis a distance f behind the lens. On the other hand, if f is negative, the spherical wave is diverging about a point on-axis a distance $|f|$ in front of the lens. The same convention is used for other lens transmission functions. A lens with a positive focal length is called a converging lens, or simply a positive lens; it forms a real image behind the lens. A lens with a negative f is a diverging (negative) lens; it forms a virtual image in front of the lens. Following this convention, several types of lenses with various combinations of convex and concave surfaces are described by Equation (B1), as long as the correct sign of f is used. For a cylindrical lens (one that is a portion of a right circular cylinder), the transmission function is similar to (B1), only the factor $(x^2 + y^2)$ is replaced by $x^2$ [21].

Combining (B1) with Equation (A4), which describes the effect of free-space propagation, the result is that the field in the back focal plane of a lens is proportional to the Fourier transform of the field in the front focal plane. More generally, the field in the back focal plane of a lens is the Fourier transform of the field in any plane F (normal to

the optical axis--general direction of propagation) in front of the lens, multiplied by a position-dependent phase factor. In a region over which this phase variation is negligible, the amplitude distribution in the back focal plane is simply proportional to the Fourier transform of the light amplitude in F. And if one measures the intensity of the light in the back focal plane (e.g., by recording on photographic film), the two-dimensional power spectrum of the light distribution on F is always obtained. Since light intensity is proportional to the absolute square of the amplitude, the phase factor is irrelevant. The nature and magnitude of the errors in the Fourier transform approximation are discussed in detail in Reference 19.

The foregoing remarks are illustrated in Figure B1. If the waves at planes $P_1$, $P_2$, and $P_3$ are denoted by $E_1(x_1, y_1)$, $E_2(x_2, y_2)$, and $E_3(x_3, y_3)$, respectively, then (again note that the fields are treated as complex):

1) $E_3$ and $E_1$ form a Fourier transform pair to within a phase factor

$$E_3(x_3, y_3) = \mathfrak{F}\left[E_1(x_1, y_1)\right] \quad \exp\left[i\,\beta(x_3, y_3)\right] \tag{B2}$$

where $\mathfrak{F}$ denotes the Fourier transform. Plane $P_1$ may lie anywhere between lenses $L_1$ and $L_2$, and $\beta$ is a function of the distance $Z_1$.

2) An exact Fourier transform exists between $E_3$ and $E_2$, or

$$\beta(x_3, y_3) = 0 \qquad \text{for} \qquad Z_1 = Z_2 \tag{B3}$$

($f_2$ is the focal length of lens $L_2$, in Figure B1).

3) An exact Fourier transform does not exist anywhere else (with respect to lens $L_2$):

$$\beta(x_3, y_3) \neq 0 \qquad \text{for} \qquad Z_1 \neq Z_2 \tag{B4}$$

This property of lenses makes it possible to use optical systems for performing many mathematical operations. For example, filtering may be done, making use of the convolution theorem. Several such operations are illustrated in Figure B2.

Another of the most significant characteristics of optical systems is that they possess two degrees of freedom, as represented by the two independent variables which define a point on a surface. This, along with the Fourier-transforming property of lenses, makes possible versatile processing systems, for performing two-dimensional mathematical operations

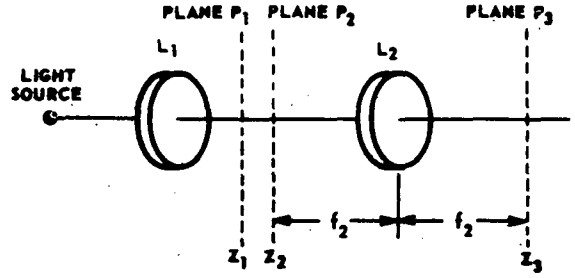


FIGURE B1. FOURIER TRANSFORMS IN AN OPTICAL SYSTEM (FROM REFERENCE 20)

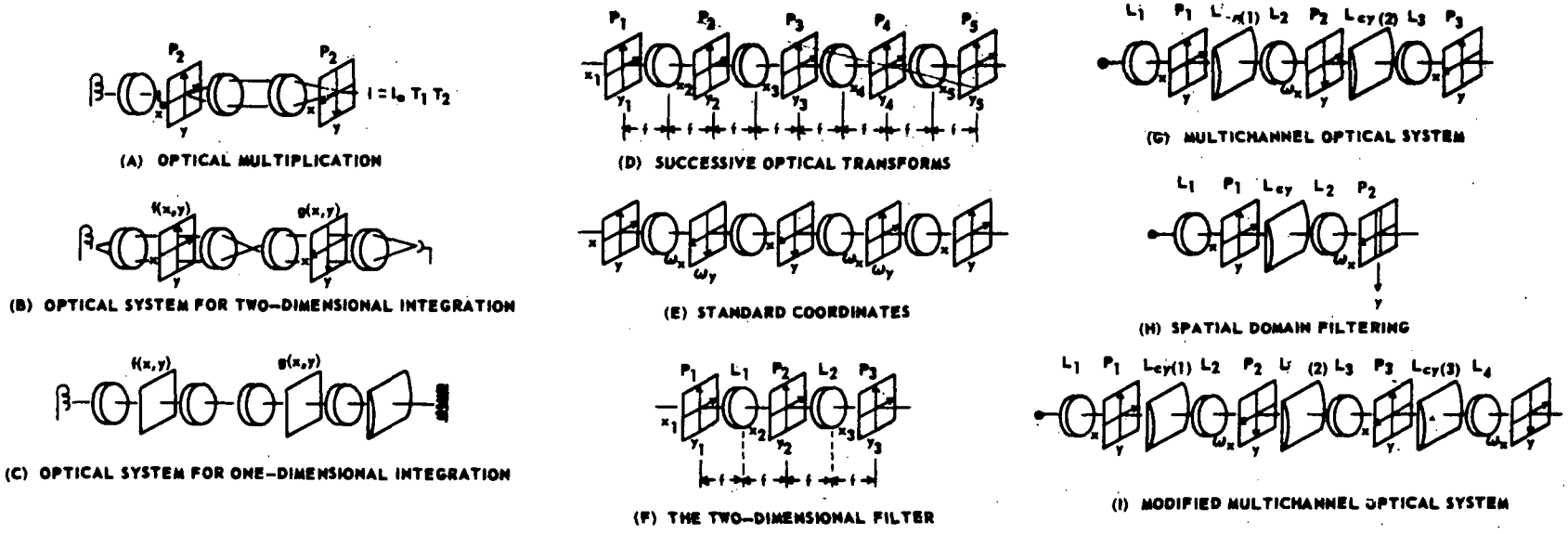


FIGURE B2. OPTICAL PROCESSING EXAMPLES (FROM REFERENCE 20)

or many one-dimensional operations in parallel. (Just as a spherical lens performs a two-dimensional Fourier transform, a cylindrical lens--such as the rightmost lens in Figure B2(c)--can be used to perform a Fourier transform with respect to one variable.)

The operation of the systems shown in Figure B2 will now be considered.

Multiplication and Integration

Figure B2(a) depicts a light source and a collimating lens, illuminating a transparency in plane $P_1$. The important property of a transparency for the type of application described here is its transmittance function. The transmittance function $T(x,y)$ relates the transmitted light intensity $I(x,y)$ with the incident (illuminating) intensity $I_0$, by

$$T(x, y) = I(x, y)/I_0 \tag{B5}$$

The two lenses to the right of plane $P_1$ image the transparency in this plane onto plane $P_2$, which contains another transparency. The intensity distribution of the light emerging from the second transparency is, therefore,

$$I(x, y) = I_0\, T_1(x, y)\, T_2(x, y) \tag{B6}$$

where $T_1$ and $T_2$ are the transmittance functions of planes $P_1$ and $P_2$, respectively. If the energy incident on plane $P_1$ is distributed uniformly over the entire transparency, as in Figure B2(a), multiplication of the (two-dimensional) functions recorded as transmittance functions is the result.

The configuration shown in Figure B2(b), which adds one more lens and a photocell or other detector, evaluates the integral

$$I = \int_{a_1}^{b_1} \int_{a_2}^{b_2} f(x, y)\, g(x, y)\, dx\, dy \tag{B7}$$

The extra lens simply images the product onto a detector whose size is greater than the image. The addition of the cylindrical lens in Figure B2(c) results in the computation of

$$I(y) = \int_{a(y)}^{b(y)} f(x, y)\, g(x, y)\, dx \qquad \text{(B8)}$$

The cylindrical lens counteracts, for the y dimension only, the tendency of the spherical lens to integrate the light emerging from the plane $P_2$. By the simple expedient of transporting the strip of film containing the g transparency across the aperture in the x direction, the expression

$$I(y, x_0) = \int_{a(y)}^{b(y)} f(x, y)\, g(x - x_0, y)\, dx \qquad \text{(B9)}$$

is evaluated by the system shown in Figure B2(c).

## Coherent Optical Systems

If the source of light is coherent, the relative phases of the light waves in various parts of the system are invariant with time. Then the considerations leading up to Equation (B2) are meaningful, and Fourier methods may be used in the analysis of coherent optical systems. A point source of light (e.g., a lamp and a pinhole) is coherent, but in order to obtain useful light intensities a laser is usually used as the source of illumination in coherent optical systems.

One advantage of coherent optical systems pertains to the transparencies used to represent signals. The transmittance functions described previously are simply energy ratios and must, therefore, always be non-negative, between 0 and 1. If a signal of interest is bipolar, as is commonly the case, it must be scaled and biased to be represented by a transparency. The addition of biases to the factors in the integrand of Equation (B8), for instance, adds several error terms, whose removal presents a problem.

The possibility of synthesizing complex transparencies (in the coherent case) exists. Even without doing this, however, the Fourier-transforming property of lenses can be used to advantage. A constant bias level has only a zero-frequency component in the spatial frequency plane. (Physically, this is equivalent to saying that a uniform plane wave is focused to a point.) In some cases, the spectrum of the remaining part of the transparency is completely disjoint from this, so the effect of a bias level can be removed by an appropriately placed stop in the spatial frequency plane.

Figure B1 illustrates the Fourier property of lenses. It should be noted that the Fourier transform relationship exists between light amplitudes in successive planes of the optical systems. Light intensity, which is what is actually sensed by film, the eye, photocells, etc., is proportional to the square of the amplitude.

In Figure B2(d), the field in plane $P_2$ is (proportional to) the two-dimensional Fourier transform of the light wave in plane $P_1$, the field in $P_3$ is the Fourier transform of the field in $P_2$, etc. Successive transforms are taken, rather than a transform followed by its inverse. However, it can easily be seen that the effect of using a Fourier kernel of the wrong polarity is simply to reverse the coordinate system of the transformed function. The scheme of labeling shown in Figure B2(e) makes the optical system consistent with the usual conventions of Fourier transform theory (assuming the light wave is traveling from left to right).

## Optical Filtering

Figure B2(f) shows a simple application of the Fourier-transform property of coherent optical systems. If a signal $s(x, y)$ is inserted at plane $P_1$, in the form of a light amplitude transmission function (cf. especially Reference 19, Chapter 6), its spectrum $S(\omega_x, \omega_y)$ is displayed at plane $P_2$. A transparency $R(\omega_x, \omega_y)$ also inserted at $P_2$ modifies the spatial frequency spectral content of the signal. At plane $P_3$, the signal is transformed back to the spatial domain. By the convolution theorem of Fourier analysis, the field in plane $P_3$ is given by the convolution of the original signal $f(x, y)$ and a function $r(x, y)$, the inverse transform of R. Therefore this optical system can be used for linear filtering.

Figure B2(f) shows a configuration that could be used for two-dimensional filtering, without the scanning which would be necessary in an electronic system. If the signal is one-dimensional, however, the second variable could be used to parameterize a multiplicity of independent channels so that one-dimensional signals could be processed simultaneously. Figure B2(g) shows a simple modification that provides one-dimensional multichannel filtering. The modification consists of the addition of two cylindrical lenses. In plane $P_2$, the Fourier transform with respect to x only is desired. The addition of the first cylindrical lens, with focal power in the y direction only, yields a double Fourier transform with respect to y, while leaving a single Fourier transform with respect to x. Thus, the desired result is achieved--plane $P_1$ is merely imaged onto plane $P_2$ in the y dimension, while a Fourier transform is taken in the x dimension.

A filter element $R(\omega_x, y)$--a multichannel one-dimensional filter--is inserted at plane $P_2$. Then, the remaining two lenses result in the inverse transformation with respect to $\omega_x$, and the output plane $P_3$ contains the input function (stacked, in the y direction) after modification by the filter in the x direction only.

The filtering may be done in the spatial domain, rather than the frequency domain. The same optical system is used, except that the output is taken from the plane $P_2$ and the portion of the system beyond this plane may be eliminated. The method consists of translating the signal transparency in plane $P_1$ past a transparency containing the filter (or reference) function in the same plane. Plane $P_2$ then contains the Fourier transform with respect to x of the product. A vertical (i.e., in the y direction) slit along the line $\omega_x = 0$ therefore passes the desired convolution integral. The output, as a function of time, is the convolution, as a function of shift. As before, y is a parameter providing multichannel operation. The situation is illustrated in Figure B2(h).

Multichannel Optical Computers

Finally, the optical system of Figure B2(i) is used for evaluating integrals of the form

$$I(\omega_x, x_0, y) = \int_{a(y)}^{b(y)} f(x - x_0, y)\, g(x, y)\, \exp(-i\,\omega_x x)\,dx \qquad (B10)$$

This general form encompasses such mathematical operations as Fourier and Laplace transforms, auto- and cross-correlations, and convolution [7]. The system shown in Figure B2(i) is a versatile multichannel processor that can be used for performing these operations, which have many applications.

Additional discussion on optical processing systems can be found in many places, for instance References 12 and 21. Another optical technique of importance, which should be mentioned here, is holography [12,19,21-26]. Holography is a two-step imaging process originally developed in an attempt to improve the resolving power of electron microscopes. The first step, called "formation", consists of photographing the interference pattern between the light diffracted by an object (scene) and a coherent reference or background wave. The second step, "reconstruction", consists of placing the photographic transparency into a coherent beam of light and producing an image of the original object. The wavefronts generated at the plane of the hologram are replicas of those that impinged on the film during the first step, and these wavefronts continue on and form an image, just as the original waves would have done if they had not been interrupted. In effect, the hologram is a recording of an optical wavefront at a plane in space; both amplitude and phase information are encoded. One consequence is that the image formed is three-dimensional, and exhibits parallax as the observer moves from one place to another; in general, a hologram contains much more information than an ordinary photograph.

## REFERENCES


1. Cutrona, L. J., et al: A High-Resolution Radar Combat-Surveillance System. IRE Transactions on Military Electronics MIL-5, 127-131, April 1961.

2. Sherwin, C. W., et al: Some Early Developments in Synthetic Aperture Radar Systems. IRE Transactions on Military Electronics MIL-6, 111-116, April 1962.

3. Brown, W. M. and Porcello, L. J.: An Introduction to Synthetic-Aperture Radar. IEEE Spectrum 6, 52-62, September 1969.

4. Cutrona, L. J., et al: On the Application of Coherent Optical Processing Techniques to Synthetic-Aperture Radar. Proceedings of the IEEE 54, No. 8, 1026-1032, August 1966.

5. Harger, R. O.: Synthetic Aperture Radar Systems. Academic Press, 1970.

6. Rihazcek, A. W.: Principles of High-Resolution Radar. McGraw-Hill Book Company, 1969.

7. Papoulis, A.: Systems and Transforms with Applications in Optics. McGraw-Hill Book Company, 1968.

8. Useful Applications of Earth-Oriented Satellites, Sensors and Data Systems. National Academy of Sciences, 1969.

9. Gerchberg, R. W.: Synthetic Aperture Radar and Digital Processing. CRES Technical Report 177-10, The University of Kansas, September 1970.

10. Moore, R. K. and Rouse, J. W.: Electronic Processing for Synthetic Aperture Array Radar. Proceedings of the IEEE 55, 233-235, February 1967.

11. Cooley, J. W., Lewis, P. A. W. and Welch, P. D.: The Fast Fourier Transform Algorithm and Its Applications. IBM Research Paper RC1743, February 9, 1967.

12. Papoulis, A.: The Fourier Integral and Its Applications. McGraw-Hill Book Company, 1962.

13. Turin, G. L.: An Introduction to Matched Filters. IRE Transactions on Information Theory IT-6, 311-329, June 1960.

14. Reference Earth Orbital Research and Applications Investigations (Blue Book), Volume IV, Earth Observations, National Aeronautics and Space Administration NHB7150.1, January 15, 1971.

15. Lybanon, M.: Work of Remote Sensing Laboratory, CRES, University of Kansas. CSC Memo No. M00010-2-2, September 17, 1970.

16. Rossi, B.: Optics. Addison-Wesley Publishing Company, Inc., 1957.

17. Born, M. and Wolf, E.: Principles of Optics, Third Edition. Pergamon Press, 1965.

18. Panofsky, W. K. H. and Phillips, M.: Classical Electricity and Magnetism, Second Edition. Addison-Wesley Publishing Company, Inc., 1962.

19. Shulman, A. R.: Optical Data Processing. John Wiley & Sons, Inc., 1970.

20. Cutrona, L. J., et al: Optical Data Processing and Filtering Systems. IRE Transactions on Information Theory IT-6, 386-400, 1960.

21. Goodman, J. W.: Introduction to Fourier Optics. McGraw-Hill Book Company, 1968.

22. Gabor, D.: Microscopy by Reconstructed Wave-Fronts. Proceedings of the Royal Society (London) A197, 454-487, 1949.

23. Leith, E. N. and Upatnieks, J.: Reconstructed Wavefronts and Communication Theory. Journal of the Optical Society of America 52, 1123-1130, 1962.

24. DeVelis, J. B. and Reynolds, G. O.: Theory and Applications of Holography. Addison-Wesley Publishing Company, Inc., 1967.

25. Gabor, D., et al: Holography. Science 173, 11-23, 1971.

26. Goodman, J. W.: An Introduction to the Principles and Applications of Holography. Proceedings of the IEEE 59, 1292-1304, 1971.

27. Leith, E. N.: Quasi-Holographic Techniques in the Microwave Region. Loc. cit., 1305-1318.

28. Moore, R. K. and Thomann, G. C.: Imaging Radar for Geoscience Use. IEEE Transactions on Geoscience Electronics GE-9, 155-164, 1971.

29. Cavanaugh, G.: private communication. Texas Instruments (Houston Facility), August 9, 1972.

30. Helms, H. D.: Fast Fourier Transform Method of Computing Difference Equations and Simulating Filters. IEEE Transactions on Audio and Electroacoustics AU-15, 85-90, 1967.

31. Lybanon, M.: FFOURT - A Computer Program for Calculating the Fast Fourier Transform. Computer Sciences Corporation Interactive Data Evaluation and Analysis System (IDEAS), System Documentation, Issue 3, April 8, 1971.

32. Singleton, R. C.: Algorithm 345, An Algol Convolution Procedure Based on the Fast Fourier Transform. Communications of the ACM 12, 179-184, 1969.

33. Barnes, G. H., et al: The ILLIAC IV Computer. IEEE Transactions on Computers C-17, 746-770, 1968.

34. Pease, M. C.: An Adaptation of the Fast Fourier Transform for Parallel Processing. Journal of the Association for Computing Machinery 15, 252-264, 1968.

35. Groginsky, H. L. and Works, G. A.: A Pipeline Fast Fourier Transform. EASCON '69 Record, 22-28, 1969.

36. Bergland, G. D.: The Fast Fourier Transform Recursive Equations for Arbitrary Length Records. Mathematics of Computation 21, 236-238, 1967.

37. Zukin, A. S. and Wong, S. Y.: Architecture of a Real-Time Fast Fourier Radar Signal Processor. Spring Joint Computer Conference Proceedings, 417-435, 1970.

38. Pease, M. C.: Organization of Large Scale Fourier Processors. Journal of the Association for Computing Machinery 16, 474-482, 1969.

39. Rice, S. O.: Mathematical Analysis of Random Noise. Part 1: Bell System Technical Journal 23, 282-332, 1944. Part 2: Bell System Technical Journal 24, 46-156, 1945.

40. Brennan, P. A. and Lintz, J.: Remote Sensing of Some Sedimentary Rocks. Proceedings of the Seventh International Symposium on Remote Sensing of Environment, May 17-21, 1971, Institute of Science and Technology, The University of Michigan, Ann Arbor, Michigan, 256-268.

41. Larrowe, B. T., et al: Lake Ice Surveillance Via Airborne Radar: Some Experimental Results. Loc. cit., 511-521.

42. Johnson, J. D. and Farmer, L. D.: Determination of Sea Ice Drift Using Side-Looking Airborne Radar. Loc. cit., 2155-2168.

43. Guinard, N. W.: The Remote Sensing of Oil Slicks. Loc. cit., 1005-1026.

44. North, G. W.: Remote Sensing for Pollution and Environmental Quality Studies. Loc. cit., 973-987.

*"The aeronautical and space activities of the United States shall be conducted so as to contribute . . . to the expansion of human knowledge of phenomena in the atmosphere and space. The Administration shall provide for the widest practicable and appropriate dissemination of information concerning its activities and the results thereof."*

—NATIONAL AERONAUTICS AND SPACE ACT OF 1958

# NASA SCIENTIFIC AND TECHNICAL PUBLICATIONS

TECHNICAL REPORTS: Scientific and technical information considered important, complete, and a lasting contribution to existing knowledge.

TECHNICAL NOTES: Information less broad in scope but nevertheless of importance as a contribution to existing knowledge.

TECHNICAL MEMORANDUMS: Information receiving limited distribution because of preliminary data, security classification, or other reasons. Also includes conference proceedings with either limited or unlimited distribution.

CONTRACTOR REPORTS: Scientific and technical information generated under a NASA contract or grant and considered an important contribution to existing knowledge.

TECHNICAL TRANSLATIONS: Information published in a foreign language considered to merit NASA distribution in English.

SPECIAL PUBLICATIONS: Information derived from or of value to NASA activities. Publications include final reports of major projects, monographs, data compilations, handbooks, sourcebooks, and special bibliographies.

TECHNOLOGY UTILIZATION PUBLICATIONS: Information on technology used by NASA that may be of particular interest in commercial and other non-aerospace applications. Publications include Tech Briefs, Technology Utilization Reports and Technology Surveys.

***Details on the availability of these publications may be obtained from:***

**SCIENTIFIC AND TECHNICAL INFORMATION OFFICE**

**NATIONAL AERONAUTICS AND SPACE ADMINISTRATION**

**Washington, D.C. 20546**